IN THE UNITED STATES PATENT AND TRADEMARK OFFICE

In re application of:

WARREN WARD

Serial No.:   10/595,033

Group Art Unit: 1595

Examiner: Tigabu Kassa

Filed: January 4, 2006

For: COMPOSITIONS COMPRISING COMPONENTS COATED WITH A LIQUID IMPERMEABLE BUT GAS PERMEABLE LAYER, USE THEREOF FOR TREATING CUTANEOUS AND OTHER EXOCRINE GLAND DISEASES

Attorney Docket No.: WAW 0101 PUSA

APPEAL BRIEF UNDER 37 C.F.R. § 41.37
AND PETITION FOR EXTENSION OF TIME
UNDER 37 C.F.R. § 1.136(a)

Mail Stop Appeal Brief - Patents
Commissioner for Patents
U.S. Patent & Trademark Office
P.O. Box 1450
Alexandria, VA 22313-1450

Sir:

Applicant hereby petitions for a one (1) month extension of time to respond to the Notice of Appeal mailed September 10, 2010, thereby extending the time period within which to respond to December 10, 2010.

This is an Appeal Brief from the final rejection of claims 7-11, 24-28, 30-33, and 36-37 of the Office Action dated June 23, 2010, hereinafter "the instant final Office Action."

I. REAL PARTY IN INTEREST

The real party in interest is Warren Ward, the sole inventor and the Appellant, an individual residing in Gwynedd, United Kingdom.

II. RELATED APPEALS AND INTERFERENCES

There are no appeals or interferences known to the Appellant, the Appellant 's legal representative, or the Assignee which may be directly affected or be directly affected by or have a bearing on the Board's decision in the pending appeal.

III. STATUS OF CLAIMS

Claims 1-28, 30-34, and 36-37 are pending in this application. Claims 29 and 35 are cancelled. Claims 1-6, 12-23, and 34 are withdrawn from consideration. Claims 7-11, 24-28, 30-33, and 36-37 are rejected and are the subject of this appeal.

IV. STATUS OF AMENDMENTS

A response with claim amendments was filed on April 5, 2010 and has been accepted for entry pursuant to the instant final Office Action.

V. SUMMARY OF CLAIMED SUBJECT MATTER

The application has one (1) independent claim: Claim 24.

Independent claim 24 concerns a preparation for use as a medicament, comprising a medically efficacious substance coated with an aqueous liquid impermeable but gas permeable layer for surrounding and preventing release of the medically efficacious substance (lines 18-20 on page 7 and lines 15-18 on page 16 of the original specification and claims 3 and 26 as originally filed), wherein the layer contains a ceramic, a clay, an inorganic non-metallic material, a polymer, a natural wax, a perforated stainless steel, or beeswax hardened with cornstarch and talc (lines 27-28 on page 19 of the original specification and claims 7 and 9 as originally filed).

VI. GROUNDS OF REJECTION TO BE REVIEWED ON APPEAL

Claims stand rejected under 35 U.S.C. § 101. *See* page 2 of the instant final Office Action.

Claims 7-11, 24-28, 30-33, and 36-37 stand rejected under 35 U.S.C. § 112, first paragraph, as lacking enablement, and second paragraph, as being indefinite. *See* pages 5-8 of the instant final Office Action.

VII. ARGUMENT

The claimed invention concerns lessening and/or removing symptoms of medical conditions that are at least partially associated with blockage of exocrine glands and ducts of sweat glands in particular. *See* lines 4-7 on page 1 and lines 1-9 on page 10 of the original specification. Non-limiting examples of such medical conditions induce miliaria, migraine and asthma. *See* line 23 on page 1 to line 7 on page 3 and lines 8-16 on page 4 of the original specification. In one embodiment, the claimed invention is directed to the use of sodium chloride (NaCl) encapsulated within an aqueous liquid impermeable but gas permeable layer such that NaCl is not released into one's circulation and cannot cross epithelial barriers. *See* lines 11-16 on page 6 and lines 1-4 on page 7 of the original specification. In certain particular instances, the NaCl is encapsulated within the layer configured in a sphere with an approximate diameter of 1 millimeter to 10 millimeters. *See* lines 16-20 on page 8 of the original specification. The sphere-shaped NaCl preparation is placed in proximity to the blocked exocrine gland duct. *See* lines 11-14 on page 10 of the original specification. Without wanting to be limited to any particular theory, it is believed that the claimed invention, in one or more embodiments, provides

-3-

in the air and/or in the liquid environment of the body an amount of non-releasable sodium to induce the body to sense a sodium surplus to allow resetting to genetic habituation. *See* line 26 on page 15 to line 5 on page 16 of the original specification.

In another embodiment, and as recited in claim 36, the claimed invention is directed to a preparation wherein the coating layer contains a wax in an amount of between 20% and 45% by weight of the preparation, a ceramic, or combinations thereof. The claimed preparation of claim 36, which contains a relatively high content of wax in a range of 20% to 45% by weight for liquid impermeability, clearly departs from the conventional art which uses only a minimal amount of wax, e.g., in a range of 1% to 5% by weight, to facilitate but not to inhibit the release of drug components although in a delayed formulation.

In yet another embodiment, and as recited in claim 37, the claimed invention is directed to a preparation of claim 24 configured as a patch, having two spaced apart spheres, each of a diameter of 1 mm to 10 mm, wherein the aqueous liquid impermeable and gas permeable layer contains a beeswax hardened with cornstarch and talc. As will be detailed below, products manufactured according to claim 37 have gained substantial commercial successes and widely recognized academic acceptance.

A.   *Claim Rejection under 35 U.S.C. § 101*

As stated on page 2 of the instant final Office Action, claims stand rejected under 35 U.S.C. § 101. In making and maintaining the claim rejection for lack of patentable utility, the Examiner argues that these is insufficient evidence to support the utility, more particularly, that there is insufficient evidence to show that a compound which is not released on or into the body can have any medically beneficial effect. For at least the reasons set forth below, Appellant respectfully solicits reversal of this rejection.

a)   *prima facie* case of rejection has not yet been properly made

MPEP § 2107.02 (IV) in relevant portion provides that, to properly reject a claimed invention under 35 U.S.C. § 101, the Office must (a) make a *prima facie* showing that the claimed invention lacks utility, and (a) provide a sufficient evidentiary basis for factual assumptions relied upon in establishing the *prima facie* showing. Accordingly, the Patent Office must do more than merely question operability. The Patent Office must set forth factual reasons which would lead one skilled in the art to question the objective truth of the statement of operability. The *prima facie* showing must contain the following elements: 1) an explanation that clearly sets forth the reasoning used in concluding that the asserted utility for the claimed invention is neither both specific and substantial nor well-established; 2) support for factual findings relied upon in reaching this conclusion; and 3) an evaluation of all relevant evidence of record, including utilities taught in the closest prior art. It is imperative that Office personnel use specificity in setting forth an initial rejection under 35 U.S.C. § 101 and support any factual conclusions made in the *prima facie* showing.

In making and maintaining this lack of utility rejection, the Examiner provides a single paragraph of 73 words (reproduced below) as reasons for supporting the rejection.

> The claimed invention lacks patentable utility. The instant application fails to provide adequate evidence to support the utility of the invention. Specifically, there is insufficient evidence to show that a compound which is not released on or into the body can have any medically beneficial effect. Additionally, the agents used to form the liquid impermeable but gas permeable layer (e.g. wax) are also used in the art to form controlled release formulations of drugs.

See also the prior Office Actions of of January 7, 2009, of June 24, 2009, page 3, and of October 5, 2009, page 3.

As can be seen from the above reproduced paragraph, the Examiner sets forth the rejection with a conclusory first sentence of lack of utility, follows with a conclusory second sentence of lack of adequate evidence for supporting the utility. In so doing, the Examiner impermissibly makes and maintains the rejection without meeting the required burden pursuant to relevant portions of MPEP cited above, namely, showing clear explanation for the lack of utility assertion, providing factual findings and support thereof, and providing an evaluation of all relevant evidence of record.

Therefore, other than merely questioning operability, the Examiner has not properly established a lack of utility rejection under 35 U.S.C. § 101 in view of requirements and obligations set forth in relevant MPEP provisions cited above.

b)   notwithstanding the section a) above, sufficient evidence has been submitted for the record to support a patentable use

Argumento, even if a *prima facie* case of rejection could be argued to have been properly established, Appellant respectfully submits that ample and sufficient evidence has been made of record to support one or more patentable uses of the claimed invention.

For instance, Appellant has stated in the application that Appellant's invention can be used to reduce symptoms of and/or to treat disorders associated with medical conditions characterized by blockage of exocrine glands including ducts of sweat glands. *See* lines 4-7 on page 1 and lines 25-26 of page 4 of the original specification.

For instance also, and as stated in paragraph 16 of the Ward Declaration of April 5, 2010, the "Equiwinner" patches per one or more embodiments of the claimed invention have been sold to professional horse trainers in various countries including the United States, United Kingdom, Australia and New Zealand. The retail selling price has been between 123 and 130 US

dollars (or the equivalent) plus carriage and tax where applicable, for a box of ten patches, plus two spare patches.

Yet for instance also, and as stated in paragraph 17 of the Ward Declaration of April 5, 2010, the "Equiwinner" patches according to the claimed invention have been very well received by the trainers, representing the only effective treatment known for the market. The total numbers of the "Equiwinner" patches sold in the last four consecutive calendar years were 5,000 patches, 11,000 patches, 18,000 patches, and 24,000 patches, with a market value of several hundred thousand dollars for year 2009. The magnitude of increase in sales is further reflective the high quality of the "Equiwinner" patches according to the claimed preparation. This secondary consideration strongly supports both utility and patentability of the claimed preparation.

Yet for instance also, and as stated in paragraph 18 of the Ward Declaration of April 5, 2010, a quantity of the "Equiwinner" patches were provided to a UK veterinarian Dr. Steve Gittins, an equine specialist, a Bachelor of Veterinary Science and a member of the Royal College of Veterinary Surgeons. In his statement dated July 14, 2005, previously submitted as Exhibit 1 of April 5, 2010, Dr. Gittins reported a positive medical effect of the patches.

Yet for instance also, and as stated in paragraph 19 of the Ward Declaration of April 5, 2010, a quantity of the "Equiwinner" patches were provided to an Italian veterinarian Dr. Paola Gulden, Vice-President of the Learned Societa Italiana Veterinari per Equini (Italian Society for Equine Veterinarians) in year 2005 to 2007 and President in year 2007 to 2009. Dr. Gulden treated a number of horses having exercise induced pulmonary hemorrhage by placing on the horses the supplied "Equiwinner" patches for between three and ten days. In her statement dated December 2005, previously submitted as Exhibit 2 of April 5, 2010, Dr. Gulden reported that "All of the horse(s) had a clear improvement of the pathological condition."

Contrary to the Examiner's assertions, the commercial success and academic acceptance of the claimed invention as recited in pertinent parts of the Ward Declaration of April 5, 2010 is not only relevant to the utility analysis under 101 but also sufficient to show at least one patentable use. The Examiner's attention is respectfully directed to MPEP 2107.02 (VI), which in relevant portion provides that an applicant can rebut a lack of utility rejection using any combination of the following: amendments to the claims, arguments or reasoning, or new evidence submitted in an affidavit or declaration under 37 CFR 1.132, or in a printed publication.

c)   the examiner continues to impermissibly mis-characterize appellant's invention

The Examiner correctly admits that no prior art can be located which would teach or suggest the claimed preparation. *See* pages 6-7 of the Office Action of January 7, 2009. However, the lack of any teaching in the art of the claimed invention does not by itself entitle the Examiner to question the usefulness of the claimed invention, let alone to do so via impermissible mis-characterization of Appellant's claimed invention.

i)   a preparation does not have to be a pharmaceutical to be useful

The Examiner asserts that the claimed invention must be released to be useful as a pharmaceutical. *See* page 3 of the Office Action of June 24, 2009. However, this assertion is submitted to have been misplaced at least to the extent that the claimed invention does not have to be a pharmaceutical to be useful. By way of example, the claimed preparation can be made a part of and used as a device, and particularly a medical device, which may be regarded to as a device that is:

> intended to affect the structure or any function of the body of man
> or other animals, and which does not achieve any of it's primary
> intended purposes through chemical action within or on the body
> of man or other animals and which is not dependent upon being

metabolized for the achievement of any of its primary intended
purposes.

See Exhibit 1 of April 7, 2009. The medical effect of the claimed preparation
applied as a medical device is well shown in the examples given. *See* Example Four on pages
30-33 of the original specification.

    **ii) a preparation does not have to necessarily function via
       receptor binding**

The Examiner further asserts that the claimed preparation must bind to its receptor
to be therapeutically effective. *See* page 3-4 of the Office Action of June 24, 2009. It then
appears that the lack of utility rejection is founded on the Examiner's belief and/or assumption
that an invention must have a conventionally recognized mechanism of action, such as a cell
receptor binding, that must not be contrary to the currently accepted scientific principles, to
satisfy the utility requirement. In fact, Appellant has not suggested that the claimed invention
can only function via cell receptor mediated signaling communication. In fact, as shown in the
Ward Declaration of April 5, 2010, at paragraphs 9 and 10, wherein it is stated that changes in
external environment in proximity to the body cell surfaces may be calculated to elicit a response.
These proposed mechanisms may not have to necessarily work through cell receptor binding or
signaling as contended by the Examiner.

Moreover, and contrary to the Examiner's assertion, there are known substances
capable of exerting activities independently of any receptor binding mechanisms. Examples of
these substances can readily be found in Appellant's original specification. For instance,
metformin as referenced in Example 2 of the Appellant's original specification influences the
insulin receptors, however, there is no suggestion anywhere in current literature that metformin
binds to insulin receptors. *See* also Exhibit 4B of April 5, 2010 which states on page 59 that
metformin impacts on insulin stimulation via intermediary molecular messengers but not directly

on any cellular receptors. *See* also Exhibit 4A of April 5, 2010 which states at page 1705 paragraph 3 that metformin "is excreted unchanged in the urine". Metformin cannot both bind to receptors and be excreted unchanged in the urine. Like metformin, capsaicin as referenced in Example 1 of Appellant's original specification is another example of substances that do not function by binding to a receptor. *See* Exhibit 4C which states at page 229 that capsaicin is well known to influence but not bind to the vanilloid receptor (VR1). The Examiner must use specificity in evaluating these factual findings.

Support for activities without receptor binding can also be found in the published work of *MacKinnon*, previously submitted as Exhibit 5 of April 7, 2009, which shows that sodium is said to have a similar action to potassium i.e. proximity of both these ions to ion channels activates electrical signals. This observation is consistent with what is stated from line 20 on page 15 to line 5 on page 16 "to provide in the air and in the liquid environment of the body an amount of sodium, which appears to indicate a surplus". No binding to receptors is suggested to be involved.

d)   the examiner continues to impermissibly not been receptive to appellant's relevant remarks

In maintaining the rejection, the Examiner continues to have impermissibly not been receptive to Appellant's express assertion of utility. For instance, as stated herein elsewhere, Appellant has stated that the claimed invention is useful for reducing symptoms of and/or for treating disorders associated with medical conditions characterized by blockage of exocrine glands including ducts of sweat glands. *See* paragraphs [0016] and [0017] of Appellant's original application. Blockage of exocrine glands may be related to certain diseases including Miliaria, migraine, and hypertension. *See* lines 14-17 and 23-27 on page 1, lines 8-10 on page 4, and lines 9-10 on page 6 of the original specification.

Without wanting to be limited to any particular theory, it is believed that the

claimed preparation, when placed near to or against one's skin or placed intact in one's body, can be in signaling communication with body's exocrine glands via gases in the surrounding environment and may exert its function via influencing cell signaling and therefore delivering a desirable therapeutic effect without the substance having to be metabolized at all. *See* lines 20-23 on page 16 of the original specification. The communicating gases may include water vapor in the air and residual water vapor retained within the coating layer. In addition, as the coating layer is made aqueous liquid impermeable and hence hydrophobic, water vapor in the air is attracted through the layer.

In fact, one of the benefits provided by the claimed preparation is just to avoid the introduction of pharmaceuticals to enter one's blood circulation. Nearly all drugs in circulation have undesirable side effects at least since drugs in circulation may penetrate areas where they would be harmful, such as across the blood-brain barrier. *See* lines 6-15 on page 18 of the original specification.

In accordance with the above proposed course of action, non-limiting use of the claimed preparation may be to treat and or to reduce symptoms associated with the condition of hypertension in a patient. It is known that hypertension may be manifested by damages to skin capillary cells which are collectively called sweat ducts, a type of exocrine ducts. As a result of the damage, sweat ducts are blocked and life-saving electrolytes are not conserved.
One of the benefits of the claimed preparation is to reduce or clear exocrine duct blockage such that physiologically normal capillary functions may be resumed. Since the capillary cells can regenerate in a period as short as 24 hours, a reduction of symptoms can be realized in an accordingly short period of time.

In certain particular embodiments, the medically efficacious substance is sodium chloride (NaCl) (page 6, lines 11-16), wherein the NaCl is not intended to be released into one's blood stream. In fact, excess intake of sodium chloride rather induces, but not alleviates as is the

case for the Appellant's invention, the onset of hypertension and other metabolic diseases. Rather, NaCl as enclosed within the aqueous liquid impermeable but gas permeable layer is not released into the body and is believed to exert effects via altering surrounding gaseous environment.

It is discovered, according to one or more embodiments of the Appellant's invention, that an environment can be created for the body to sense a surplus of sodium chloride and to reset genetic habitations of the exocrine glands (page 15, lines 20-24). The environment indicating a surplus of sodium chloride can be a gaseous one in the case when the preparation is applied to one's external skin or can be a liquid one in the case when the preparation is placed intact in the gastrointestinal tract (GI tract) for a period of time prior to its fecal excretion (page 16, lines 15-18).

In his 2003 Nobel lecture "Potassium channels and the atomic basis of selective ion conduction," submitted as Exhibit 5 of April 7, 2009, Roderick MacKinnon reported the discovery of the architecture and action of potassium ion (K^+) channels applicable to all fauna, and stated that sodium (Na^+) ion channels work in the same way. These ion channels are found in all cells of the human body and other mammals. It is clear from this his paper that the proximity of a potassium ion to a cell causes electrical activity in the ion channel. One or more embodiments of Appellant's invention allow for sodium chloride and other medically efficacious substances to be placed in close proximity to body cells, and thus ion channels, the sodium chloride or other substances being surrounded by water vapour. Further water vapour, in the case of skin patches, or liquid water, in the case of ingested products, surrounds the coated invention.

In other words, the ion channel recognizes not the ion but the pattern of liquid molecules and particularly water molecules around the ion. So in the instance wherein the claimed preparation is applied as a pill passing through the GI tract in close proximity to epithelial cells causes cell ion channels to open in anticipation of receiving ions, a plurality of

electrical signals can be signified by the pattern changes in the surrounding environment generated by the opening of the ion channels as the pill moves along. Alternatively, in the instance wherein the claimed preparation is applied as the skin patches, there is no movement which is one reason why each of the patches uses two granules on the patch. *See* line 22 on page 11 to line 2 on page 12 of the specification as originally filed. This arrangement provides that dermal ion channels are opened on a flip-flop basis, mimicking of movement achieving the same effect as that of the pill. The activation of ion channels as explained above is a medical effect produced by a substance which is not released. *See* also at line 8 on page 14 to line 23 on page 16 of the specification as originally filed.

B.   *Claim Rejections Under 35 U.S.C. § 112*

Claims 7-11, 24-28, 30-33, and 36-37 stand rejected under 35 U.S.C. § 112, first paragraph for lacking enablement, and second paragraph, for being indefinite. *See* pages 5-9 of the final Office Action. The Examiner bases the rejection substantially for the same reasons asserted in the § 101 utility rejection, namely that a drug not released is effective in producing any medical effect. *See* pages 5-6 of the instant final Office Action, page 5 of the Office Action dated October 5, 2009, and page 5 of the Office Action dated June 24, 2009. Appellant respectfully solicits reversal of this rejection for at least the reasons set forth above and further wishes to state the following.

MPEP 2164.08 in relevant part states that the determination of the propriety of a rejection based upon the scope of a claim relative to the scope of the enablement involves two stages of inquiry; the first is to determine how broad the claim is with respect to the disclosure; the entire claim must be considered; and the second inquiry is to determine if one skilled in the art is enabled to make and use the entire scope of the claimed invention without undue experimentation. In addition, not everything necessary to practice the invention need be

disclosed. *In re Buchner*, 929 F.2d 660, 661, 18 USPQ2d 1331, 1332 (Fed. Cir. 1991). All that is necessary for finding sufficient enablement is that one skilled in the art would be able to practice the claimed invention, given the level of knowledge and skill in the art, the scope of enablement only needs to bear a "reasonable correlation" to the scope of the claims. *In re Fisher*, 427 F.2d 833, 839, 166 USPQ 18, 24 (CCPA 1970). *See* also MPEP 2164.08. A specification disclosure which contains a teaching of the manner and process of making and using those used in describing and defining the subject matter sought to be patented must be taken as in compliance with the enabling requirement of the first paragraph of § 112 unless there is reason to doubt the objective truth of the statements contained therein which must be relied on for enabling support. *In re Marzocchi*, 439 F.2d 220, 223, 169 USPQ 367, 369 (CCPA 1971). Limitations and examples in the specification do not generally limit what is covered by the claims. MPEP 2160.

a)   the claim scope is sufficiently narrow

As stated herein elsewhere, independent claim 24 concerns a preparation for use as a medicament, comprising a medically efficacious substance coated with an aqueous liquid impermeable but gas permeable layer for surrounding and preventing release of the medically efficacious substance, wherein the layer contains a ceramic, a clay, an inorganic non-metallic material, a polymer, a natural wax, a perforated stainless steel, or beeswax hardened with cornstarch and talc. In particular, the claim scope is sufficiently narrow at least to the extent of the coating layer of the claimed preparation is not just of any material but material that is aqueous liquid impermeable and gas permeable, wherein the coating layer is of certain specified categories – ceramic, clay, inorganic non-metallic material, polymer, natural wax,, perforated stainless steel, or beeswax hardened with cornstarch and talc.

b)   the claimed invention can be made and used without undue
        experimentation

One example of the coating layer used in the claimed preparation is a wax matrix, which is inherently gas permeable. *See* lines 21-22 on page 20 of the original specification. The gas permeability of the illustrated wax matrix coating layer is well known in the art such that there involves no undue testing. The gas permeability property inherent to the wax matrix has many known extended uses, including to make fabrics breathable and to preserve freshness of citrus fruits by allowing ingress of air oxygen. These assertions have been addressed herein above, which are not reproduced for brevity. In brief, the claimed preparation does not have to be a pharmaceutical, nor does the claimed preparation depend on release of the encapsulated substance to be released for therapeutic action. In one example, the encapsulated substance can function via effecting surrounding environment and inducing changes in the vicinity.

Another example of the coating layer used in the claimed preparation is beeswax hardened with cornstarch and talc. *See* lines 1-2 on page 9 of the original specification. The information given at lines 11-22 on page 20 is ample for any person skilled in the art to manufacture the invention. It will be apparent to anyone skilled in the art that the coating can firstly be made and tested. There are only two parameters, namely the quantity of cornstarch and talc to be used. A set of samples can be set up with incremental increases in the amounts of talc and cornstarch until it is estimated that the wax is just sufficiently hardened to prevent dissolution. The set of coatings can then be applied to the active with the excipient ratio as given at lines 11-22 on page 20 of the original specification at between 20% and 45% by weight. The resulting samples may then be tested as described at lines 5-10 on page 21 of the original specification. For a person skilled in the art, the number of samples is unlikely to exceed ten in number, and the entire experimentation is unlikely to exceed 12 hours bench time plus the 27 hours liquid impermeability testing mentioned herein elsewhere.

Yet another example of the coating layer used in the claimed preparation is a polymer. *See* lines 26-27 on page 19 and lines 23-24 on page 20 of the original specification. The attached "Permeation of Gases and Vapours in Polymers" from the textbook "Polymer Permeability" ed. J. Comyn (Springer, 1985), previously submitted as Exhibit 2 of April 7, 2009, explains at pages19-20 the reason that polymeric materials are inherently gas permeable.

In "Diffusion in and Through Polymers" (Wolf R. Vieth, 1991 Oxford University Press), previously submitted as Exhibit 3 of April 7, 2009, is stated "[I]n strong contrast to gas penetration, polymer membranes may be highly swollen by a penetrating liquid, and their properties thus altered." The whole of the introduction to this book makes it clear that polymers are inherently gas permeable, and the quoted sentence illustrates that it is not difficult to ascertain by examination whether or not the polymer has been penetrated by water and swollen as a result. The sentence shows the clear difference between a membrane which has been hardened so as not to allow the passage of water but to only permit the passage of gas, and a membrane which has not been hardened so that liquids can pass.

"Tuning Nanoscopic Water Layers on Hydrophobic and Hydrophilic Surfaces with Laser Light" by Andrei P. Sommer, *et al.*, previously submitted as Exhibit 4 of April 7, 2009, shows the way that nanoscopic interfacial water vapor permeates through the surface of hydrophobic materials, such as hardened polymers.

Moreover, U.S. Patent 5827538 "Osmotic Devices Having Vapor-Permeable Coatings", as cited by the Examiner, illustratively teaches that water vapor, which is a gas, permeates the polymer layers. This occurs naturally from atmospheric water vapor. No pressure, device or procedure is needed to have the water vapor permeate the layers. The wax or other polymer coating of the claimed preparation is permeated with water vapor and, in the case of sodium chloride, the sodium chloride within the coating is surrounded by water vapor. Sodium chloride does not dissolve in gas, only in liquid. The coating layer prevents ingress of liquid or

egress of NaCl.

Using commercially available polymers is also simple. For example Eudragit RS 30 D is a well known polymethacrylate resin used for coating tablets, including controlled release tablets. *See* the previously submitted Exhibit 7 of April 7, 2009. The manufacturers (EVONIK Röhm GmbH, Pharma Polymers, Darmstadt, Germany) specify the addition of 6% of Triethyl Citrate to the resin in water. The manufactures specify a number of tests, well known to those in the art, for testing for film formation. In the case of the instant invention the only remaining parameter for successful non-dissolution of a coated substance is the amount of hardener to be added to the coating solution. Talc is a suitable hardener and is well known to be used as such. 25% to 30% by weight is a suitable amount of talc and it is unlikely that a formulation scientist would take more than a day to arrive at a value within this ratio. In the case of the Eudragit polymer plus talc as above, the addition of the talc hardening the polymer prevents the liquid water uptake, but the polymer retains its inherent property, permeability to gas (in this case water vapour), as is well known to any person skilled in the art.

The claimed invention can be used as a medical device. The examples given in the original specification are adequate to show the medical effect of the devices and to fully inform anyone skilled in the art in their formulation. The original specification at lines 5-10 on page 21 illustratively describes the testing needed to be done. Unlike those in the art wherein making pharmaceuticals are concerned with many parameters including dissolution, absorption, bioavability, metabolisation, elimination and so on, requiring extensive experimentation and therefore explanation and direction, these considerations do not necessarily apply to Appellant's invention. The encapsulated medically efficacious substance is not released or dissolved and is eliminated intact.

Therefore, contrary to the Examiner's assertions, the making and using of the present invention is well enabled by the original specification in view of what was known in the art at the time of invention.

The Appeal Brief fee of *$270.00* and Petition Fee of *$65.00* is being charged to Deposit Account No. 02-3978 via electronic authorization submitted concurrently herewith. The Commissioner is hereby authorized to charge any additional fees or credit any overpayments as a result of the filing of this paper to Deposit Account No. 02-3978.

Respectfully submitted,

WARREN WARD

By: /Junqi Hang/
Junqi Hang
Registration No. 54,615
Attorney for Appellant

Date: December 9, 2010

BROOKS KUSHMAN P.C.
1000 Town Center, 22nd Floor
Southfield, MI 48075-1238
Phone: 248-358-4400
Fax: 248-358-3351

Enclosure - Appendices

VIII. CLAIMS APPENDIX

7.   The preparation of claim 30, wherein said substance is sodium chloride.

8.   The preparation according to claim 7 wherein the agent is a ceramic, a polymer or a natural wax.

9.   The preparation according to claim 7 wherein the agent encapsulates sodium chloride to form a sphere.

10.   The preparation according to claim 9 wherein the sphere is of a diameter between 1 mm and 10 mm.

11.   The preparation according to claim 9 wherein the sphere comprises sodium chloride crystals coated with beeswax hardened with cornstarch and talc.

24.   A preparation for use as a medicament, comprising a medically efficacious substance coated with an aqueous liquid impermeable but gas permeable layer for surrounding and preventing release of the medically efficacious substance, wherein the layer contains a ceramic, a clay, an inorganic non-metallic material, a polymer, a natural wax, a perforated stainless steel, or beeswax hardened with cornstarch and talc.

25.   The preparation according to claim 24, in a form selected from the group consisting of: a pill, a tablet, a lozenge, a bolus, a capsule, a caplet, a granule, a nanoparticle, and a microparticle.

26.   The preparation according to claim 25, being in granular, nanoparticle or

microparticle form selected from the group consisting of: a suspension, a cream, and a paste.

27.   The preparation according to claim 24, prepared for use with a patch for holding said preparation near to or against the skin of a patient.

28.   The preparation according to claim 24, prepared for implantation into the body of a patient.

30.   The preparation according to claim 24, wherein said substance is selected from the group consisting of: sodium chloride, capsaicin, metformin, salicylic acid, and a derivative of salicylic acid.

31.   The preparation according to claim 24, wherein said substance is selected from the group consisting of; a substance endogenous to the body, a food substance, a plant material, and a drug.

32.   The preparation according to claim 24, combined with a preparation of at least one ingredient designed for delivery into solution.

33.   The preparation according to claim 24 combined with a preparation of at least one ingredient designed for delivery into solution for a therapeutic purpose.

36.   The preparation of claim 24, wherein the layer contains a wax in an amount of between 20% and 45% by weight of the preparation, a ceramic, or combinations thereof.

37.   The preparation of claim 24, prepared for use with a patch for holding said preparation near to or against the skin of a patient, wherein the aqueous liquid impermeable but

gas permeable layer encapsulates the medically efficacious substance to form a pair of spaced apart spheres each having a diameter of between 1 mm to 10 mm, and wherein the aqueous liquid impermeable but gas permeable layer comprises a beeswax hardened with cornstarch and talc.

IX. EVIDENCE APPENDIX

Exhibits	Key Term(s)	Entered for Record Per the Office Action of
Exhibit 1 of April 7, 2009	medical device	June 24, 2009
Exhibit 2 of April 7, 2009	permeation of gases and vapors in polymers	June 24, 2009
Exhibit 3 of April 7, 2009	diffusion in and through polymers	June 24, 2009
Exhibit 4 of April 7, 2009	turning nanoscopic water layers on hydrophobic and hydrophilic surfaces with laser light	June 24, 2009
Exhibit 5 of April 7, 2009	potassium channels and the atomic basis of selective ion conduction, by MacKinnon	June 24, 2009
Exhibit 7 of April 7, 2009	specification and test methods for Eudragit RL 30D	June 24, 2009
Ward Declaration of April 5, 2010	declaration under rule 1.132	June 23, 2010
Exhibit 1 of April 5, 2010	letter of Dr. Steve Gittins	June 23, 2010
Exhibit 2 of April 5, 2010	letter of Dr. Paola Gulden	June 23, 2010
Exhibit 4A of April 5, 2010	insulin, oral hypoglycemic agents, by Goodmans	June 23, 2010
Exhibit 4B of April 5, 2010	Metformin modulates insuling post receptor signaling transduction in chronically insulin-treated Hep G2 cells, by Li et al.	June 23, 2010

| Exhibit 4C of April 5, 2010 | the endogenous lipid anandamide is a full agonist at the human vanilloid receptor, by Smart et al. | June 23, 2010 |

X. RELATED PROCEEDINGS APPENDIX

None.

EXHIBIT 1

of April 7, 2009

FDA Home Page | CDRH Home Page | Search | A-Z Index

Questions?

III VII IIIVII I

Device Advice Home   CDRH Home | Comments
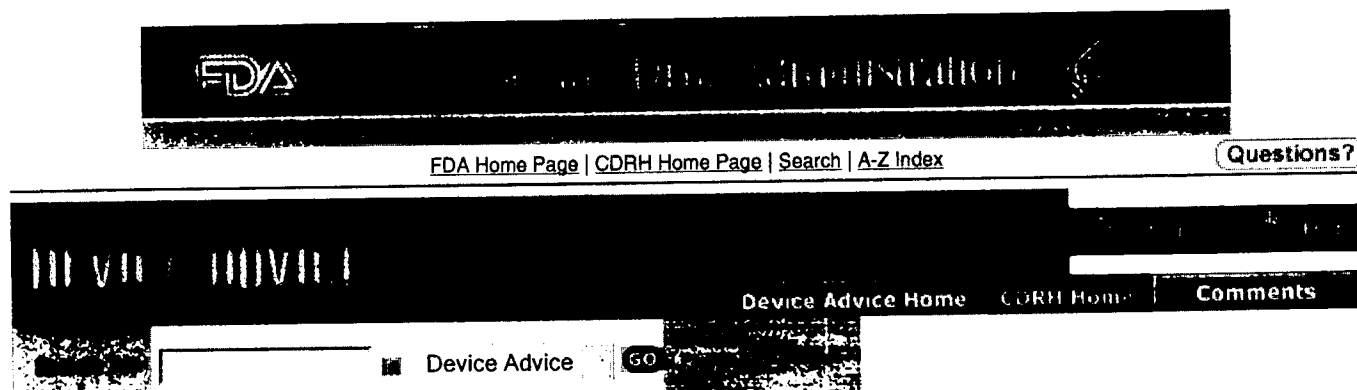
■ Device Advice   GO

CDRH > Device Advice > Is The Product A Medical Device

Please note: as of October 1, 2002, FDA charges fees for review of <u>Premarket Notification 510(k)s</u> and <u>Premarket Approvals</u>

Is The Product A Medical Device?

- Introduction
- Medical Device Definition
- Getting to Market with a Medical Device
- Other FDA Components

Introduction

Determine if your product meets the Definition of a device. If it does, there are FDA requirements that apply. First, see the definition below.

Medical Device Definition

Medical devices range from simple tongue depressors and bedpans to complex programmable pacemakers with micro-chip technology and laser surgical devices. In addition, medical devices include in vitro diagnostic products, such as general purpose lab equipment, reagents, and test kits, which may include monoclonal antibody technology. Certain electronic radiation emitting products with medical application and claims meet the definition of medical device. Examples include diagnostic ultrasound products, x-ray machines and medical lasers. If a product is labeled, promoted or used in a manner that meets the following definition in section 201(h) of the Federal Food Drug & Cosmetic (FD&C) Act it will be regulated by the Food and Drug Administration (FDA) as a medical device and is subject to premarketing and postmarketing regulatory controls. A device is:

- "an instrument, apparatus, implement, machine, contrivance, implant, in vitro reagent, or other similar or related article, including a component part, or accessory which is:
  - recognized in the official National Formulary, or the United States Pharmacopoeia, or any supplement to them,
  - intended for use in the diagnosis of disease or other conditions, or in the cure, mitigation, treatment, or prevention of disease, in man or other animals, or
  - intended to affect the structure or any function of the body of man or other animals, and which does not achieve any of it's primary intended purposes through chemical action within or on the body of man or other animals and which is not dependent upon being metabolized for the achievement of any of its primary intended purposes."

This definition provides a clear distinction between a medical device and other FDA regulated products such as drugs. If the primary intended use of the product is achieved through chemical action or by being metabolized by the body, the product is usually a drug. Human drugs are regulated by FDA's Center for Drug Evaluation and Research (CDER). Biological products which include blood and blood products, and blood banking equipment are regulated by FDA's Center for Biologics Evaluation and Research (CBER). FDA's Center for Veterinary Medicine (CVM) regulates products used with animals. If your product is not a medical device but regulated by another Center in the FDA, each component of the FDA has an office to assist with questions about the products they regulate. In cases where it is not clear whether a product is a medical device there are procedures in place to use DSMICA Staff Directory to assist you in making a determination.

Check the Precedent Correspondence (Previous decisions on products) for information on a related product that may assist

you in determining the requirements you need to consider for your product.

Updated February 28, 2002

Choose another topic: Select a topic

● Accessibility   ✗ Disclaimer

CDRH Home Page | CDRH A-Z Index | Contact CDRH | Accessibility | Disclaimer
FDA Home Page | Search FDA Site | FDA A-Z Index | Contact FDA | HHS Home Page

Center for Devices and Radiological Health / CDRH

EXHIBIT 2

of April 7, 2009

Chapter 2

Permeation of Gases and Vapours in Polymers

C. E. ROGERS

Department of Macromolecular Science, Case Western Reserve University, Cleveland, Ohio, USA

1. INTRODUCTION

The solution and transport behaviour of low molecular weight substances in polymeric materials is a topic of interest for many fields of science and technology. The importance and relevance of such behaviour has become more apparent in recent years with the accelerating development of separation membrane systems, highly impermeable or selectively permeable packaging or barrier films, and the overall increase in the use of polymeric materials for diverse applications with consequent exposure to various environmental agents.

The selection or development of polymeric materials for use in applications with stringent design specifications relating to their solution and transport behaviour requires knowledge and appreciation

diffusion behaviour, often observed in biological systems, is related to the directional flux effects observed in systems with a polymer membrane possessing a gradient of chemical composition,[1]-[46] or temperature, or stress, or other variable which affects diffusion in terms of irreversible thermodynamics.

The transport of a penetrant through a homogeneous membrane, in the absence of gross defects such as pores or cracks, is usually considered to occur by the following process: solution (condensation and mixing) of the gas or vapour in the surface layers, migration to the opposite surface under a concentration (chemical potential) gradient, and evaporation from that surface into the ambient phase. The migration of the penetrant can be visualised as a sequence of unit diffusion steps or jumps during which the particle passes over a potential barrier separating one position from the next.

The unit diffusion or jump involves a cooperative rearrangement of the penetrant molecule and its surrounding polymer chain segments. It is not necessary that a 'hole' per se be formed in the polymer structure between two successive penetrant positions (although this is often the basis for model calculations); the penetrant molecule and its surrounding chain segments may share some common volume before and after the diffusion jump. However, a certain number of van der Waals type or other interactions between the component molecules and chain segments must be broken to allow a rearrangement of the local structure. The amount of energy required for this rearrangement (or 'hole formation') will increase as the size and shape of the penetrant molecule increase. Several jumps may need to occur in the same direction before the molecule has been displaced by a distance equal to its size.

This process requires a localisation of energy to be available to the diffusing molecule and its polymer chain segment neighbours to provide the energy needed for rearrangement against the cohesive forces of the medium with effective movement of the penetrant for a successful jump. In a polymer above its glass temperature, as in simple liquids, fluctuations in density ('holes') are constantly disappearing and reforming as a result of thermal fluctuations. Low density regions resulting from an outward expansion of chain segments from a central point can be associated with a localised accumulation of energy causing the expansion.

Diffusive motion thus depends on the relative mobilities of penetrant molecules and polymeric chain segments as they are affected by

changes in size, shape, concentration, component interactions, temperature and other factors which affect polymeric segmental mobility. Since diffusion requires rearrangement of the relative molecular conformations within a mixture, the behaviour is closely related to the rheological and mechanical properties of the solid in the presence of penetrant. In many cases, relatively long-term relaxation processes may delay the rate of approach to equilibrium with consequent marked effect on concurrent diffusion and solution behaviour.

Studies of concurrent solution/diffusion and stress relaxation or creep in a given system can be used to advantage for elucidating the nature of polymer chain segmental motions as they affect both viscoelastic and transport behaviours.[4,47-50] However, it must be emphasised that the molecular and segmental motions are somewhat different for the two processes, especially when diffusion is compared with the bulk viscosity of the polymer. For the diffusion of small molecules only relatively local coordination of segmental motions are involved. In viscous flow processes, there is an actual displacement of polymer molecules requiring more coordination of these segmental motions. The two processes utilise different spectra of the distribution of segmental motions (or free volume fluctuation distribution). It is to be expected that any correlation between the processes will be closer for low penetrant concentrations or large-size penetrants where the segmental motions involved in the two processes are more nearly equivalent.

The overall transport process in a polymer therefore depends on two major factors which, in turn, are governed by a wide variety of factors related to composition, fabrication and experimental conditions. One factor is polymer chain segmental mobility and the other is defect structures, such as voids, microcracks and other non-thermodynamic variations in polymer structure and morphology. Defect structures are usually difficult to either define or characterise, but their effect on transport and solution behaviour can be profound. Gross defects, such as pinholes and cracks, are of great experimental concern but are not to be considered here since their effects on transport are overwhelming and usually obvious to the investigator—the film leaks profusely. It is the smaller defects which give more subtle, but important, contributions to the overall transport and solution processes that we need to consider. These include spherulitic and lamellar boundary regions in semi-crystalline polymers and permanent or transient voids (excess free volume, 'frozen holes', etc.) found in glassy polymers.

EXHIBIT 3

of April 7, 2009

1

OVERVIEW

1.0 INTRODUCTION

In recent years, there has been a rapid increase in the number and variety of challenges and opportunities facing practitioners of chemical engineering and applied chemistry in the areas of permeability-controlled devices and processes. Conventional techniques are insufficiently flexible or too costly in many cases, and advanced processes are being developed to meet new needs.

One of the most interesting of the applications of the principles of *diffusion in and through polymers* is the use of selective permeation through membranes to effect separations. Two aspects of the field logically emerge and are addressed here: the basic nature of the transport process itself and the engineering factors important in achieving successful designs, varying from small-scale appliances to large-scale industrial operations. The former has been accorded considerable attention in the published literature, and the latter is being given increasing attention. One purpose of this book, then, is to examine the present state of the art with respect to interrelated scientific and engineering aspects, expanding the latter to include consideration of bioprocess applications, such as those encountered with biosensors, controlled release, and bioreactors.

In order to understand the mechanisms of transport in the various polymers of interest, it is useful to consider features of the two principal microstructural conditions of polymeric materials: the glassy and rubbery states. In the glassy state, a polymer is hard and may be brittle, these properties being intimately related to restricted polymer chain mobility. Rotation about the chain axis is limited and motion within the structure is largely vibratory within a frozen quasi-lattice. Polymers of this type are very dense structures, with very little internal void space (ca. 2 to 10%). Hence, it is not surprising that penetrant diffusivities through such a structure are low but that discrimination between penetrants on the basis of size is excellent. Glassy behavior is

2 Diffusion In and Through Polymers

associated with chain stiffness, strong intermolecular forces between backbone chains, and the presence of bulky side groups.

In contrast, polymers in the rubbery state typically are tough and flexible, with such properties associated with freer chain motion. In this case, larger segments are thought to participate in the diffusion process due to internal micromotions of chain rotation and translation, as well as vibration. Basically, then, a larger amount of free volume in which diffusion may take place is more readily accessible.

In both glassy and rubbery states, these properties can be further modified by the presence of a crystalline phase, or by stress-induced orientation. Both crystallization and orientation tend to place additional constraints on the mobility of the amorphous phase through which diffusion takes place. Also, the crystalline phase is usually impermeable, which results in longer and more tortuous diffusion paths.

Focusing for a moment on the topic of glassy polymers per se, their inherent versatility places them among the most important materials of the present time. As a result, scientific and technological investigations involving the triadic relationship between structure, property and function, or application, for polymeric glasses have increasingly become a common mode for research workers. As has been observed, the behavior of the properties of a polymeric material at a temperature below the glass transition region can be quite complex and also rather unique. Much of this pattern has been ascribed to the nonequilibrium nature of the structurally-arrested glassy state, with properties generally and appropriately characterized as history-dependent and time-dependent.

From a practical point of view, a better understanding of the nonequilibrium molecular characteristics of the glassy state and their effects on the properties and applications of glassy polymers is deemed crucial in improving the predictability of the performance of a material to optimize its end-uses. From a theoretical point of view, deeper understanding will assist in consolidating the framework required for the attainment of a unified picture of the glassy state and a sound theory or model capable of fully describing its complex behavior. Hence, the inherent nonequilibrium structure of the glassy state and its effects on the properties and functions of glassy polymers continues to be of lively interest to researchers, as will become apparent throughout this book.

It is generally not such a simple task to select the appropriate types of experiments whose results will impart meaningful understanding regarding the intimate link between structural changes and the direct consequence involving a certain property, functionality or prac-

tical application. This link or interrelationship may often seem somewhat ambiguous, for a variety of properties and practical end-uses. The difficulty is further compounded by the relative paucity of analytical means to examine the microstructure of an amorphous polymeric material per se, or at least to detect a structural change at the microscopic level. Conventional and available experimental techniques such as x-ray analysis are sometimes not of major benefit, other than to show that the material is free of crystallites, confirming the assumed amorphous structure. It is encouraging to note that sophisticated resonance techniques such as NMR or ESR (electron-spin resonance) are coming into play for the elucidation of the interaction of penetrants with glassy polymer microstructures. Mikhailov and Kuzina (1990) observed what they termed micro- and macro-diffusion in polystyrene, related to the kinetic inhomogeneity of the matrix which resulted in a wide spectrum of activational barriers (ca. 5-20 kcal/mol). Cain et al. (1989) employed NMR spin relaxation experiments to show that the translational diffusion coefficients of CO_2 in silicone rubber have a wide distribution, and the self-diffusion coefficients span a range of nearly four orders of magnitude (10^{-10} to 10^{-6} cm^2/s) at ca. 300K. The small fraction of the CO_2 with diffusion coefficients of 10^{-6} to 10^{-4} cm^2/s apparently reflects those channels suitable for rapid transport of CO_2 through the rubber. In studies of Xe diffusion in bisphenol A polycarbonate, a distribution of relaxation times arising from the inhomogeneous character of the polymeric matrix is observed. Ohno and Suzuki (1986) have applied broad-line NMR spectroscopy to develop a new quantitative parameter, $(\Delta H^2)_{inter}$, to describe the packing state of polymers. In this way, the intermolecular terms of the second moment are found to correlate well with membrane gas permeability coefficients.

ficients.

As has been pointed out in a host of more recent studies within the last decade, the nonequilibrium nature of the glassy state may be surfacing or mechanistically pertaining in the behavior of a polymer throughout its existence. Thus, the perturbation may well be occurring either during a processing cycle or within the service lifetime of a polymer. Besides thermal annealing, other types of perturbations such as static mechanical pressure, tensile strain, or even exposure to a gaseous substance could result in - or could lead to - a complex response which may in fact be a nonequilibrium or glassy one. The specific manner whereby a disturbance is introduced could also play an important role.

The effects of exposure of glassy polymers to small molecules are of particular interest to chemical engineers, since many of their in-

4 Diffusion in and Through Polymers

volvements with polymer applications include sorption and transport of permanent gases. For instance, Langsam and Robeson (1989) recently reported on the effects of oxygen partial pressure and temperature on the lifetime of polymer films used in gas separation processes studied by a combination of test procedures based on thermogravimetric analysis and mechanical properties. The use of commercial antioxidants increased the temperature at which the film was usable in a separation process. The decline in permeability during accelerated aging was associated with a chain scission process and an embrittlement of the film. The lifetime of the protected films at ambient conditions (25°/170 mm O_2) was greater than five years. The flux decline was due to the contamination of films with hydrocarbon vapor. Water vapor had no effect on the permeabilities or the selectivity of the gas pair, O_2/N_2, in surface-fluorinated polymer films.

Indeed, the examination of sorption and transport properties of small molecules in polymeric materials has long been known to be a promising means to progress toward the goal of a unified concept along one main avenue. Having already obtained a reasonable degree of success in interpreting the microstructure of semicrystalline and glassy polymers via these properties, the use of small molecules as micro-structural probes is being more and more enthusiastically adopted by chemical engineers and chemists who are involved in applied research on polymeric materials, in search of polymer microstates with superior membrane selection and/or retention properties for industrial and bio-medical applications. In following the advances which have been achieved by these workers, the transport portion of the ultimate triadic relationship appears to be naturally attainable since many of the prac-tical applications and end-uses of glassy polymers involve sorption and transport of small molecules as fundamental processes. These include a wide variety of applications, ranging from small scale uses such as packaging materials for consumer products and protective coatings, to large scale industrial processes such as permselective membranes for gas separations (Dao, 1989).

1.1 GAS PERMEATION

In the permeation of non-condensible gases in polymeric membranes, equilibrium levels of gas sorption in the solid are low because interactions between solute molecules and the polymer are weak. Diffusion constants are independent of penetrant concentration in the membrane. Application of Fick's law and Henry's law results in a

transport equation in which the flux rate is given by the product of a new constant, the permeability, and the partial pressure gradient across the membrane. In this case, the permeability is the product of the diffusivity and the Henry's law constant. It has been found that the permeability varies with temperature according to an Arrhenius-type equation. The apparent activation energy for permeation is the sum of a diffusion activation energy and the enthalpy of solution, each in turn related to the temperature dependence of diffusivity and solubility.

Because of limited polymer chain mobility, penetrant molecular size and shape are important parameters in determining the diffusion coefficient. Indeed, it is this capacity of a polymeric membrane to discriminate between penetrants with subtle steric differences that contributes significantly to membrane selectivity and ultimate value in a separations process. A second important factor is the chemical similarity between penetrant and polymer. The qualitative solubility rule of "like dissolves like" is obeyed. Thus, gas molecules which have a solubility parameter close to that of the membrane material will tend to be more soluble, possibly resulting in higher fluxes.

Where specific interactions between penetrant and polymer become important, such as when hydrogen bonding is involved, the relationship among diffusivity, solubility, and measured permeability is more complicated. Permeation of solvating vapors, such as, for example, water in ethyl cellulose and many hydrocarbons in polyethylene, shows a concentration dependence of both diffusivity and solubility.

1.2 LIQUID AND VAPOR PERMEATION

Liquid permeation involves the solution of liquid at the upstream face of the membrane, followed by diffusion through the membrane, and desorption from the downstream face. In strong contrast to gas permeation, polymer membranes may be highly swollen by a penetrating liquid, and their properties thus altered. For liquids in polymers, sorbed volumes can be 10 to 20% or even higher, compared to gas-polymer systems where sorbed volumes are vanishingly small in most cases. Thus, liquids open up the structure, with the result that the absolute flux rates through the membrane can be 2 to 3 orders of magnitude higher for a liquid than for a noncondensible gas.

However, similar ideas which are useful in describing the "ideal" behavior of gas-polymer solutions can be modified to describe the liquid permeation process. The transport equation is again based on

6 Diffusion Is and Through Polymers

Fick's law but diffusion coefficients are strong functions of concentration (typically exponential). Since the driving force is the concentration of dissolved liquid, liquid solubility in the polymer brings in the relationship between chemical structure of penetrant and membrane.

Diffusion constants, apart from their concentration dependence, also depend on molecular size and shape, and as in gas permeation, crystallinity and orientation have important effects on the transport process. In the presence of a swelling liquid, crystalline polymer membranes actually undergo structural rearrangements as a result of the interactions between penetrant and polymer. At these levels of sorption, sufficient liquid is present within the polymer phase to depress the melting point of crystals, and thus generate changes in the crystalline size and texture of an organic polymer. In fact, this process can be used to advantage to "tailor" membranes and a body of literature has developed from attempts to increase the selectivity of membrane separation by such methods.

1.3 REVERSE OSMOSIS

In a closed system with pure solvent separated from a solution by a membrane permeable to solvent only, solvent will flow into solution in the direction of decreasing solvent activity by a process known as osmosis. If the activity of solvent in solution is raised above its level in the pure state at one atmosphere, such as by application of hydrostatic pressure, net solvent flow will proceed from solution to pure solvent, a process which has been named reverse osmosis. Thus, applying a hydrostatic pressure in excess of the osmotic pressure to an aqueous salt solution in contact with a hydrophilic membrane will result in

Author:
Prof. Wolf R. Vieth
College of Engineering, Rutgers University, Piscataway NJ 08854 USA

EXHIBIT 4

of April 7, 2009

635

Tuning Nanoscopic Water Layers on Hydrophobic and Hydrophilic Surfaces with Laser Light

Andrei P. Sommer,*,† Arnaud Caron,† and Hans-Joerg Fecht†,‡

Institute of Micro and Nanomaterials, University of Ulm, 89081 Ulm, Germany, and Institute for Nanotechnology, Forschungszentrum Karlsruhe, 76021 Karlsruhe, Germany

The evolutional function of ordered interfacial water near solid surfaces was postulated by Szent-Györgyi: "Life actually, may have started with building these water structures." Here we report their tunability with laser light on both hydrophobic and hydrophilic surfaces. On the former, the light caused their depletion—on the latter, an increase in fluidity—as measured by atomic force acoustic microscopy. Interfacial water layers play a key role in cellular recognition. Their tunability promises to revolutionize various fields in biomedical engineering and life sciences.

The biochemical and biological implications of ordered nanoscopic water layers are enormous. Presumably, they not only mask proteins, thereby modifying their reactivity,[1] but also play the role of informational blueprints in first contact events in cell–cell and cell–material contacts.[2] One of the pioneering investigations indicating the prevalence of ordered nanoscopic water layers on solid surfaces exposed to air has been conducted exemplarily on hydrophobic polymers.[3] By using a near-field scanning optical microscope (NSOM), it was shown that the profile of the water layer adsorbed onto a translucent polymer film could be instantly modulated by 670 nm laser light, applied at an intensity as low as the solar intensity (1000 W m^{-2}) (i.e., the sample was thinner in response to its irradiation). Considering that water is practically transparent to 670 nm light, it was concluded that the resonant laser energy induced fluctuations in the fraction of the water molecules that are partially immobilized in the near-field substrate and thereby ordered.[4] In our earlier experiment, irradiation of the polymer film and simultaneous NSOM were conducted collinearly (normal to the surface of the sample), restricting the approach to translucent samples. The configuration employed here allows us to probe nanoscopic water layers even on samples that are not transparent (e.g., silicon wafers). In particular, the laser irradiation and simultaneous probing of the near-field responses occurred on the same side of the samples—irradiation by a 670 nm laser (power 0.8 mW, local intensity 50 W m^{-2}) and recording resonance spectra via atomic force acoustic microscopy (AFAM).[5] AFAM (Fries Research & Technology, Germany) was carried out under ambient conditions (dim light, temperature 24 °C, relative humidity 61%) by sweeping the frequency in the range of 160 to 230 kHz. It is worth mentioning that with 50 W m^{-2} the applied laser intensity was extremely low: the intensity of a laser pointer of a 1 mW laser (beam Ø ≈ 1 mm) is on the order of 1.3 kW m^{-2}.

Figure 1 shows the basic components of the AFAM experiment and illustrates its principle. The method consists of performing contact mode atomic force microscopy (AFM) on a sample that is mounted on an ultrasonic transducer. Specific contact resonance spectra with typical amplitudes smaller than 1 nm are obtained
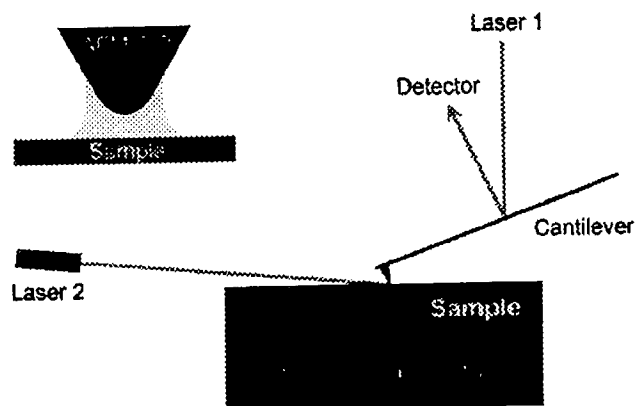

Figure 1. AFAM consists of performing contact mode AFM on an ultrasonically excited sample. The tip–sample interface is irradiated with a 670 nm laser (laser 2) at an angle of incidence of 11.5°. The experimental setup permits the detection of nanoscopic water layers on ultrasmooth substrates. The inset shows the nanoscopic water layer acting as a damping element between the AFM tip and sample.

by recording the vibrational amplitude of the AFM cantilever as a function of the corresponding ultrasonic excitation frequency.

In the simplest model interpreting the coupling between the AFM tip and sample surface, the tip–sample interaction is described in terms of the classical single spring constant, representing the system's contact stiffness.[6] At moderate oscillations, the resonance curves become symmetric, and changes in the resonance amplitude become manifest. Traditionally, the variation experienced by the oscillating AFM tip is expressed in terms of the quality factor (Q factor), which is inversely proportional to the damping. At resonance, the Q factor is proportional to the vibrational amplitude and can be calculated by dividing the resonance frequency ν_{res} by the half width Δ of the resonance curve: $Q = \nu_{res}/\Delta$. When AFAM is performed at constant resonance frequency and constant excitation amplitude, the resonance amplitude is proportional to the Q factor and inversely proportional to the damping. In general, the resonance amplitude increases with increasing stiffness of the surface.[7] From this perspective, we can expect that nanoscopic water layers adhering to both the sample and tip (hemispherical approximation) and penetrating into the interface (inset of Figure 1) would act

* Corresponding author. E-mail: samoan@gmx.net.
† University of Ulm.
‡ Forschungszentrum Karlsruhe.
(1) Szent-Györgyi, A. *Perspect. Biol. Med.* **1971**, *14*, 239–249.
(2) Sommer, A. P. *J. Phys. Chem. B* **2004**, *108*, 8096–8098.
(3) Sommer, A. P.; Franke, R. P. *Nano Lett.* **2003**, *3*, 19–20.
(4) Sommer, A. P.; Pavlath, A. E. *Cryst. Growth Des.* **2007**, *7*, 18–24.
(5) Rabe, U.; Janser, K.; Arnold, W. *Rev. Sci. Instrum.* **1996**, *67*, 3281–3293.

(6) Hurley, D. C.; Kopycinska-Müller, M.; Kos, A. B.; Geiss, R. H. *Adv. Eng. Mater.* **2005**, *7*, 713–718.
(7) Rabe, U.; Amelio, S.; Kester, E.; Scherer, V.; Hirsekorn, S.; Arnold, W. *Ultrasonics* **2000**, *38*, 430–437.
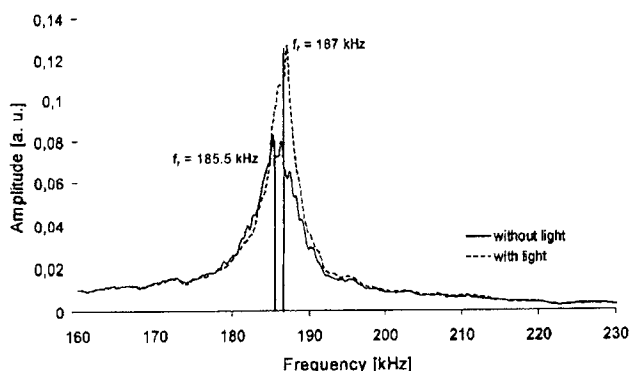
Figure 2. Acoustic atomic force microscopy on polystyrene (hydrophobic), without and with a 670 nm laser. The Q factors for the resonance curves indicate the presence of a water layer between the tip and substrate, which can be tuned by the laser light. The Q factor changed from 26.5 to 39.3, from dim light to laser irradiation, respectively.
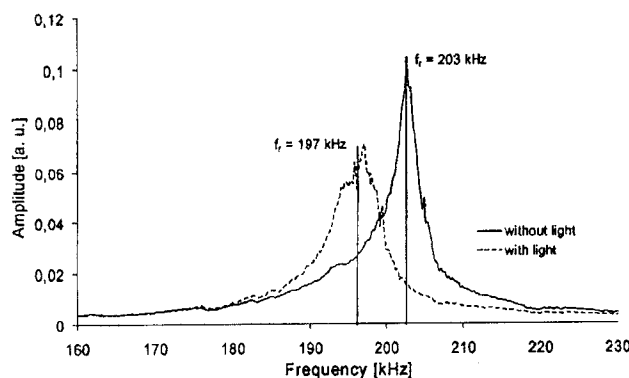

Figure 3. Acoustic atomic force microscopy on silicon (hydrophilic), without and with a 670 nm laser. The Q factors for the resonance curves indicate that there is a more pronounced damping of the tip when the laser is on (cf. Figure 2). The Q factor changed from 34 to 24.5, from dim light to laser irradiation, respectively.

as a damping element operating as a film between the tip and substrate and as a collar around the tip, thereby softening the contact. Consequently, depletion of the damping element would increase the contact stiffness.

Indeed, this is exactly what we observed in the present study. Figure 2 is representative of the resonance behavior on a hydrophobic sample (cover of a polystyrene Petri dish), without and with laser irradiation, confirming our earlier result:[3] $Q_D <$ Q_L, where Q_D and Q_L stand for the Q factor without and with laser irradiation of the tip—sample interface, respectively. For the measurements, we used a single-crystal silicon tip mounted on a soft cantilever (0.2 N m^{-1}) and applied a loading force of 5 nN. Next, we investigated the resonance behavior on hydrophilic samples. Interestingly, it was opposite to that found on hydrophobic samples. Figure 3 shows a measurement on a (100) silicone wafer (loading force 10 nN). The Q factors calculated for the resonance curves in Figure 3 indicate that laser irradiation increased the damping in the space between the tip and substrate, expressed in terms of the Q factors: $Q_D > Q_L$.

The increase in damping following laser exposure can be explained on the basis of recent AFM experiments performed in air, which indicated an extremely increased viscosity of interfacial water confined in the space between a hydrophilic tip (Si) and hydrophilic substrates.[8-10] It is probable that this increase (compared to that of bulk water and water layers on hydrophobic

surfaces) is simply due to ordered water layers that are thicker on hydrophilic surfaces than on hydrophobic ones.

A qualitative description of viscosity is resistance to flow. Thus, the effect of the applied laser light apparently resulted in a considerable increase in the fluidity of this very viscous water layer, reflected in an increase in damping between the tip and sample, thus facilitating its penetration into the tip—sample interspace. An increase in fluidity is probably equivalent to a decrease in density, where because of the unilateral restriction in mobility the packing density of the molecules constituting the interfacial water layers is probably higher than for those in bulk water. A decrease in density would automatically result in a higher meniscus around the tip, which could explain the increase in damping in response to irradiation. Consistent with the prevalence of thicker water layers on hydrophilic substrates compared to hydrophobic ones, the laser light intensity of 50 W m^{-2} is presumably too small to cause a substantial depletion of the water layers on the silicon wafer. Importantly, the tuning of the water layer was reversible: after switching the laser off, the resonance curve returns to its initial form. And more importantly, the observed shift in amplitude (frequency) disappeared at relative humidity levels of 48% (and below), thus excluding the heating of the AFM tip and/or substrate as the cause of the observed effect. In summary, we established a simple and versatile method based on conventional AFM and an ultrasonic transducer to obtain direct access to the nature of nanoscopic water layers on ultrasmooth substrates. The advantage of the method, whose principle was inspired by the NSOM-based technique introduced by us earlier,[3] is that its applicability is not restricted to translucent substrates. Noting the relevance of nanoscopic water layers as information carriers during cell—cell and cell—biomaterial contacts (first contact events), we expect that the novel method will advance to a central tool in the design of smart biomaterials (i.e., biomaterials with reversibly switchable surface properties[11]). As recently shown, nanoscopic water layers persist in the near-field of solids even in an aqueous environment[4] and therefore have the highest relevance in biological systems. However, in contrast to metallic systems in which the coexistence of an amorphous and a crystalline phase is well characterized[12,13] both theoretically and experimentally, a precise physical picture of the interfacial zone between bulk water and ordered water layers is still lacking, principally because of the indirect nature of the experiments describing this extremely sensitive zone.[4,14] Nevertheless, even without further details it is clear that differently structured nanoscopic water masks on molecules of different polarity are a key element in protein folding (i.e., the hydrophobic effect). Thus, we expect that our results will have a significant impact on life sciences in general and proteomics in particular.

(8) Goertz, M. P.; Houston, J. E.; Zhu, X. Y. *Langmuir* **2007**, *23*, 5491−5497.

(9) Jinesh, K. B.; Frenken, J. W. M. *Phys. Rev. Lett.* **2006**, *96*, 166103.
(10) Li, T. D.; Gao, J.; Szoszkiewicz, R.; Landman, U.; Riedo, E. *Phys. Rev. B* **2007**, *75*, 115415.
(11) Lahann, J.; Mitragotri, S.; Tran, T. N.; Kaido, H.; Sundaram, J.; Choi, I. S.; Hoffer, S.; Somorjai, G. A.; Langer, R. *Science* **2003**, *299*, 371−374.
(12) Fecht, H. J. *Nature* **1992**, *356*, 133−135.
(13) Lojkowski, W.; Fecht, H. J. *Prog. Mater. Sci.* **2000**, *45*, 339−568.
(14) Sommer, A. P.; Zhu, D.; Brühne, K. *Cryst. Growth Des.* **2007**, *7*, 2298−2301.

EXHIBIT 5

of April 7, 2009

POTASSIUM CHANNELS AND THE ATOMIC BASIS OF SELECTIVE ION CONDUCTION

Nobel Lecture, December 8, 2003

by

RODERICK MACKINNON

Howard Hughes Medical Institute, Laboratory of Molecular Neurobiology and Biophysics, Rockefeller University, 1230 York Avenue, New York, NY 10021, USA.

INTRODUCTION

All living cells are surrounded by a thin, approximately 40 Å thick lipid bilayer called the cell membrane. The cell membrane holds the contents of a cell in one place so that the chemistry of life can occur, but it is a barrier to the movement of certain essential ingredients including the ions Na^+, K^+, Ca^{2+} and Cl^-. The barrier to ion flow across the membrane – known as the dielectric barrier – can be understood at an intuitive level: the cell membrane interior is an oily substance and ions are more stable in water than in oil. The energetic preference of an ion for water arises from the electric field around the ion and its interaction with neighboring molecules. Water is an electrically polarizable substance, which means that its molecules rearrange in an ion's electric field, pointing negative oxygen atoms in the direction of cations and positive hydrogen atoms toward anions. These electrically stabilizing interactions are much weaker in a less polarizable substance such as oil. Thus, an ion will tend to stay in the water on either side of a cell membrane rather than enter and cross the membrane. And yet numerous cellular processes, ranging from electrolyte transport across epithelia to electrical signal production in neurons, depend on the flow of ions across the membrane. To mediate the flow, specific protein catalysts known as ion channels exist in the cell membrane. Ion channels exhibit the following three essential properties: (1) they conduct ions rapidly, (2) many ion channels are highly selective, meaning only certain ion species flow while others are excluded, (3) their function is regulated by processes known as gating, that is, ion conduction is turned on and off in response to specific environmental stimuli. Figure 1 summarizes these properties (figure 1).

The modern history of ion channels began in 1952 when Hodgkin and Huxley published their seminal papers on the theory of the action potential in the squid giant axon (Hodgkin and Huxley, 1952a; Hodgkin and Huxley, 1952b; Hodgkin and Huxley, 1952c; Hodgkin and Huxley, 1952d). A fundamental element of their theory was that the axon membrane undergoes changes in its permeability to Na^+ and K^+ ions. The Hodgkin-Huxley theory
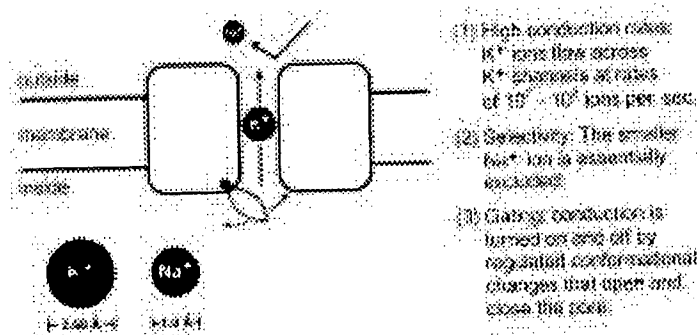
214

Figure 1. Ion channels exhibit three basic properties depicted in the cartoon. They conduct specific ions (for example K⁺) at high rates, they are selective (a K⁺ channel essentially excludes Na⁺), and conduction is turned on and off by opening and closing a gate, which can be regulated by an external stimulus such as ligand-binding or membrane voltage. The relative size of K⁺ and Na⁺ ions is shown.

did not address the mechanism by which the membrane permeability changes occur: ions could potentially cross the membrane through channels or by a carrier-mediated mechanism. In their words 'Details of the mechanism will probably not be settled for some time' (Hodgkin and Huxley, 1952a). It is fair to say that the pursuit of this statement has accounted for much ion channel research over the past fifty years.

As early as 1955 experimental evidence for channel mediated ion flow was obtained when Hodgkin and Keynes measured the directional flow of K⁺ ions across axon membranes using the isotope ⁴²K⁺ (Hodgkin and Keynes, 1955). They observed that K⁺ flow in one direction across the membrane depends on flow in the opposite direction, and suggested that 'the ions should be constrained to move in single file and that there should, on average, be several ions in a channel at any moment'. Over the following two decades Armstrong and Hille used electrophysiological methods to demonstrate that Na⁺ and K⁺ ions cross cell membranes through unique protein pores – Na⁺ channels and K⁺ channels – and developed the concepts of selectivity filter for ion discrimination and gate for regulating ion flow (Hille, 1970; Hille, 1971; Hille, 1973; Armstrong, 1971; Armstrong et al., 1973; Armstrong and Bezanilla, 1977; Armstrong, 1981). The patch recording technique invented by Neher and Sakmann then revealed the electrical signals from individual ion channels, as well as the extraordinary diversity of ion channels in living cells throughout nature (Neher and Sakmann, 1976).

The past twenty years have been the era of molecular biology for ion channels. The ability to manipulate amino acid sequences and express ion channels at high levels opened up entirely new possibilities for analysis. The advancement of techniques for protein structure determination and the development of synchrotron facilities also created new possibilities. For me, a scientist who became fascinated with understanding the atomic basis of life's electrical system, there could not have been a more opportune time to enter the field.

215

MY EARLY STUDIES: THE K^+ CHANNEL SIGNATURE SEQUENCE

The cloning of the *Shaker* K^+ channel gene from *Drosophila melanogaster* by Jan, Tanouye, and Pongs revealed for the first time a K^+ channel amino acid sequence and stimulated efforts by many laboratories to discover which of these amino acids form the pore, selectivity filter, and gate (Tempel *et al.*, 1987; Kamb *et al.*, 1987; Pongs *et al.*, 1988). At Brandeis University in Chris Miller's laboratory I had an approach to find the pore amino acids. Chris and I had just completed a study showing that charybdotoxin, a small protein from scorpion venom, inhibits a K^+ channel isolated from skeletal muscle cells by plugging the pore and obstructing the flow of ions (MacKinnon and Miller, 1988). In one of those late night 'let's see what happens if' experiments while taking a molecular biology course at Cold Spring Harbor I found that the toxin – or what turned out to be a variant of it present in the charybdotoxin preparation – inhibited the Shaker K^+ channel (MacKinnon *et al.*, 1988; Garcia *et al.*, 1994). This observation meant I could use the toxin to find the pore, and it did not take very long to identify the first site-directed mutants of the Shaker K^+ channel with altered binding of toxin (MacKinnon and Miller, 1989). I continued these experiments at Harvard Medical School where I began as assistant professor in 1989. Working with my small group at Harvard, including Tatiana Abramson, Lise Heginbotham, and Zhe Lu, and sometimes with Gary Yellen at Johns Hopkins University, we reached several interesting conclu-
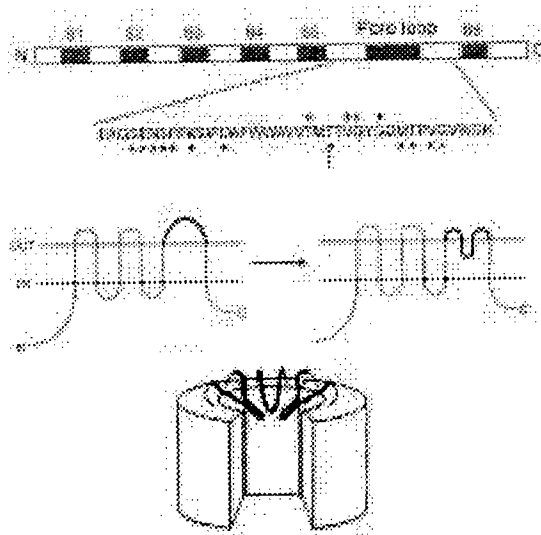

Figure 2. Early picture of a tetramer K^+ channel with a selectivity filter made of pore loops. A linear representation of a Shaker K^+ channel subunit on top shows shaded hydrophobic segments S1 to S6 and a region designated the pore loop. A partial amino acid sequence from the Shaker K^+ channel pore loop highlights amino acids shown to interact with extracellular scorpion toxins (*), intracellular tetraethylammonium ($\uparrow$) and K^+ ions (+). The pore loop was proposed to reach into the membrane (middle) and form a selectivity filter at the center of four subunits (bottom).

216

Figure 3. The K+ channel signature sequence shown as single letter amino acid code (blue) is highly conserved in organisms throughout the tree of life. Some K+ channels contain six membrane-spanning segments per subunit (6TM) while others contain only two (2TM). 2TM K+ channels correspond to 6TM K+ channels without the first four membrane-spanning segments (S1-S4 in figure 2).

sions concerning the architecture of K+ channels. They had to be tetramers in which four subunits encircle a central ion pathway (MacKinnon, 1991). This conclusion was not terribly surprising but the experiments and analysis to reach it gave me great pleasure since they required only simple measurements and clear reasoning with binomial statistics. We also deduced that each subunit presents a 'pore loop' to the central ion pathway (figure 2) (MacKinnon, 1995). This 'loop' formed the binding sites for scorpion toxins (MacKinnon and Miller, 1989; Hidalgo and MacKinnon, 1995; Ranganathan *et al.,* 1996) as well as the small-molecule inhibitor tetraethylammonium ion (MacKinnon and Yellen, 1990; Yellen *et al.,* 1991), which had been used by Armstrong and Hille decades earlier in their pioneering analysis of K+ channels (Armstrong, 1971; Armstrong and Hille, 1972). Most important to my thinking, mutations of certain amino acids within the 'loop' affected the channel's ability to discriminate between K+ and Na+, the selectivity hallmark of K+ channels (Heginbotham *et al.,* 1992; Heginbotham *et al.,* 1994). Meanwhile, new K+ channel genes were discovered and they all had one obvious feature in common: the very amino acids that we had found to be important for K+ selectivity were conserved (figure 3). We called these amino acids the K+ channel signature sequence, and imagined four pore loops somehow forming a selectivity filter with the signature sequence amino acids inside the pore (Heginbotham *et al.,* 1994; MacKinnon, 1995).

When you consider the single channel conductance of many K+ channels found in cells you realize just how incredible these molecular devices are. With typical cellular electrochemical gradients, K+ ions conduct at a rate of 10^7 to 10^8 ions per second. That rate approaches the expected collision frequency of K+ ions from solution with the entryway to the pore. This means that K+ ions flow through the pore almost as fast as they diffuse up to it. For this to occur the energetic barriers in the channel have to be very low, something like those encountered by K+ ions diffusing through water. All the more

217

remarkable, the high rates are achieved in the setting of exquisite selectivity: the K^+ channel conducts K^+, a monovalent cation of Pauling radius 1.33 Å, while essentially excluding Na^+, a monovalent cation of Pauling radius 0.95 Å. And this ion selectivity is critical to the survival of a cell. How does nature accomplish high conduction rates and high selectivity at the same time? The answer to this question would require knowing the atomic structure formed by the signature sequence amino acids, that much was clear. The conservation of the signature sequence amino acids in K^+ channels throughout the tree of life, from bacteria (Milkman, 1994) to higher eukaryotic cells, implied that nature had settled upon a very special solution to achieve rapid, selective K^+ conduction across the cell membrane. For me, this realization provided inspiration to want to directly visualize a K^+ channel and its selectivity filter.

THE KCSA STRUCTURE AND SELECTIVE K^+ CONDUCTION

I began to study crystallography, and although I had no idea how I would obtain funding for this endeavor, I have always believed that if you really want to do something then you will find a way. By happenstance I explained my plan to Torsten Wiesel, then president of Rockefeller University. He suggested that I come to Rockefeller where I would be able to concentrate on the problem. I accepted his offer and moved there in 1996. In the beginning I was joined by Declan Doyle and my wife Alice Lee MacKinnon and within a year others joined including João Morais Cabral, John Imredy, Sabine Mann and Richard Pfuetzner. We had to learn as we went along, and what we may have lacked in size and skill we more than compensated for with enthusiasm. It was a very special time. At first I did not know how we would ever reach the point of obtaining enough K^+ channel protein to attempt crystallization, but the K^+ channel signature sequence continued to appear in a growing number of prokaryotic genes, making expression in *Escherichia coli* possible. We focused our effort on a bacterial K^+ channel called KcsA from *Streptomyces lividans*, discovered by Schrempf (Schrempf *et al.*, 1995). The KcsA channel has a simple topology with only two membrane spanning segments per subunit corresponding to the Shaker K^+ channel without S1 through S4 (figure 2). Despite its prokaryotic origin KcsA closely resembled the Shaker K^+ channel's pore amino acid sequence, and even exhibited many of its pharmacological properties, including inhibition by scorpion toxins (MacKinnon *et al.*, 1998). This surprised us from an evolutionary standpoint, because why should a scorpion want to inhibit a bacterial K^+ channel! But from the utilitarian point of view of protein biophysicists we knew exactly what the scorpion toxin sensitivity meant, that KcsA had to be very similar in structure to the Shaker K^+ channel.

The KcsA channel produced crystals but they were poorly ordered and not very useful in the X-ray beam. After we struggled for quite a while I began to wonder whether some part of the channel was intrinsically disordered and interfering with crystallization. Fortunately my neighbor Brian Chait and his postdoctoral colleague Steve Cohen were experts in the analysis of soluble proteins by limited proteolysis and mass spectrometry, and their techniques
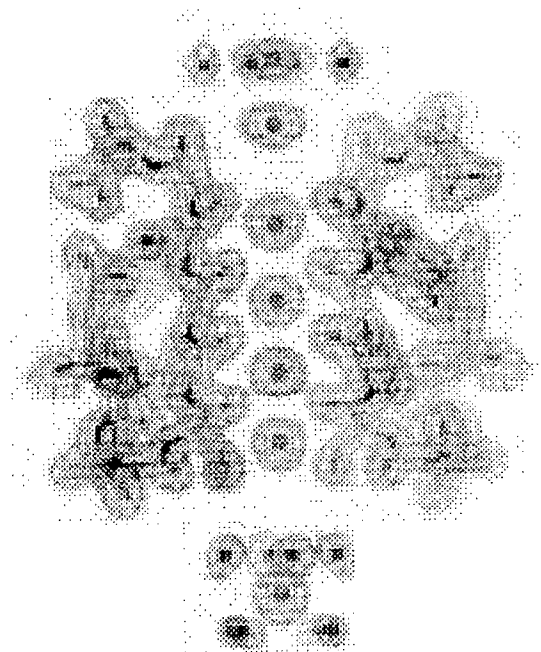
Figure 4. Electron density ($2F_o$-F_c contoured at 2 σ) from a high-resolution structure of the KcsA K$^+$ channel is shown as blue mesh. This region of the channel features the selectivity filter with K$^+$ ions and water molecules along the ion pathway. The refined atomic model is shown in the electron density. Adapted from (Zhou *et al.*, 2001b).

applied beautifully to a membrane protein. We found that KcsA was as solid as a rock, except for its C-terminus. After removing disordered amino acids from the c-terminus with chymotrypsin the crystals improved dramatically, and we were able to solve an initial structure at a resolution of 3.2 Å (Doyle *et al.*, 1998). We could not clearly see K$^+$ in the pore at this resolution, but my years of work on K$^+$ channel function told me that Rb$^+$ and Cs$^+$ should be valuable electron dense substitutes for K$^+$, and they were. Rubidium and Cs$^+$ difference Fourier maps showed these ions lined up in the pore – as Hodgkin and Keynes might have imagined in 1955 (Hodgkin and Keynes, 1955).

The KcsA structure was altogether illuminating, but before I describe it, I will depart from chronology to explain the next important technical step. A very accurate description of the ion coordination chemistry inside the selectivity filter would require a higher resolution structure. With 3.2 Å data we could infer the positions of the main-chain carbonyl oxygen atoms by applying our knowledge of small molecule structures, that is our chemical intuition, but we needed to see the selectivity filter atoms in detail. A high-resolution structure was actually quite difficult to obtain. After more than three additional years of work by João and then Yufeng (Fenny) Zhou we finally managed to produce high-quality crystals by attaching monoclonal Fab fragments to KcsA. These crystals provided the information we needed, a structure at a resolution of 2.0 Å in which K$^+$ ions could be visualized in the grasp of selec-
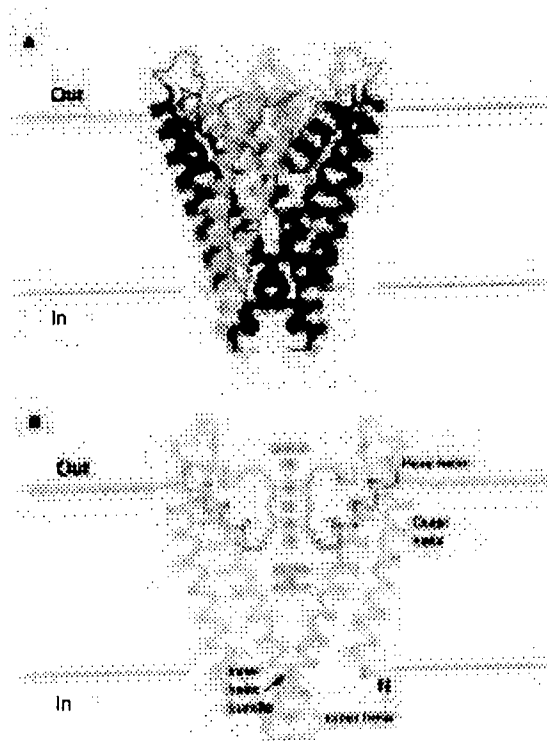
Figure 5. (A) A ribbon representation of the KcsA K$^+$ channel with its four subunits colored uniquely. The channel is oriented with the extracellular solution on top. (B) The KcsA K$^+$ channel with front and back subunits removed, colored to highlight the pore-helices (red) and selectivity filter (yellow). Electron density in blue mesh is shown along the ion pathway. Labels identify the pore, outer, and inner helices and the inner helix bundle. The outer and inner helices correspond to S5 and S6 in figure 2.

tivity filter protein atoms (figure 4) (Zhou *et al.*, 2001b). What did the K$^+$ channel structure tell us and why did nature conserve the K$^+$ channel signature sequence amino acids?

Not all protein structures speak to you in an understandable language, but the KcsA K$^+$ channel does. Four subunits surround a central ion pathway that crosses the membrane (figure 5A). Two of the four subunits are shown in figure 5B with electron density from K$^+$ ions and water along the pore. Near the center of the membrane the ion pathway is very wide, forming a cavity about 10 Å in diameter with a hydrated K$^+$ ion at its center. Each subunit directs the C-terminal end of a 'pore helix', shown in red, toward the ion. The C-terminal end of an α-helix is associated with a negative 'end charge' due to carbonyl oxygen atoms that do not participate in secondary structure hydrogen bonding, so the pore helices are directed as if to stabilize the K$^+$ ion in the cavity. At the beginning of this lecture I raised the fundamental issue of the cell membrane being an energetic barrier to ion flow because of its oily interior. KcsA allows us to intuit a simple logic encoded in its structure, and electrostatic calculations support the intuition (Roux and MacKinnon, 1999): the K$^+$ channel lowers the membrane dielectric barrier by hydrating a K$^+$ ion deep inside the membrane, and by stabilizing it with α-helix end charges.
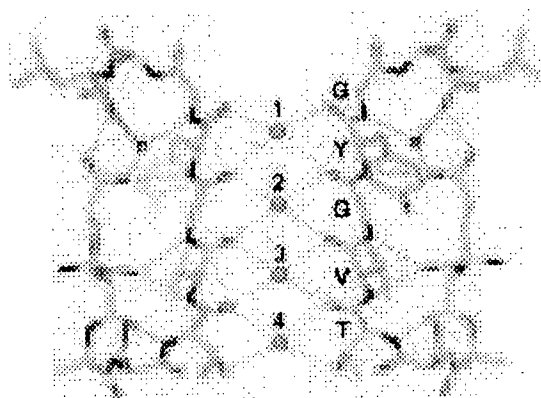
220

Figure 6. Detailed structure of the K^+ selectivity filter (two subunits). Oxygen atoms coordinate K^+ ions (green spheres) at positions 1 to 4 from the extracellular side. Single letter amino acid code identifies select signature sequence amino acids. Yellow, blue and red correspond to carbon, nitrogen and oxygen atoms, respectively. Green and gray dashed lines show oxygen-K^+ and hydrogen bonding interactions.

How does the K^+ channel distinguish K^+ from Na^+? Our earlier mutagenesis studies had indicated that the signature sequence amino acids would be responsible for this most basic function of a K^+ channel. Figure 6 shows the structure formed by the signature sequence – the selectivity filter – located in the extracellular third of the ion pathway. The glycine amino acids in the sequence TVGYG have dihedral angles in or near the left-handed helical region of the Ramachandran plot, as does the threonine, allowing the main-chain carbonyl oxygen atoms to point in one direction, toward the ions along the pore. It is easy to understand why this sequence is so conserved among K^+ channels: the alternating glycine amino acids permit the required dihedral angles, the threonine hydroxyl oxygen atom coordinates a K^+ ion, and the side-chains of valine and tyrosine are directed into the protein core surrounding the filter to impose geometric constraint. The end result when the subunits come together is a narrow tube consisting of four equal spaced K^+ binding sites, labeled 1 to 4 from the extracellular side. Each binding site is a cage formed by eight oxygen atoms on the vertices of a cube, or a twisted cube called a square antiprism (figure 7). The binding sites are very similar to the single alkali metal site in nonactin, a K^+ selective antibiotic with nearly identical K^+-oxygen distances (Dobler *et al.*, 1969; Dunitz and Dobler, 1977). The principle of K^+ selectivity is implied in a subtle feature of the KcsA crystal structure. The oxygen atoms surrounding K^+ ions in the selectivity filter are arranged quite like the water molecules surrounding the hydrated K^+ ion in the cavity. This comparison conveys a visual impression of binding sites in the filter paying for the energetic cost of K^+ dehydration. The Na^+ ion is apparently too small for these K^+-sized binding sites, so its dehydration energy is not compensated.

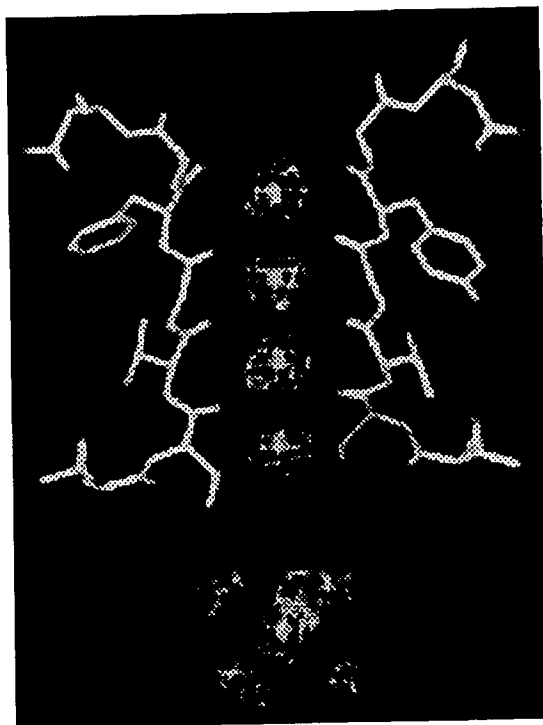The question that compelled us most after seeing the structure was exactly

Figure 7. A K$^+$ channel mimics the hydration shell surrounding a K$^+$ ion. Electron density (blue mesh) for K$^+$ ions in the filter and for a K$^+$ ion and water molecules in the central cavity are shown. White lines highlight the coordination geometry of K$^+$ in the filter and in water. Adapted from (Zhou *et al.*, 2001b).

how many ions are in the selectivity filter at a given time? To begin to understand how ions move through the filter we needed to know the stoichiometry of the ion conduction reaction, and that meant knowing how many ions can occupy the filter. Four binding sites were apparent, but are they all occupied at once? Four K$^+$ ions in a row separated by an average center-to-center distance of 3.3 Å seemed unlikely for electrostatic reasons. From an early stage we suspected that the correct number would be closer to two, because two ions more easily explained the electron density we observed for the larger alkali metal cations Rb$^+$ and Cs$^+$ (Doyle *et al.*, 1998; Morais-Cabral *et al.*, 2001). Quantitative evidence for the precise number of ions came with the high-resolution structure and with the analysis of Tl$^+$ (Zhou and MacKinnon, 2003). Thallium is the most ideally suited 'K$^+$ analog' because it flows through K$^+$ channels, has a radius and dehydration energy very close to K$^+$, and has the favorable crystallographic attributes of high electron density and an anomalous signal. The one serious difficulty in working with Tl$^+$ is its insolubility with Cl$^-$. Fenny meticulously worked out the experimental conditions and determined that on average there are between two and two and a half conducting ions in the filter at once, with an occupancy at each position around one half.
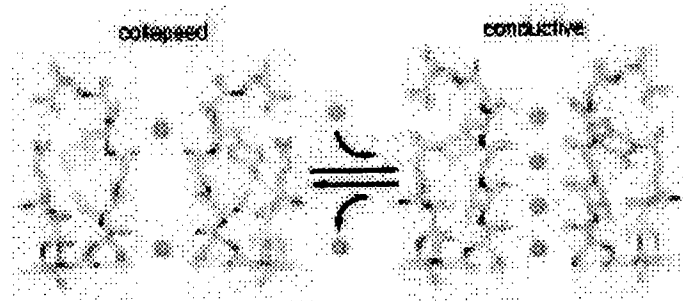
222

Figure 8. The selectivity filter can adopt two conformations. At low concentrations of K^+ on average one K^+ ion resides at either of two sites near the ends of the filter, which is collapsed in the middle. At high concentrations of K^+ a second ion enters the filter as it changes to a conductive conformation. On average, two K^+ ions in the conductive filter reside at four sites, each with about half occupancy.

We also observed that if the concentration of K^+ (or Tl^+) bathing the crystals is lowered sufficiently (below normal intracellular levels) then a reduction in the number of ions from two to one occurs and is associated with a structural change to a 'collapsed' filter conformation, which is pinched closed in the middle (Zhou *et al.*, 2001b; Zhou and MacKinnon, 2003). At concentrations above 20 mM the entry of a second K^+ ion drives the filter to a 'conductive' conformation, as shown in figure 8. Sodium on the other hand does not drive the filter to a 'conductive' conformation even at concentrations up to 500 mM.

The K^+-induced conformational change has thermodynamic consequences for the affinity of two K^+ ions in the 'conductive' filter. It implies that a fraction of the second ion's binding energy must be expended as work to bring about the filter's conformational change, and as a result the two ions will bind with reduced affinity. To understand this statement at an intuitive level, recognize that for two ions to reside in the filter they must oppose its tendency to collapse and force one of them out, i.e. the two-ion 'conductive' conformation is under some tension, which will tend to lower K^+ affinity. This is a desirable property for an ion channel because weak binding favors high conduction rates. The same principle, referred to as the 'induced fit' hypothesis, had been proposed decades earlier by enzymologists to explain high specificity with low substrate affinity in enzyme catalysis (Jencks, 1987).

In the 'conductive' filter if two K^+ ions were randomly distributed then they would occupy four sites in six possible ways. But several lines of evidence hinted to us that the ion positions are not random. For example Rb^+ and Cs^+ exhibit preferred positions with obviously low occupancy at position 2 (Morais-Cabral *et al.*, 2001; Zhou and MacKinnon, 2003). In K^+ we observed an unusual doublet peak of electron density at the extracellular entryway to the selectivity filter, shown in figure 9 (Zhou *et al.*, 2001b). We could explain this density if K^+ is attracted from solution by the negative protein surface charge near the entryway and at the same time repelled by K^+ ions inside the filter. Two discrete peaks implied two distributions of ions in the filter. If K^+ ions
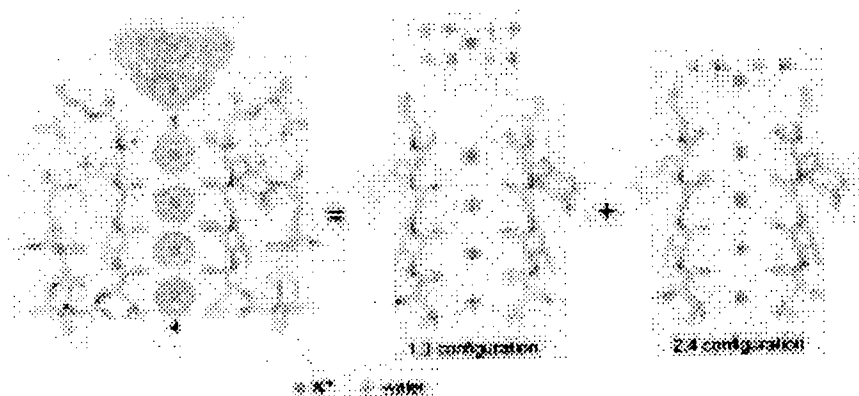
223

Figure 9. Two K$^+$ ions in the selectivity filter are hypothesized to exist predominantly in two specific configurations 1,3 and 2,4 as shown. K$^+$ ions and water molecules are shown as green and red spheres, respectively. Adapted from (Zhou *et al.*, 2001b).

tend to be separated by a water molecule for electrostatic reasons then the two dominant configurations would be 1,3 (K$^+$ ions in positions 1 and 3 with a water molecule in between) and 2,4 (K$^+$ ions in positions 2 and 4 with a water molecule in between). A mutation at position 4 (threonine to cysteine) was recently shown to influence K$^+$ occupancy at positions 2 and 4 but not at 1 and 3, providing strong evidence for specific 1,3 and 2,4 configurations of K$^+$ ions inside the selectivity filter (Zhou and MacKinnon, 2004).

Discrete configurations of an ion pair suggested a mechanism for ion conduction (figure 10A) (Morais-Cabral *et al.*, 2001). The K$^+$ ion pair could diffuse back and forth between 1,3 and 2,4 configurations (bottom pathway), or alternatively an ion could enter the filter from one side of the membrane as the ion-water queue moves and a K$^+$ exits at the opposite side (the top pathway). Movements would have to be concerted because the filter is no wider than a K$^+$ ion or water molecule. The two paths complete a cycle: in one complete cycle each ion moves only a fraction of the total distance through the filter, but the overall electrical effect is to move one charge all the way. Because two K$^+$ ions are present in the filter throughout the cycle we expect there should be electrostatic repulsion between them. Together with the filter conformational change that is required to achieve a 'conductive' filter with two K$^+$ ions in it, electrostatic repulsion should favor high conduction rates by lowering K$^+$ affinity.

Absolute rates from 10^7 to 10^8 ions per second are truly impressive for a highly selective ion channel. One aspect of the crystallographic data suggests that very high conductance K$^+$ channels such as KcsA might operate near the maximum rate that the conduction mechanism will allow. All four positions in the filter have a K$^+$ occupancy close to one half, which implies that the 1,3 and 2,4 configurations are equally probable, or energetically equivalent, but there is no *a priori* reason why this should be. A simulation of ions diffusing around the cycle offers a possible explanation: maximum flux is achieved when the energy difference between the 1,3 and 2,4 configurations is zero be-
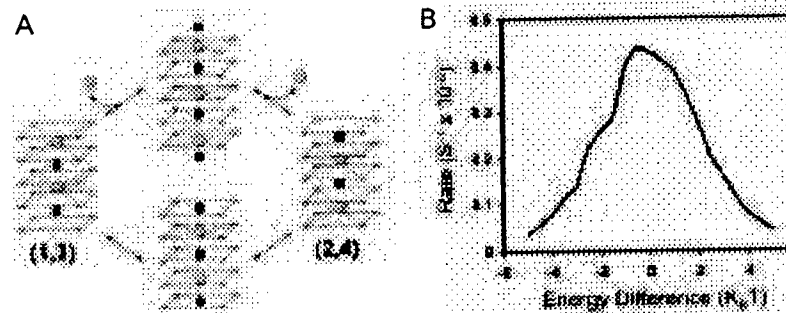
Figure 10. (A) Through-put cycle for K^+ conduction invoking 1,3 and 2,4 configurations. The selectivity filter is represented as five square planes of oxygen atoms. K^+ and water are shown as green and red spheres, respectively. (B) Simulated K^+ flux around the cycle is graphed as a function of the energy difference between the 1,3 and 2,4 configurations. Adapted from (Morais-Cabral *et al.*, 2001).

cause that is the condition under which the 'energy landscape' for the conduction cycle is smoothest (figure 10B). The energetic balance between the configurations therefore might reflect the optimization of conduction rate by natural selection (Morais-Cabral *et al.*, 2001). It is not so easy to demonstrate this point experimentally but it is certainly fascinating to ponder.

COMMON STRUCTURAL PRINCIPLES UNDERLIE K^+ AND Cl^- SELECTIVITY

The focus of this lecture is K^+ channels, but for a brief interlude I would like to show you a Cl^- selective transport protein. By comparing a K^+ channel and a Cl^- 'channel' we can begin to appreciate familiar themes in nature's solutions to different problems: getting cations and anions across the cell membrane. ClC Cl^- channels are found in many different cell types and are associated with a number of physiological processes that require Cl^- ion flow across lipid membranes (Jentsch *et al.*, 1999; Maduke *et al.*, 2000). As is the case for K^+ channels, ClC family genes are abundant in prokaryotes, a fortunate circumstance for protein expression and structural analysis. When Raimund Dutzler joined my laboratory he, Ernest Campbell and I set out to address the structural basis of Cl^- ion selectivity. We determined crystal structures of two bacterial members of the ClC Cl^- channel family, one from *Escherichia coli* (EcClC) and another from *Salmonella typhimurium* (StClC) (Dutzler *et al.*, 2002). Recent studies by Miller on the function of EcClC have shown that it is actually a Cl^- – proton exchanger (Accardi and Miller, 2004). We do not yet know why certain members of this family of Cl^- transport proteins function as channels and others as exchangers, but the crystal structures are fascinating and give us a view of Cl^- selectivity. Architecturally the ClC proteins are unrelated to K^+ channels, but if we focus on the ion pathway certain features are similar (figure 11). As we saw in K^+ channels, the ClC proteins have α-helices pointed at the ion pathway, but the direction is reversed with the positive
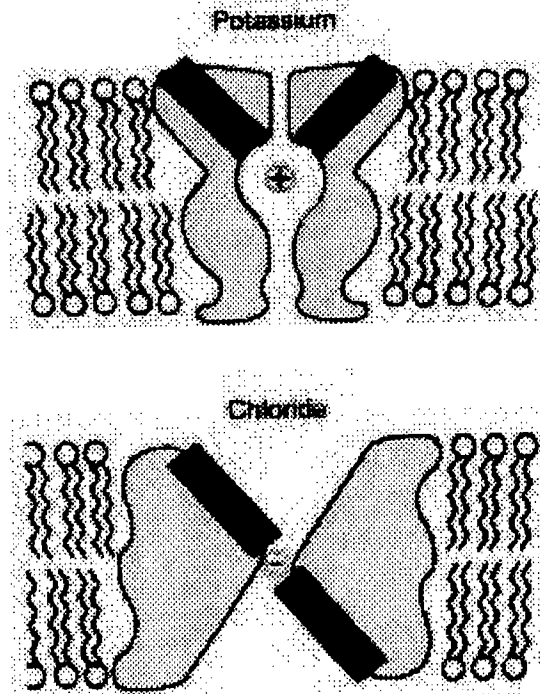
Figure 11. The overall architecture of K⁺ channels and ClC Cl⁻ transport proteins is very different but certain general features are similar. One similarity shown here is the use of α-helix end charges directed toward the ion pathway. The negative C-terminal end charge (red) points to K⁺. The positive N-terminal end charge (blue) points to Cl⁻.

charge of the N-terminus close to Cl⁻. This makes perfect sense for lowering the dielectric barrier for a Cl⁻ ion. In ClC we see that ions in its selectivity filter tend to be coordinated by main chain protein atoms, with amide nitrogen atoms surrounding Cl⁻ instead of carbonyl oxygen atoms surrounding K⁺ (figure 12). We also see that both the K⁺ and Cl⁻ selectivity filters contain multiple close-spaced binding sites and appear to contain more than one ion, perhaps to exploit electrostatic repulsion between ions in the pore. I find these similarities fascinating. They tell us that certain basic physical principles are important, such as the use of α-helix end charges to lower the dielectric barrier when ions cross the lipid membrane.

TRYING TO SEE A K⁺ CHANNEL OPEN AND CLOSE

Most ion channels conduct when called upon by a specific stimulus such as the binding of a ligand or a change in membrane voltage (Hille, 2001). The processes by which ion conduction is turned on are called gating. The conduction of ions occurs on a time scale that is far too rapid to involve very large protein conformational changes. That is undoubtedly one of the reasons why a single KcsA structure could tell us so much about ion selectivity and con-
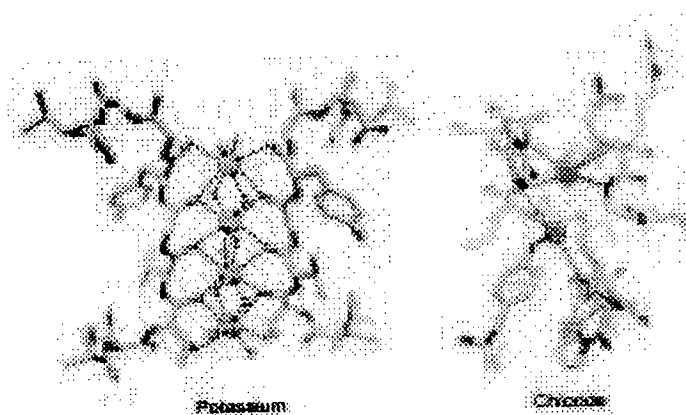
226

Figure 12. K⁺ and Cl⁻ selectivity filters make use of main chain atoms to coordinate ions: carbonyl oxygen atoms for K⁺ ions (green spheres) and amide nitrogen atoms for Cl⁻ ions (red spheres). Both filters contain multiple close-spaced ion binding sites. The Cl⁻ selectivity filter is that of a mutant ClC in which a glutamate amino acid was changed to glutamine (Dutzler *et al.*, 2003).

duction. Gating on the other hand occurs on a much slower time scale and can involve large protein conformational changes. The challenge for a structural description of gating is to capture a channel in both opened (on) and closed (off) conformations so that they can be compared.

In the KcsA K⁺ channel gating is controlled by intracellular pH and lipid membrane composition, but unfortunately the KcsA channel's open probability reaches a maximum value of only a few percent in functional assays (Cuello *et al.*, 1998; Heginbotham *et al.*, 1998). At first we had no definitive way to know whether a gate was open or closed in the crystal structures. In the 1970s Armstrong had proposed the existence of a gate near the intracellular side of the membrane in voltage dependent K⁺ channels because he could 'trap' large organic cations inside the pore between a selectivity filter near the extracellular side and a gate near the intracellular side (Armstrong, 1971; Armstrong, 1974). Following these ideas we crystallized KcsA with a heavy atom version of one of his organic cations, tetrabutyl antimony (TBA), and found that it binds inside the central cavity of KcsA (Zhou *et al.*, 2001a). This was very interesting because the ~10 Å diameter of TBA far exceeds the pore diameter leading up to the cavity: in KcsA the intracellular pore entryway is constricted to about 3.5 Å by the inner helix bundle (figure 5B). Seeing TBA 'trapped' in the cavity behind the inner helix bundle evoked Armstrong's classical view of K⁺ channel gating, and implied that the inner helix bundle serves as a gate and is closed in KcsA. Mutational and spectroscopic studies in other laboratories also pointed to the inner helix bundle as a possible gate-forming structural element (Perozo *et al.*, 1999; del Camino *et al.*, 2000).

Youxing Jiang and I hoped we could learn more about K⁺ channel gating by determining the structures of new K⁺ channels. From gene sequence analysis we noticed that many prokaryotic K⁺ channels contain a large C-ter-
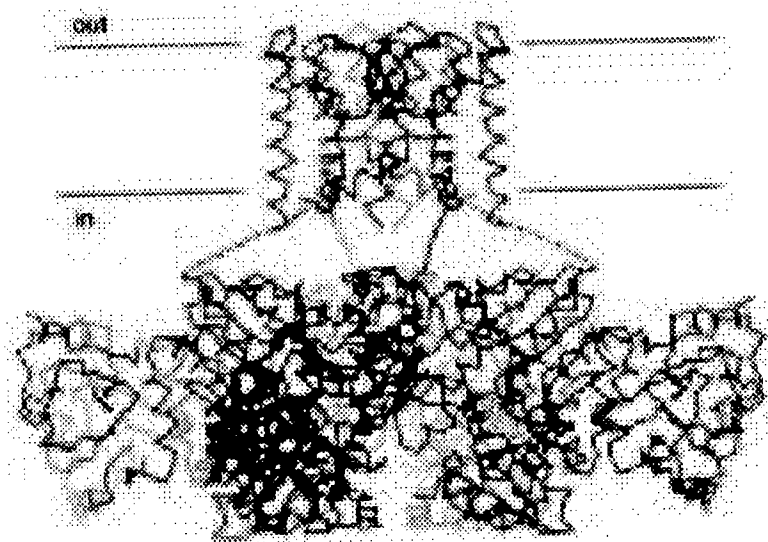
227

Figure 13. The MthK K⁺ channel contains an intracellular gating ring (bottom) attached to its ion conduction pore (top). Ca^{2+} ions (yellow spheres) are bound to the gating ring in clefts in between domains. The connections between the gating ring and the pore, which were poorly ordered in the crystal, are shown as dashed lines.

minus that encodes what we called RCK domains and we suspected that these domains control pore opening, perhaps through binding of an ion or a small-molecule. Initally we determined the structure of isolated RCK domains from an *Escherichia coli* K⁺ channel, but by themselves they were not very informative beyond hinting that a similar structure exists on the C-terminus of eukaryotic Ca^{2+}-dependent 'BK' channels (Jiang *et al.*, 2001). We subsequently determined the crystal structure of MthK, complete K⁺ channel containing RCK domains, from *Methanobacterium thermoautotrophicus* (figure 13) (Jiang *et al.*, 2002a). This structure was extremely informative. The RCK domains form a 'gating ring' on the intracellular side of the pore. In clefts between domains we could see what appeared to be divalent cation binding sites, and the crystals had been grown in the presence of Ca^{2+}. In functional assays we discovered that the open probability of the MthK channel increased as Ca^{2+} or Mg^{2+} concentration was raised, giving us good reason to believe that the crystal structure should represent the open conformation of a K⁺ channel.

In our MthK structure the inner helix bundle is opened like the aperture of a camera (figure 14) (Jiang *et al.*, 2002b). As a result, the pathway leading up to the selectivity filter from the intracellular side is about 10 Å wide, explaining how Armstrong's large organic cations can enter the cavity to block a K⁺ channel, and how K⁺ ions gain free access to the selectivity filter through aqueous diffusion. By comparing the KcsA and MthK channel structures it seemed that we were looking at examples of closed and opened K⁺ channels, and could easily imagine the pore undergoing a conformational change from closed to open. To open, the inner helices would have to bend at a point halfway across
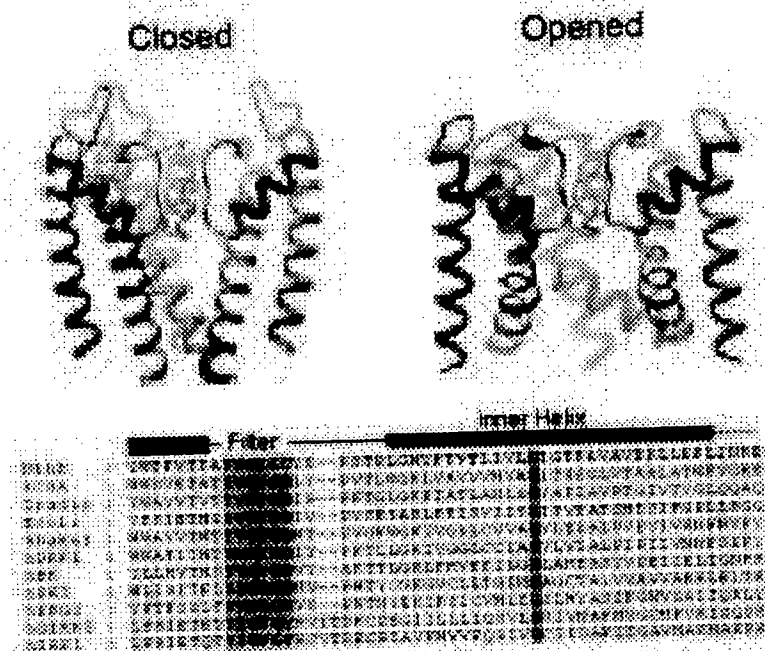
228

Figure 14. KcsA and MthK represent closed and opened K⁺ channels. Three subunits of the closed KcsA K⁺ channel (left) and opened MthK K⁺ channel (right) are shown. The inner helices of MthK are bent at a glycine gating hinge (red), allowing the inner helix bundle to open. Partial amino acid sequences from a variety of K⁺ channels with different gating domains are compared. Colors highlighting the selectivity filter sequence (gold) and inner helix glycine hinge (red) match colors used in the structures. Adapted from (Jiang *et al.*, 2002b).

the membrane as their C-terminus is displaced laterally away from the pore axis by conformational changes in the gating ring. A glycine amino acid facilitates the bending in MthK by introducing a hinge point in the middle of the inner helix. Like MthK, KcsA and many other K⁺ channels contain a glycine at the very same location; its conservation suggests that the inner helices move in a somewhat similar manner in many different K⁺ channels (figure 14).

Gating domains convert a stimulus into pore opening. Further studies are needed to understand how the free energy of Ca²⁺ binding is converted into pore opening in the MthK channel. And the mechanistic details of ligand gating will vary from one channel type to the next because nature is very modular with ion channels, just like with other proteins. Gene sequences show us that a multitude of different domains can be found attached to the inner helices of different K⁺ channels, allowing ions such as Ca²⁺ or Na⁺, small organic molecules, and even regulatory proteins to control the conformational state of the pore and so gate the ion channel (http://www.ncbi.nlm.nih.gov/BLAST/) (Atkinson *et al.*, 1991; Schumacher *et al.*, 2001; Yuan *et al.*, 2003; Kubo *et al.*, 1993).

A fundamentally different kind of gating domain allows certain K⁺, Na⁺, Ca²⁺ and nonselective cation channels to open in response to membrane volt-
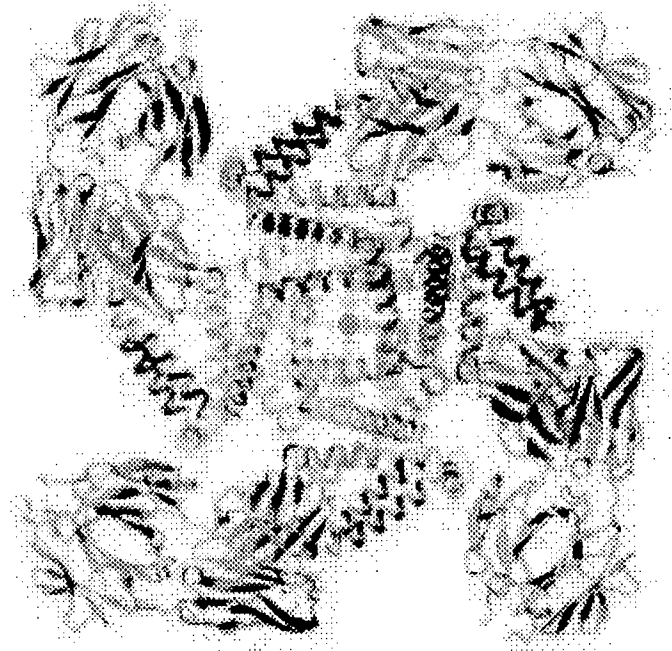
229

Figure 15. Crystal structure of the KvAP K⁺ channel in complex with monoclonal antibody Fab fragments. The channel is viewed along the pore axis from the intracellular side of the membrane, with α-helical subunits colored in blue, yellow, cyan, and red. One Fab fragment (green) is bound to the helix-turn-helix element of the voltage sensor on each subunit. From (Jiang *et al.*, 2003a).

age changes. Referred to as voltage sensors, these domains are connected to the outer helices of the pore and form a structural unit within the membrane. The basic principle of operation for a voltage sensor is the movement of protein charges through the membrane electric field coupled to pore opening (Armstrong and Bezanilla, 1974; Sigworth, 1994; Bezanilla, 2000). Like transistors in an electronic device, voltage-dependent channels are electrical switches. They are a serious challenge for crystallographic analysis because of their conformational flexibility. Youxing Jiang and I working with Alice Lee and Jiayun Chen solved the structure of a voltage-dependent K⁺ channel, KvAP, from the thermophilic Archea *Aeropyrum pernix* (Ruta *et al.*, 2003; Jiang *et al.*, 2003a) (figure 15). In the crystal of KvAP the voltage sensors, held by monoclonal Fab fragments, adopted a non-native conformation. This observation in itself is meaningful as it underscores the intrinsic flexibility of voltage sensors: in contrast Fab fragments had little effect on the more rigid KcsA K⁺ channel and ClC Cl⁻ channel homolog, both of which we determined in the presence and absence of Fab fragments (Doyle *et al.*, 1998; Zhou *et al.*, 2001b; Dutzler *et al.*, 2002; Dutzler *et al.*, 2003). KvAP's voltage sensors contain a hydrophobic helix-turn-helix element with arginine residues beside the pore (Jiang *et al.*, 2003a), and functional experiments using tethered bi-

230

otin and avidin show that this element moves relative to the plane of the membrane (Jiang et al., 2003b). Additional structures revealing different channel conformations will be needed to better understand the mechanistic details of voltage-dependent gating. But the KvAP structure and associated functional studies have provided a conceptual model for voltage-dependent gating – one in which the voltage sensors move at the protein-lipid interface in response to a balance between hydrophobic and electrostatic forces. Rees and colleagues at the California Institute of Technology determined the structure of a voltage regulated mechanosensitive channel called MscS, and although it is unrelated to traditional voltage-dependent channels, it too contains hydrophobic helix-turn-helix elements with arginine residues apparently against the lipid membrane (Bass et al., 2002). MscS and KvAP are fascinating membrane protein structures. They do not fit into the standard category of membrane proteins with rigid hydrophobic walls against the lipid membrane core. I find such proteins intriguing.

We are only just beginning to understand the structural principles of ion channel gating and regulation. Electrophysiological studies have uncovered a multitude of connections between cellular biochemical pathways and ion channel function (Hille, 2001). New protein structures are now beginning to do the same. Beta subunits of certain eukaryotic voltage-dependent channels are structurally related to oxido-reductase enzymes (Gulbis et al., 1999; Gulbis et al., 2000). PAS domains on other K^+ channels belong to a family of sensory molecules (Morais Cabral et al., 1998), and a specialized structure on G protein-gated channels forms a binding site for regulatory G protein subunits (Nishida and MacKinnon, 2002). The interconnectedness of ion channel function with many aspects of cell function is beginning to reveal itself as complex and fascinating.

CONCLUDING REMARKS

I think the most exciting time in ion channel studies is just beginning. So many of the important questions are waiting to be answered and we have the tools in hand to answer them. I am very optimistic about the future, and for the great possibilities awaiting young scientists who are now setting out to study ion channels and other membrane proteins. I consider myself very fortunate to have contributed to some small part of the knowledge we have today. Of course, my contributions would never have been possible without the efforts and enthusiasm of the young scientists who have come from around the world to study ion channels with me (figure 16). I also owe thanks to the Rockefeller University, the Howard Hughes Medical Institute, and the National Institutes of Health for supporting my scientific research.

MACKINNON LABORATORY: 1989–2003

Postdoctoral	Students	Staff Scientists	Collaborators
Laura Escobar	Lise Heginbotham	Tatiana Abramson	Gary Yellen
Zhe Lu	Michael Root	John Lewis	Maria Garcia
Adrian Gross	Patricia Hidalgo	Alice Lee MacKinnon	Gerhard Wagner
Kenton Swartz	Sanjay Aggarwal	Sabine Mann	Andrzej Krezel
Chul-Seung Park	James Morrell	Richard Pfuetzner	Brian Chait
Rama Ranganathan	Alexander Pico	Anling Kuo	Steve Cohen
Chinfei Chen	Vanessa Ruta	Minhui Long	Martine Cadene
Declan Doyle	Ian Berke	Amelia Kaufman	Benoit Roux
John Imredy		Ernest Campbell	Tom Muir
João Morais Cabral		Jiayun Chen	
Youxing Jiang			
Jacqueline Gulbis			
Raimund Dutzler			
Francis Valiyaveetil			
Xiao-Dan Pfenninger-Li			
Ming Zhou			
Ofer Yifrach			
Yufeng Zhou			
Sebastien Poget			
Motohiko Nishida			
Uta-Maria Ohndorf			
Steve Lockless			
Qiu-Xing Jiang			
Seok-Yong Lee			
Stephen Long			

Thanks to Rockefeller University, HHMI, NIH, to the synchrotrons CHESS, NSLS, ALS, APS and ESRF and to my assistant Wendell Chin.

Figure 16. MacKinnon laboratory from 1989 to 2003.

REFERENCE LIST

Accardi, A. and Miller, C. (2004) Proton-coupled chloride transport mediated by ClC-ec1, a bacterial homologue of the ClC chloride channels. Biophys.J. *86[1]*, 286a.

Armstrong, C. M. (1971). Interaction of tetraethylammonium ion derivatives with the potassium channels of giant axons. J. Gen. Physiol. *58*, 413–437.

Armstrong, C. M. (1981). Sodium channels and gating currents. Physiol. Rev. *61*, 645–683.

Armstrong, C. M. and Bezanilla,F. (1974). Charge movement associated with the opening and closing of the activation gates of the Na^+ channels. J. Gen. Physiol. *63*, 533–552.

Armstrong, C. M., Bezanilla, F., and Rojas, E. (1973). Destruction of sodium conductance inactivation in squid axons perfused with pronase. J. Gen. Physiol. *62*, 375–391.

Armstrong, C. M. and Hille, B. (1972). The inner quaternary ammonium ion receptor in potassium channels of the node of Ranvier. J. Gen. Physiol. *59*, 388–400.

Armstrong, C. M. (1974). Ionic pores, gates, and gating currents. Q. Rev. Biophys. *7*, 179–210.

Armstrong, C. M. and Bezanilla, F. (1977). Inactivation of the sodium channel. II. Gating current experiments. J. Gen. Physiol *70*, 567–590.

Atkinson, N. S., Robertson, G. A., and Ganetzky, B. (1991). A component of calcium-activated potassium channels encoded by the Drosophila slo locus. Science *253*, 551–555.

Bass, R. B., Strop, P., Barclay, M., and Rees, D. C. (2002). Crystal structure of *Escherichia coli* MscS, a voltage-modulated and mechanosensitive channel. Science *298*, 1582–1587.

Bezanilla, F. (2000). The voltage sensor in voltage-dependent ion channels. Physiol Rev. *80*, 555–592.

Cuello, L. G., Romero, J. G., Cortes, D .M., and Perozo, E. (1998). pH-dependent gating in the Streptomyces lividans K^+ channel. Biochemistry *37*, 3229–3236.

del Camino, D., Holmgren, M., Liu, Y., and Yellen, G. (2000). Blocker protection in the pore of a voltage-gated K^+ channel and its structural implications. Nature *403*, 321–325.

Dobler,v. M., Dunitz, J. D., and Kilbourn, B. T. (1969). Die struktur des KNCS-Komplexes von nonactin. Helvetica Chimica Acta *52*, 2573–2583.

Doyle, D. A., Morais Cabral, J. H., Pfuetzner, R. A., Kuo, A., Gulbis, J. M., Cohen, S. L., Chait, B. T., and MacKinnon,R. (1998). The structure of the potassium channel: molecular basis of K^+ conduction and selectivity. Science *280*, 69–77.

Dunitz, J. D. and Dobler, M. (1977). Structural studies of ionophores and their ion-complexes. In Biological aspects of inorganic chemistry, A. W. Addison, W. R. Cullen, D. Dolphin, and B. R. James, eds. John Wiley & Sons, Inc.), pp. 113–140.

Dutzler, R., Campbell, E. B., Cadene, M., Chait, B. T., and MacKinnon,R. (2002). X-ray structure of a ClC chloride channel at 3.0 Å reveals the molecular basis of anion selectivity. Nature *415*, 287–294.

Dutzler, R., Campbell, E. B., and MacKinnon, R. (2003). Gating the selectivity filter in ClC chloride channels. Science *300*, 108–112.

Garcia, M. L., Garcia-Calvo, M., Hidalgo, P., Lee, A., and MacKinnon, R. (1994). Purification and charaterization of three inhibitors of voltage-dependent K^+ channels from Leiurus quinquestriatus var. hebraeus venom. Biochemistry *33*, 6834–6839.

Gulbis, J. M., Mann, S., and MacKinnon, R. (1999). Structure of a voltage-dependent K^+ channel beta subunit. Cell *97*, 943–952.

Gulbis, J. M., Zhou, M., Mann, S., and MacKinnon, R. (2000). Structure of the cytoplasmic β subunit-T1 assembly of voltage-dependent K^+ channels. Science *289*, 123–127.

Heginbotham, L., Abramson, T., and MacKinnon, R. (1992). A functional connection between the pores of distantly related ion channels as revealed by mutant K^+ channels. Science *258*, 1152–1155.

Heginbotham, L., Lu, Z., Abramson, T., and MacKinnon, R. (1994). Mutations in the K^+ channel signature sequence. Biophys. J. *66*, 1061–1067.

Heginbotham, L., Kolmakova-Partensky, L., and Miller, C. (1998). Functional reconstitution of a prokaryotic K^+ channel. J. Gen. Physiol. *111*, 741–749.

Hidalgo, P. and MacKinnon, R. (1995). Revealing the architecture of a K$^+$ channel pore through mutant cycles with a peptide inhibitor. Science 268, 307–310.

Hille, B. (1970). Ionic channels in nerve membranes. Prog. Biophys. Mol. Biol. 21, 1–32.

Hille, B. (1973). Potassium channels in myelinated nerve. Selective permeability to small cations. J. Gen. Physiol. 61, 669–686.

Hille, B. (2001). Ion Channels of Excitable Membranes. (Sunderland, MA: Sinauer Associates, Inc.).

Hille, B. (1971). The permeability of the sodium channel to organic cations in myelinated nerve. J. Gen. Physiol. 58, 599–619.

Hodgkin, A. L. and Huxley, A. F. (1952a). A quantitative description of membrane current and its application to conduction and excitation in nerve. J. Physiol. 117, 500–544.

Hodgkin, A. L. and Huxley, A. F. (1952b). Currents carried by sodium and potassium ions through the membrane of the giant axon of Loligo. J. Physiol. 116, 449–472.

Hodgkin, A. L. and Huxley, A. F. (1952c). The components of membrane conductance in the giant axon of Loligo. J. Physiol. 116, 473–496.

Hodgkin, A. L. and Huxley, A. F. (1952d). The dual effect of membrane potential on sodium conductance in the giant axon of Loligo. J. Physiol. 116, 497–506.

Hodgkin, A. L. and Keynes, R. D. (1955). The potassium permeability of a giant nerve fibre. J. Physiol. (Lond) 128, 61–88.

Jencks, W. P. (1987). Catalysis in Chemistry and Enzymology. (Dover Publications, Inc.).

Jentsch, T. J., Friedrich, T., Schriever, A., and Yamada, H. (1999). The CLC chloride channel family. Pflugers Arch. 437, 783–795.

Jiang, Y., Lee, A., Chen, J., Ruta, V., Cadene, M., Chait, B., and MacKinnon, R. (2003a). X-ray structure of a voltage-dependent K$^+$ channel. Nature 423, 33–41.

Jiang, Y., Ruta, V., Chen, J., Lee, A., and MacKinnon, R. (2003b). The principle of gating charge movement in a voltage-dependent K$^+$ channel. Nature 423, 42–48.

Jiang, Y., Lee, A., Chen, J., Cadene, M., Chait, B. T., and MacKinnon, R. (2002a). Crystal structure and mechanism of a calcium-gated potassium channel. Nature 417, 515–522.

Jiang, Y., Lee, A., Chen, J., Cadene, M., Chait, B. T., and MacKinnon, R. (2002b). The open pore conformation of potassium channels. Nature 417, 523–526.

Jiang, Y., Pico, A., Cadene, M., Chait, B. T., and MacKinnon, R. (2001). Structure of the RCK domain from the E. coli K$^+$ channel and demonstration of its presence in the human BK channel. Neuron 29, 593–601.

Kamb, A., Iverson, L. E., and Tanouye, M. A. (1987). Molecular characterization of Shaker, a Drosophila gene that encodes a potassium channel. Cell 50, 405–413.

Kubo, Y., Reuveny, E., Slesinger, P. A., Jan, Y. N., and Jan, L. Y. (1993). Primary structure and functional expression of a rat G-protein-coupled muscarinic potassium channel. Nature 364, 802–806.

MacKinnon, R. (1991). Determination of the subunit stoichiometry of a voltage-activated potassium channel. Nature 350, 232–235.

MacKinnon, R. (1995). Pore loops: an emerging theme in ion channel structure. Neuron 14, 889–892.

MacKinnon, R., Cohen, S. L., Kuo, A., Lee, A., and Chait, B. T. (1998). Structural conservation in prokaryotic and eukaryotic potassium channels. Science 280, 106–109.

MacKinnon, R. and Miller, C. (1988). Mechanism of charybdotoxin block of the high-conductance, Ca^{2+}-activated K$^+$ channel. J. Gen. Physiol. 91, 335–349.

MacKinnon, R. and Miller, C. (1989). Mutant potassium channels with altered binding of charybdotoxin, a pore-blocking peptide inhibitor. Science 245, 1382–1385.

MacKinnon, R., Reinhart, P. H., and White, M. M. (1988). Charybdotoxin block of Shaker K$^+$ channels suggests that different types of K$^+$ channels share common structural features. Neuron 1, 997–1001.

MacKinnon, R. and Yellen G. (1990). Mutations affecting TEA blockade and ion permeation in voltage-activated K$^+$ channels. Science 250, 276–279.

Maduke, M., Miller, C., and Mindell, J. A. (2000). A decade of CLC chloride channels: structure, mechanism, and many unsettled questions. Annu. Rev. Biophys. Biomol. Struct. *29*, 411–438.

Milkman, R. (1994). An *Escherichia coli* homologue of eukaryotic potassium channel proteins. Proc. Natl. Acad. Sci. 91[9], 3510–3514.

Morais-Cabral, J. H., Zhou, Y., and MacKinnon, R. (2001). Energetic optimization of ion conduction rate by the K^+ selectivity filter. Nature *414*, 37–42.

Morais-Cabral, J. H., Lee, A., Cohen, S. L., Chait, B. T., Li, M., and MacKinnon, R. (1998). Crystal structure and functional analysis of the HERG potassium channel N-terminus: a eukaryotic PAS domain. Cell *95*, 649–655.

Neher, E. and Sakmann, B. (1976). Single-channel currents recorded from membrane of denervated frog muscle fibres. Nature *260*, 799–802.

Nishida, M. and MacKinnon, R. (2002). Structural basis of inward rectification: Cytoplasmic pore of the G protein-gated inward rectifier GIRK1 at 1.8 Å resolution. Cell *III*, 957–965.

Perozo, E., Cortes, D. M., and Cuello, L. G. (1999). Structural rearrangements underlying K^+-channel activation gating. Science *285*, 73–78.

Pongs, O., Kecskemethy, N., Muller, R., Krah-Jentgens, I., Baumann, A., Kiltz, H. H., Canal, I., Llamazares, S., and Ferrus, A. (1988). Shaker encodes a family of putative potassium channel proteins in the nervous system of *Drosophila*. EMBO J. *7*, 1087–1096.

Ranganathan, R., Lewis, J. H., and MacKinnon, R. (1996). Spatial localization of the K^+ channel selectivity filter by mutant cycle-based structure analysis. Neuron *16*, 131–139.

Roux, B. and MacKinnon, R. (1999). The cavity and pore helices in the KcsA K^+ channel: electrostatic stabilization of monovalent cations. Science *285*, 100–102.

Ruta, V., Jiang, Y., Lee, A., Chen, J., and MacKinnon, R. (2003). Functional analysis of an archeabacterial voltage-dependent K^+ channel. Nature *422*, 180–185.

Schrempf, H., Schmidt, O., Kummerlen, R., Hinnah, S., Muller, D., Betzler, M., Steinkamp, T., and Wagner, R. (1995). A prokaryotic potassium ion channel with two predicted transmembrane segments from *Streptomyces lividans*. EMBO J. *14*, 5170–5178.

Schumacher, M. A., Rivard, A. F., Bachinger, H. P., and Adelman, J. P. (2001). Structure of the gating domain of a Ca2+-activated K^+ channel complex with Ca^{2+}/calmodulin. Nature *410*, 1120–1124.

Sigworth, F. J. (1994). Voltage gating of ion channels. Q. Rev. Biophys. *27*, 1–40.

Tempel, B. L., Papazian, D. M., Schwarz, T. L., Jan, Y. N., and Jan, L. Y. (1987). Sequence of a probable potassium channel component encoded at Shaker locus of *Drosophila*. Science *237*, 770–775.

Yellen, G. Jurman, M. E., Abramson, T., and MacKinnon, R. (1991). Mutations affecting internal TEA blockade identify the probable pore-forming region of a K^+ channel. Science *251*, 939–942.

Yuan, A., Santi, C. M., Wei, A., Wang, Z. W., Pollak, K., Nonet, M., Kaczmarek, L., Crowder, C. M., and Salkoff, L. (2003). The sodium-activated potassium channel is encoded by a member of the Slo gene family. Neuron *37*, 765–773.

Zhou, M. and MacKinnon, R. (2004). A mutant KcsA K^+ channel with altered conduction properties and selectivity filter ion distribution. J.Mol.Biol. 338, 839–846.

Zhou, M., Morais-Cabral, J. H., Mann, S., and MacKinnon, R. (2001a). Potassium channel receptor site for the inactivation gate and quaternary amine inhibitors. Nature *411*, 657–661.

Zhou, Y. and MacKinnon, R. (2003). The occupancy of ions in the K^+ selectivity filter: Charge balance and coupling of ion binding to a protein conformational change underlie high conduction rates. J. Mol. Biol. *333*, 965–975.

Zhou, Y., Morais-Cabral, J. H., Kaufman, A., and MacKinnon, R. (2001b). Chemistry of ion coordination and hydration revealed by a K^+ channel- Fab complex at 2.0 Å resolution. Nature *414*, 43–48.

EXHIBIT 7

of April 7, 2009

Specifications and test methods for

EUDRAGIT® RL 30 D and EUDRAGIT® RS 30 D

"Ammonio Methacrylate Copolymer Type A" Ph. Eur.
"Ammonio Methacrylate Copolymer Type B" Ph. Eur.
"Ammonio Methacrylate Copolymer Dispersion, Type A and B" USP/NF
"Aminoalkylmethacrylate Copolymer RS" JPE

1   Commercial form

Aqueous dispersions of EUDRAGIT® RL 100 / EUDRAGIT® RS 100 with 30 % dry substance. The water is tested according to the specifications of "Purified Water in bulk" Ph. Eur. and according to the specifications for Conductivity of "Purified Water" USP. The dispersions contain 0.25 % sorbic acid Ph. Eur. / NF as a preservative as well as 0.1 % of sodium hydroxide Ph. Eur. / NF as an alkalizing agent.

EUDRAGIT® RL 30 D (Type A) and EUDRAGIT® RS 30 D (Type B) are described in the USP/NF monograph quoted above.

EUDRAGIT® RL 100 (Type A) and EUDRAGIT® RS 100 (Type B) are described in the Ph. Eur. and JPE monographs quoted above.

2   Chemical structure

EUDRAGIT® RL 100 and EUDRAGIT® RS 100 are copolymers of ethyl acrylate, methyl methacrylate and a low content of a methacrylic acid ester with quaternary ammonium groups (trimethylammonioethyl methacrylate chloride). The ammonium groups are present as salts and make the polymers permeable.
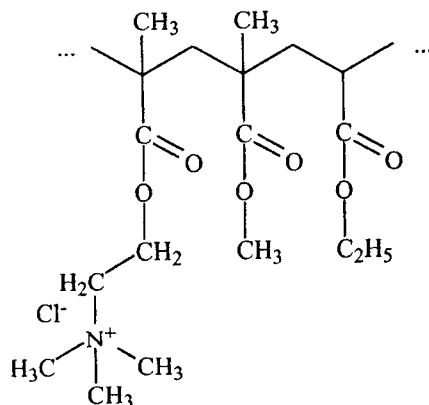
The average molecular weight is approx. 150,000.

3 Characters

Description

Milky-white liquids of low viscosity with a faint characteristic odour.

Solubility

The aqueous dispersions are miscible with water in any proportion, the milky-white appearance being retained. 1 part EUDRAGIT® RL 30 D / RS 30 D dissolves in 5 parts acetone, ethanol or isopropyl alcohol to give clear to slightly cloudy solutions.

When mixed with methanol in a ratio of 1:5, EUDRAGIT® RL 30 D dissolves completely, EUDRAGIT® RS 30 D only partially. When mixed with 1 N sodium hydroxide in a ratio of 1:2, none of the dispersions dissolve.

4 Tests

Film formation

10 g EUDRAGIT® RL 30 D / RS 30 D are mixed with 0.6 g triethyl citrate. When poured onto a glass plate, a transparent film forms upon evaporation of the water.

Dry substance / Residue on evaporation

28.5 - 31.5 %
The test is performed according to Ph. Eur. 2.2.32 method d.
1 g of the dispersions is dried in an oven for 3 hrs at 110 °C. After drying, the dispersion must form a transparent film.

Loss on drying

68.5 – 71.5 %
The test is performed according to "Dry substance / Residue on evaporation."

Assay

EUDRAGIT® RL 30 D: 10.18 - 13.73 % ammonio methacrylate units on dry substance (DS).
Alkali value: 27.5 - 37.1 mg KOH per g DS.
EUDRAGIT® RS 30 D: 6.11 - 8.26 % ammonio methacrylate units on DS.
Alkali value: 16.5 - 22.3 mg KOH per g DS.

The alkali value (AV) is defined similarly to the acid value. It states how many mg KOH are equivalent to the basic groups contained in 1 g dry substance (DS).

The assay is performed according to Ph. Eur. 2.2.20 "Potentiometric titration" or USP <541>.
2 g EUDRAGIT® RL 30 D or 4 g EUDRAGIT® RS 30 D are dried in vacuo in an oven for 30 minutes at 90 °C. Subsequently the sample is dissolved in 75 ml glacial acetic acid within about 30 minutes at approx. 50 °C. After the solution has cooled down, 25 ml copper (II) acetate solution (0.6 % solution in anhydrous acetic acid) are added and 0.1 N perchloric acid is used as the titrant.

$$AV \text{ (mg KOH / g DS)} = \frac{ml\ 0.1\ N\ HClO_4 \cdot 561}{\text{sample weight (g)} \cdot DS\ (\%)}$$

$$AV \text{ (mg KOH / g DS)} = \text{ammonio methacrylate units (\%)} \cdot 2.701$$

Assay USP/NF: the test is performed according to the USP/NF monograph.
EUDRAGIT® RL 30 D: 10.18 - 13.73 % ammonio methacrylate units on DS
EUDRAGIT® RS 30 D: 6.11 – 8.26 % ammonio methacrylate units on DS

Viscosity / Apparent viscosity

Max. 100 mPa · s
The viscosity of the dispersions is determined by means of a Brookfield viscometer
(spindle 1 / 30 rpm / 20 °C).

pH

4.0 – 6.0
The pH is determined according to Ph. Eur. 2.25.

Relative density

d_{20}^{20}: 1.047 - 1.057
The relative density of the dispersions is determined according to Ph. Eur. 2.2.5.

Coagulum content

Max. 1,000 mg / 100 g
A stainless steel wire cloth with a mesh size of 0.125 mm (mesh number 125, ISO) is accurately
weighed. 100 g of the dispersions are filtered through this cloth, which is then washed with water
until a clear filtrate is obtained, dried to constant weight at 105 °C and weighed to determine the
filtration residue.

5   Purity

Sulphated ash / Residue on ignition

Max. 0.5 %
The test is performed according to Ph. Eur. 2.4.14 or USP <281>.
1 g of the dispersions is used for the test.

Heavy metals

Max. 20 ppm
The test is performed according to Ph. Eur. 2.4.8 method C or USP <231> method II.
1 g of the dispersions is used for the test.

Methanol

Max. 1.0 %
The test is performed on according to Ph. Eur. 2.4.24, sample preparation 2.
0.200 g is used for the test.

Monomers

Ethyl acrylate: max. 30 ppm
Methyl methacrylate: max. 20 ppm
The test is performed according to the Ph. Eur. or USP/NF Monograph.

Microbial count

Total aerobic microbial count (TAMC): max. 1,000 CFU / g
Total combined yeasts and moulds count (TYMC): max. 100 CFU / g
(Acceptance criteria according to Ph. Eur. 5.1.4 / USP 1111)
The test is performed according to Ph. Eur. 2.6.12 or USP <61>.

6   Identity testing

First identification

The material must comply with the tests for "Assay" and "Viscosity / Apparent viscosity."

Second identification

IR spectroscopy on a dry film approx. 15 μm thick. The film is obtained by applying one drop of EUDRAGIT® RL 30 D / RS 30 D to a glass plate and covering with a water-resistant crystal disc (AgCl, KRS 5). By lightly pressing on and then removing the crystal disc, a clear film is obtained after a drying period of about 15 minutes at 60 °C.

The figures on page 4 show the characteristic bands of the ester groups at 1,150 - 1,190 and 1,240 and 1,270 cm^{-1}, as well as the C = O ester vibration at 1,730 cm^{-1}. In addition, CH_x vibrations can be discerned at 1,385, 1,450, 1,475 and 2,950 - 3,000 cm^{-1}.

A small absorption at 1,570 cm^{-1} is caused by the sorbic acid.

EUDRAGIT® RL 30 D
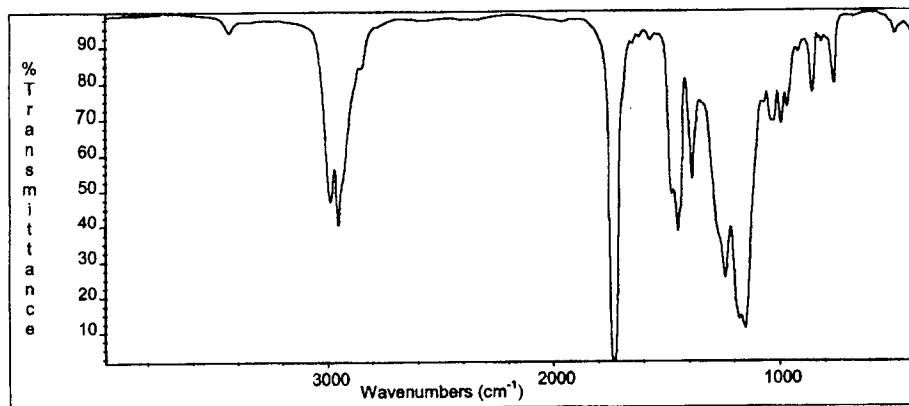
EUDRAGIT® RS 30 D
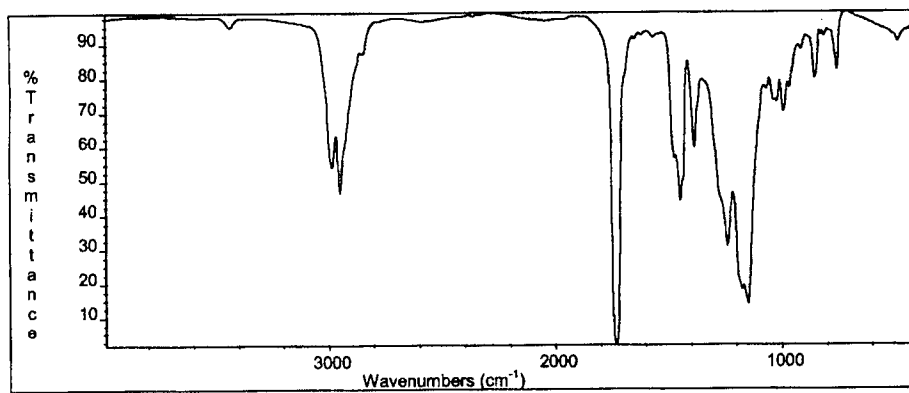
7   Detection in dosage forms

The dosage forms are extracted using the solvents listed under "Solubility" if necessary after crushing. Insoluble substances are isolated by filtration or centrifugation. The clear filtrate is boiled down and the residue identified by IR spectroscopy.

8   Storage

EUDRAGIT® RL 30 D: Store at temperatures up to 25 °C. Protect from freezing. Any storage between 8°C and 25°C fulfils this requirement.

EUDRAGIT® RS 30 D: Store at controlled room temperatures (USP, General Notices). Protect from freezing. Any storage between 8°C and 25°C fulfils this requirement.

Avoid contamination during sampling. Containers that have been opened for use should be closed again immediately and the content used up within the next few weeks.

9   Stability

Minimum stability dates are given on the product labels and batch-related Certificates of Analysis. Storage Stability data are available upon request.

WARD DECLARATION OF
April 5, 2010

IN THE UNITED STATES PATENT AND TRADEMARK OFFICE

In re application of:

WARREN WARD

Group Art Unit: 1595

Examiner: Tigabu Kassa

Serial No.:   10/595,033

Filed: January 4, 2006

For: COMPOSITIONS COMPRISING COMPONENTS COATED WITH A LIQUID IMPERMEABLE BUT GAS PERMEABLE LAYER, USE THEREOF FOR TREATING CUTANEOUS AND OTHER EXOCRINE GLAND DISEASES

Attorney Docket No.:   WAW0101PUSA

DECLARATION OF WARREN WARD
UNDER 37 C.F.R. § 1.132

Commissioner for Patents
U.S. Patent and Trademark Office
P.O. Box 1450
Alexandria, VA 22313-1450

I, Warren Ward, do hereby declare and state as follows:

1.   I graduated from UK Grammar School with certificates in English, French, English Literature, Pure Maths, Applied Maths, Physics, Chemistry, Art, and Advanced Level Pure Maths and Applied Maths.

2.   My professional background is one of executive or general manager, with employment associated with the management of large holiday centres in the UK from 1964 to 1979. From 1979 to 1996, I held a Chief Officer appointment in UK Local Government. From 1996 to 2000, I lectured in information technology at Llandrillo College, UK. I was also a Fellow of the Institute of Trade Valuers UK, and pursued that profession until 2002. From 1984 onwards, I undertook part time investigation into the health status of UK citizens and the etiology of chronic conditions. By 2002 this became a full time occupation.

3.   I am the sole inventor of the claimed subject matter of U.S.

Application Serial No. 10/595,033, hereinafter the "Application" and am familiar with the

content of the Application and the Office Action dated October 5, 2010 received from the

United States Patent and Trademark Office, hereinafter the "Office Action."

4.   I understand the pending claims 7-11, 24-28, 30-33 and 36 are rejected

under 35 U.S.C. § 101 as lacking patentable utility (Office Action, pages 2-3). In particular,

the Examiner opines that "there is insufficient evidence to show that a compound which is not

released on or into the body can have any medically beneficial effect." *Id.*

5.   The pending claims in current form are directed to a preparation for use

as a medicament. The claimed preparation is not a conventional pharmaceutical composition

or compound that must generally be dissolved into body circulation for cellular uptake and

subsequent metabolization. See for instance Applicants' Amendment dated September 23,

2009 at pages 7-10.

6.   The claimed preparation is at least partly based on the understanding

that all living cells sense and respond to their environment by means of mechanisms known

as cell signaling pathways. These mechanisms are part of a complex system of

communications that govern basic cellular activities and coordinate the actions of cells.

7.   Cell signaling refers to the process by which extracellular substances

produce an intracellular response. This is an essential and widespread biological

phenomenon by which hormones, neurotransmitters, and other agents regulate cellular

function. In some cases, the natural agent inducing the response is present on the surface of a

nearby cell, or is present in the extracellular matrix on which cells reside.

8.   From 2001 onwards, I set out to experiment and investigate the

creation of an exogenous signaling pathway as a therapeutic method of cell signaling via

epithelial surfaces and thus activating total body cellular signaling. This therapeutic method

is particularly useful for chronic conditions where the physiology has moved away from

normal natural interactive controls or homeostasis, e.g. essential hypertension. There are five great advantages of this method of treatment:

- Molecules can be used to affect cell signaling without the molecules having to be dissolved in body fluids.
- Molecules can be used to reinstate normal homeostasis of humans and animals with chronic conditions, in contrast to conventional drugs which often interfere with normal physiological processes.
- Molecules which are found naturally in the body can be used to beneficially affect cell signaling pathways.
- Since, in contrast to conventional drugs, there is no dissolution or elimination, the molecules can be carefully targeted to avoid all side effects, creating a high level of safety.
- Molecules, including established therapeutic molecules, can be used to affect cell signaling pathways more effectively, but much more safely than conventional drugs.

9.   I reasoned that the creation of an exogenous signaling pathway would require both the presence of introduced molecules in proximity to the epithelial surfaces, and transient presentation of such chemicals in microscopic quantities, or apparent microscopic quantities, to the cells of the epithelial surfaces. Induced changes in their immediate environment could be calculated to elicit a response by the epithelial cells.

10.   After a large number of experiments, it was found that a rapid response could be achieved by transient presentation of appropriate chemicals to the epithelial surface. A working method was determined to enclose chemicals within a microscopically perforated robust coating together with arrangements to ensure that these coated chemicals had constant movement, or apparent constant movement. A number of coated products can be formulated in this way. I termed this methodology 'Smart Cell Signal'™ .

11.   My research and elucidation of the 'Smart Cell Signal'™ led to the development and manufacture of the unique Equiwinner™ patches.

12.   As recited in the pending claims with particular reference to the new claim 37, the said Equiwinner™ patches are constructed to have two spheres containing sodium chloride mounted on one side of the patch and spaced apart, and the sodium chloride

is coated with an aqueous liquid impermeable but gas permeable layer comprising white beeswax hardened with talc and cornstarch, all as set out in the Application.

13.   Equiwinner™ patches were originally designed to activate angiogenesis of skin capillaries so as to reduce the excessively high blood pressure of racehorses under maximum exertion. This high pressure was known to cause exercise induced pulmonary haemorrhage (EIPH), or horse bleeding. This is a very common problem in horses. Equiwinner™ also corrects anhidrosis, or non-sweating, another previously untreatable condition in horses, particularly those in hot climates. The 'Smart Cell Signal'™ is also effective throughout the body in restoring full hydration of horse body tissues, indicating persistence of the induced cell to cell signaling. Another condition for which Equiwinner™ is rapidly effective is equine rhabdomyolysis, or azoturia, commonly known as "tying-up".

14.   I, the discoverer of the 'Smart Cell Signal'™, believe that I have described for the first time in history the full aetiology of the previously unknown cause of automatic head shaking in horses, which can be corrected using Equiwinner™.

15.   Further information related to the Equiwinner™ patches may be found at www.equiwinner.com, www.signal-health.com, and www.equinereset.co.nz.

16.   The "Equiwinner" patches have been sold to professional horse trainers in various countries including the United States, United Kingdom, Australia and New Zealand. The retail selling price has been between 123 and 130 US dollars (or the equivalent) plus carriage and tax where applicable, for a box of ten patches, plus two spare patches.

17.   The Equiwinner™ patches according to the claimed invention and in particular new claim 37, have been very well received by the horse trainers, representing the only effective treatment known for the market. The total number of Equiwinner™ patches sold in the last five consecutive calendar years were 5000 patches, 11.000 patches, 18,000 patches, 24,000 patches and 25,000 patches, with a capital value at year 2010 of several

hundred thousand dollars. The magnitude of the increase in sales is further reflective of the high quality of the Equiwinner™ patches, all constructed according to the claimed invention.

18.   In 2005, I supplied a quantity of Equiwinner™ patches, constructed according to the claimed invention and in particular according to new claim 37, to a UK veterinarian Dr. Steve Gittins. Dr Gittins is an equine specialist, a Bachelor of Veterinary Science and a Member of the Royal College of Veterinary Surgeons. In his statement dated 14 July 2005, submitted herewith as Exhibit 1, Dr. Gittins reported a positive medical effect of the said supplied Equiwinner™ patches.

19.   Later in 2005, I supplied a quantity of Equiwinner™ patches, constructed according to the claimed invention and in particular according to new claim 37, to an Italian veterinarian Dr. Paola Gulden. Dr Gulden was Vice-President of the learned Societa Italiana Veterinari per Equini (Italian Society for Equine Veterinarians) in year 2005-2007 and President in year 2007-2009. Dr Gulden treated a number of horses having Exercise Induced Pulmonary Haemorrhage by placing on the horses the said supplied Equiwinner™ patches for between three and ten days. In her statement dated December 2005, submitted herewith as Exhibit 2, Dr. Gulden reported that "All of the horse(s) had a clear improvement of the pathological condition."

20.   I understand the pending claims 7-11, 24-28, 30-33 and 36 are rejected under 35 U.S.C. § 112, first paragraph, as failing to comply with the enablement requirement (Office Action, pages 5-8). In particular, the Examiner opines that substances enclosed within a layer which is not permeable to liquid but permeable to gas cannot have any effect outside the layer when in water. For at least the following, I contend that the said substances can be detected from outside the layer and therefore can influence the environment outside the layer when in water.

21.   I made two solid spheres of about 9 mm diameter comprising sodium chloride crystals coated with white wax USP, a pharmaceutical grade of beeswax, hardened with talc and cornstarch as described in the description of the patent application para 0093.

These were each placed on a piece of aluminium, 30mm by 35mm x 2mm labelled A1 and A2, in two glass vessels and immersed in purified water BP. The vessels were covered and left in a room at 22 degrees C for 96 hours. The two spheres remained resting in the same place on the aluminium at this time. They did not float. The same two solid spheres were then carefully examined using both visual and microscopic assessment and found to be unchanged by the immersion in water. The place on the aluminium where the spheres had each been resting was the photographed at about 60 x magnification with the results shown in Exhibit 3A1 and 3A2.

22.   On examination and by photography the aluminium was found to be substantially corroded, including the removal of aluminium to a depth of 1mm, only in the place where each of the spheres had been placed. Throughout this document, I intend the word "corroded" or the like to mean that the metal or the metals have been eaten away.

23.   I then placed the two spheres on two fresh pieces of the same aluminium of the same size labelled B1 and B2, placed in the two glass vessels and immersed in fresh purified water BP. The vessels were then covered and left in a room at 22 degrees C for 96 hours. The two spheres remained resting in the same place on the aluminium at this time. The two spheres were then carefully examined using both visual and microscopic assessment and found to be unchanged by the immersion in water. The spheres did not float. The place on the aluminium where the spheres had each been resting was the photographed at about 60 x magnification with the results shown in Exhibit 3B1 and 3B2.

24.   On examination and by photography the aluminium was found to be substantially corroded, including the removal of aluminium to a depth of 1mm, only in the place where each of the spheres had been placed.

25.   I then made two solid cylinders of about 8mm length and 4mm diameter comprising sodium chloride crystals coated with white wax USP, a pharmaceutical grade of beeswax, hardened with talc and cornstarch as described in the description of the patent application para 0093. The two cylinders were each placed on two fresh pieces of the

same aluminium of the same size labelled C1 and C2, placed in the two glass vessels and immersed in fresh purified water BP. The vessels were then covered and left in a room at 22 degrees C for 96 hours. The two spheres remained resting in the same place on the aluminium at this time. The two cylinders were then carefully examined using both visual and microscopic assessment and found to be unchanged by immersion in water. The cylinders did not float. The place on the aluminium where the cylinders had each been resting was the photographed, with each of C1 and C2 requiring two photographs to cover the length of the cylinder, at about 60 x magnification with the results shown in Exhibit 3C1 and 3C2.

26.   On examination and by photography the aluminium was found to be substantially corroded, including the removal of aluminium to a depth of up to 1mm, only in the place where each of the cylinders had been placed.

27.   I made two spheres of about 9mm diameter comprising white wax USP, hardened with cornstarch and talc. However these were found to float in water and were discarded.

28.   I then made two spheres of about 9mm diameter comprising a core of a PVC sphere of about 2mm diameter coated with white wax USP, hardened with cornstarch and talc, as described in the description of the patent application para 0093. PVC was chosen as an inert substance of high enough specific gravity to prevent the spheres from floating. The two spheres were then placed on two fresh pieces of the same aluminium of the same size labelled D1 and D2 placed in the two glass vessels, and immersed in purified water BP. The two vessels were then covered and left in a room at 22 degrees C for 96 hours. The two spheres remained resting in the same place on the aluminium at this time. The two pieces of aluminium were carefully examined using both visual and microscopic assessment and found to be unchanged. I then took the two pieces of the aluminium labelled D1 and D2 and placed these in the two glass vessels. I then added to each vessel 25 ml of purified water BP in which two tenths of a gram of sodium chloride crystals had been dissolved. The vessels were then covered and left in a room at 22 degrees C for 96 hours. The two pieces of aluminium

were then carefully examined using both visual and microscopic assessment and found to be unchanged by being used. The place on the aluminium where the spheres had previously each been resting was the photographed at about 60 x magnification with the results shown in Exhibit 3D1 and 3D2.

29.   On examination and by photography the no corrosion of the aluminium was found.

30.   The same two spheres comprising sodium chloride coated with white wax BSP hardened with cornstarch and talc, used earlier with aluminium were now placed each on a zinc coated mild steel washer labelled E1 and E2 of about 30mm diameter placed in the two glass vessels and covered with purified water BP. The vessels were then covered and left in a room at 22 degrees C for 24 hours to 48 hours. The two spheres remained resting in the same place on the washer at this time. The two spheres were then carefully examined using both visual and microscopic assessment and found to be unchanged. The place on the washers where the spheres had each been resting was the photographed, with two photographs required to cover the area for E1, at about 60 x magnification with the results shown in Exhibits 3E1 and 3E2.

31.   On examination and by photography, the area under the spheres was seen to have had the zinc coating removed. The same two spheres of about 9mm diameter comprising a core of a PVC sphere of about 2mm diameter coated with white wax USP, hardened with cornstarch and talc were placed each one on a zinc coated washer of the same type, labelled F1 and F2 and placed in the two glass vessels immersed in purified water BP. The vessels were then covered and left in a room at 22 degrees C for 24 hours to 48 hours. The two spheres remained resting in the same place on the washers at this time.

32.   The two washers were then examined and found to be unchanged by being used. The place on the washers where the spheres had each been resting was the photographed at about 60 x magnification with the results shown in Exhibits 3F1 and 3F2.

33.   I have now provided an affidavit as stated above demonstrating that the substance, sodium chloride, enclosed within the liquid impermeable but gas permeable layer, does affect its immediate surrounding environment without the preparation of the invention being changed in any way. The effect on the surrounding metals is solely the result of the construction of the spheres is demonstrated by the observation that a similar amount of sodium chloride to that included in the spheres and cylinders, when dissolved in water has no corrosive effect on the metals. It should be noted that the same two spheres containing coated sodium chloride were used for periods of 96 hours then 96 hours then 48 hours in water and on inspection were not found to be changed in any way. As shown by the above test at para 27, if in fact after the whole of the time in water the sodium chloride had leaked into solution the remaining hardened beeswax layer would have become buoyant and floated upwards. This did not occur. Secondly as previously noted within Exhibit 3 submitted in response to the Office Action of January 7, 2009, "polymer membranes may be highly swollen by a penetrating liquid." Swelling did not occur with the spheres in the test. The spheres remained unchanged. It should additionally be noted that if the sodium chloride had escaped from the coating this could not be responsible for the action on the metals, only the sodium chloride within the layer had that action. The tests further support my assertion that gaseous water molecules are adjacent to the medically efficacious substance, and form a continuous thread of water between the substance, through the gas permeable liquid impermeable coating, to the surrounding liquid water.

34.   I further refer to the textbook titled "Permeation of Gases and Vapours in Polymers" previously submitted as Exhibit 2 dated April 7, 2009. This textbook clearly shows why water vapour is attracted through the polymer layer (including a wax layer) so as to be in contact with the substance within the layer, and in use to provide a thread of water between the substance and body cells.

35.   I declare that all statements made herein of my own knowledge are true and that all statements made on information and belief are believed to be true; and further that these statements were made with the knowledge that willful false statements and the like so made are punishable by fine or imprisonment, or both, under Section 1001 of Title 18 of the United States Code and that such willful false statements may jeopardize the validity of the Application and any patent issued therein.

Signed: _Warren Ward_

Warren Ward

Date: _4 APRIL 2010_

EXHIBIT 1
of April 5, 2010

Premier Veterinary Centre

S.R. Gittins BVSc GPCert (EqP) MRCVS   **S.R. Evans** BVSc MRCVS   **K. Williams**

<div>

2 Aberconwy Road
Prestatyn
Denbighshire
LL19 9HH
Tel :-01745 854646
Fax: - 01745 857707

23 Brynford Street,
Holywell,
Flintshire
CH8 7RD
Tel: - 01352 713319
Fax: - 01352 714 876

</div>

Please reply to: - **Holywell**

14th July 2005

Dear Warren

Just to give you some feedback on the Equiwinner patches.

I have used them in a number of cases as recommended and have had very good success. I have used Equiwinner for many bleeders (Exercise Induced Pulmonary Haemorrhage), some of which have been chronic cases. So far they are all doing well with no relapses. In one case a second course was needed.

A most pleasing case was a fifteen year old cob mare who had been tying up since last November. She is now back in work, doing well and 'looking fantastic'.

I have also seen Equiwinner used in showing horses and again the owners are very pleased with the shine they put on the horses and how well they look.

I am currently trialling them in poor performance and under performing horses. Although I have only so far used them on four animals, each one has shown an improvement in performance and racing time.

Yours sincerely,

Steve Gittins

EXHIBIT 2
of April 5, 2010

PRELIMINARY CLINICAL TRIAL ON "EQUIWINNER PATCH"

Introduction

Exercise-Induced Pulmonary Haemorrage (EIPH) is a widespread condition which affects the most breeds of horses undergoing strenuous athletic events. The aetiology and the pathogenesis are still unclear, several theories have been advanced concerning its developing.
Underventilated lung regions, due to small airways disease, can cause an extreme fluctuations in the alveolar pressure, which can results in parenchymal tearing or alveolar capillary rupture (Robinson et al., 1980). Also, small airways disease, coupled with maximal exercise, induces a localized hypoxia, resulting in bronchial angiogenesis, pulmonary vasoconstriction with a greater proportion of bronchial blood flowing to the alveolar capillary bed trough bronchial anastomotic connection. The advancing margin of the new vascular growth of the bronchial vessels, could be indicate as the site of haemorrage. (Clarke, 1985)

Its prevalence is estimate to be between 75% and 26% in the Thoroughbred and in the Standarbred. The prevalence of EIPH increases with the age of the horse, there is no clear correlation between EIPH and the location of stables, condition or type of the track (Pascoe et al., 1981, Voynick et al., 1986). It has been statistically demonstrated that EIPH is a cause of reduced performance in race horses (Hinchcliff, 2004).

Diagnosis is based on the assessment of the presence of blood in the upper respiratory tract. The presence of epistaxis or traces of blood at the nostrils, is usually only present in the most severe cases of EIPH, therefore tracheobronchoscopic examination is considered the elective diagnostic tool (Mac Namara et al, 1990, Birks et al, 2002). Cytologic count on fluid obtained by bronchoalveolar lavage is another method which can give a quantification of the haemorrage (Meyer et al, 1998). The collection of lavage fluid may detect haemorrage that is not evident on endoscopic examination, but this technique is considered to be impractical, being invasive and requiring sedation of the horse and often, administration of local anesthetic solution into the airways (Hinchcliff et al, 2004).

There are no effective treatments for EIPH. A better management of the environment has been recommended, with the aim to reduce any source of dust or mold. Medical treatments, such as corticosteroids to reduce the inflammatory reaction in the lung, bronchodilators to improve ventilation and airway secretions and to increase mucociliary clearence, diuretics (furosemide) to reduce pulmonary

pressure and resistance, have been and are currently used to try to minimize the negative effects of EIPH associated with poor performances (Ainsworth et al., 2000).

Equiwinner Patch is a device which works on the equine organism to restore normal homeostasis, balancing intra and extra cellular fluids, using a patented messenger cell signalling technology. The device is totally drug free, therefore there is no chemical action on the body of the horse.

In this clinical study Equiwinner Patches have been used, following the instruction of the manufacturer, to treat EIPH in Standardbred horses. This study, which has not the features of a clinical experiment on a scientist basis, aims to give a preliminary idea of the effectiveness of the Equiwinner Patches.

Materials and methods

Five Standarbred horses with a known history of EIPH of different grade of severity, were considered. The horses, three stallions, one female and one gelding, of age between three and six year old, were regularly trained all in the same stable, in the North-West of Italy. All the horses were fed, managed and trained in a similar way.
All the horses were vaccinated and wormed on a regular basis. All the horses were not on any kind of medical treatments during the period of this study.
This study was performed over a period of time of five months, from July to November 2005.

Assessment of severity of EIPH was performed by endoscopic examination of the upper airways, and classification of gravity of EIPH was based on a grading system which consists of five levels (0-4), based upon the amount and location of blood in the upper respiratory tract (Hinchcliff et al., 2004). In one case, (horse C) EIPH was revealed by the bronchoalveolar lavage (BAL) during a previous complete examination on high speed treadmill. The cytological examination of the BAL revealed a number of red cells and of hemosiderophages consistent with recent episodes of haemorrage, despite of the endoscopic examination which revealed no presence of blood (grade 0).

The five horses were divided into two groups. The first group was composed by three horses, two (horses A, B) with history of EIPH of grade 4, and one with history of EIPH of grade 0, but episodes of significant EIPH were revealed by the BAL cytological examination (horse C). The second group (horses D,E) included horses with EIPH from grade 1 to 2.

In the first group, horses were rested for a period of ten days. During this period of time the Equiwinner Patch was applied daily, at the top of the hindquarter, as recommended. Horses were walked by hand or in the walker twice a day. No access to paddocks was allowed to the horses because of the hot climate at the time of the experiment. Horses were gradually put back on normal training at the end of the treatment and raced as soon as they were considered ready for it.

Horses belonging to the second group were kept on normal training and treated with Equiwinner Patches, once a day, for five days prior the day of the race. In one case the course of treatment was reduced to three days, because the declaration of participants was to close to the date of the race. Equiwinner Patch was removed only during the actual exercise, and replaced after the horses were showered and dried.

In both groups, endoscopic examination was performed 45 to 60 minutes after racing, the horses were unsedated and restrained by use of a nose twitch.
As a part of normal health checking during training, all horses were tested for lactate serum level after each session of training.

Results

First group

Horse A: 6yo, bay stallion. Known history of EIPH grade 4.
Very good performance at the first race, ten days after the end of treatment (second after a brake at the start). Endoscopic examination after race revealed no blood in the upper airways (grade 0). Lactate serum level were improved during normal training. At the second race after treatment the horse performance was lower, endoscopic examination revealed presence of mucus and some flecks of blood in trachea (grade 1).

Horse B: 4yo, bay stallion. Known history of EIPH grade 4.
This horse was put back in training and checked at the stable after the first fast training. This horse was used to be trained at this speed after furosemide (Lasix) administration. In this case, with no pharmacological treatment, the endoscopic examination 45 minutes after exercise was completely negative. Also the serum lactate level was under usual values. Good performance on first and second race after treatment, despite the presence of a narrow stream of blood in the trachea at endoscopic examination (grade 1).

Horse C: 6yo, bay gelding. History of poor performances in the last few months, complete clinical examination revealed signs of recent episodes of EIPH at the

BAL cytological count. Never had evidence of blood at the endoscopic examination after exercise.

Very good results at the first and second race after treatment, improved serum lactate level. Endoscopy always negative, unfortunately it was not possible to perform a BAL to check the cytological count. This horse was also definitely in a better general conditions after the period of treatment.

Second group

Horse D: 3yo, chestnut female. History of EIPH grade 2.
Treated twice with a course of five days prior of the day of race. Moderate improvement of performances at both races, presence of flecks and very narrow stream of blood (grade 1), lactate serum level not significantly changed during normal training.

Horse E: 5yo, bay stallion. History of EIPH grade 1 to 2.
Treated twice with a five days course and one with a three days course because declaration of participants was closer to the day of race.
Good performances at the first two races, not very well at the third. Endoscopic examination negative at the first and second time, presence of one long stream of blood in the trachea at the third examination after racing. Presence of flakes of witish mucus suggested the presence of a subclinic respiratory disease.

Finally, horse A, belonging to group one, received other two course of five days the first time prior to the day of race, with the same protocol followed for the group two, about two months after the end of the primary treatment. The horse performed well again, endoscopic examination was of grade 1 on both occasion, with very narrow stream of blood in the trachea (grade 1).

Discussion

Even if the number of horses examined is too low to assess effectiveness of Equiwinner Patches, results are definitely very encouraging. All the horse had a clear improvement of the pathologic condition, particularly the ones belonging to the first group, who received a longer treatment coupled with a period of rest. The association of other stressful factors with poor performances, such as travelling, and the individual capability to react to these factors, needs to be further investigated, to clear up if the uncomplete response to the treatment with Equiwinner patch can be related to these factors. Furthermore, period of rest plays a determinant rule in reducing the severity of EIPH.

Good results were also obtained treating a horse for ten days and giving a shorter course of treatment two or three months later. Further studies are required to optimise the use of this device in treatment and prevention of EIPH.

Bibliography

- Robinson NE, Derksen FJ : Small airways obstruction as a cause of EIPH : an hypothesis. Am. Assoc. Equine Pract. 26:41, 1980
- Clarke AF: review of EIPH and its possible relationship with mechanical stress. Equine Vet. J.17:166, 1985
- Pascoe JR, Ferraro GL,Cannon JH et al: EIPH in racing thoroughbreds: a preliminary study. Am. J. Vet. Res. 42:701, 1981
- Voynick BR, Sweeney CR: EIPH in polo and racing horses. J .Am. Vet. Med. Ass. 188:301, 1986
- Hinchcliff KW, Jackson MA, Morley PS et al: Association between EIPH and performance by thoroughbred race horses. Report for the Rural Ind. Res. And Development Corp. 6-17, 2005
- Mac Namara B, Bauer S, Iafe J: Endoscopic evaluation of EIPH and chronic obstructive pulmonary disease in association with poor performances in racing Standardbred. J. Am. Vet. Med. Ass. 26: 482-485, 1990
- Birks EK, Shuler KM, Soma LR et al: EIPH: post race endoscopic evaluation of Standarbreds and Thoroughbreds. Equine Vet. J. Supplement 34, 375-378, 2002.
- Hinchcliff KW, Jackson MA, Brown JA, et al: Tracheobronchocopic assessment of EIPH in Thouroghbred race horses. Report for the Rural Ind. Res. And Development Corp. 2-5, 2005
- Ainsworth DM, Biller DS: Respiratory System, in: Reed SM, Bayly WM: Equine Internal Medicine, 281-282 Saunders Edition, 2000

Pooly Gulden

Paola Gulden, DMV
Italy, December 2005

EXHIBIT 4A

of April 5, 2010

pancreatic β cells. The drug is absorbed rapidly from the gastrointestinal tract; peak blood levels are obtained within one hour. The half-life of the drug is about one hour. These features of the drug allow for multiple preprandial use, as compared to the classical once- or twice-daily dosing of sulfonylureas. Repaglinide is metabolized primarily by the liver. Metabolites of the drug do not have a hypoglycemic action. Repaglinide should be used cautiously in patients with hepatic insufficiency. Because a small proportion (about 10%) of repaglinide is metabolized by the kidney, increased dosing of the drug in patients with renal insufficiency also should be performed cautiously. As with sulfonylureas, the major side effect of repaglinide is hypoglycemia.

Nateglinide

Nateglinide (STARLIX) is an orally effective insulin secretagogue derived from D-phenylalanine. Like sulfonylureas and repaglinide, nateglinide stimulates insulin secretion by blocking ATP-sensitive potassium channels in pancreatic β cells. Nateglinide promotes a more rapid but less sustained secretion of insulin than do other available oral antidiabetic agents (Kalbag *et al.*, 2001). The drug's major therapeutic effect is reducing postprandial glycemic elevations in type 2 diabetic patients. Nateglinide recently has been approved by the United States Food and Drug Administration (FDA) for use in type 2 DM and is most effective if administered 1 to 10 minutes before a meal in a dose of 120 mg. Nateglinide is metabolized primarily by the liver and thus should be used cautiously in patients with hepatic insufficiency. About 16% of an administered dose is excreted by the kidney as unchanged drug. Dosage adjustment is unnecessary in renal failure. Early studies have suggested that nateglinide therapy may produce fewer episodes of hypoglycemia than do other currently available oral insulin secretagogues (Horton *et al.*, 2001).

Biguanides

Metformin (GLUCOPHAGE) and phenformin were introduced in 1957 and buformin was introduced in 1958. The latter was of limited use, but metformin and phenformin were widely used. Phenformin was withdrawn in many countries during the 1970s because of an association with lactic acidosis. Metformin has been associated only rarely with that complication and has been widely used in Europe and Canada; it became available in the United States in 1995. Metformin given alone or in combination with a sulfonylurea improves glycemic control and lipid concen-

trations in patients who respond poorly to diet or to a sulfonylurea alone (DeFronzo *et al.*, 1995).

Metformin is absorbed mainly from the small intestine. The drug is stable, does not bind to plasma proteins, and is excreted unchanged in the urine. It has a half-life of about 2 hours. The maximum recommended daily dose of metformin in the United States is 2.5 g, taken in three doses with meals.

Metformin is antihyperglycemic, not hypoglycemic (*see* Bailey, 1992). It does not cause insulin release from the pancreas and does not cause hypoglycemia, even in large doses. Metformin has no significant effects on the secretion of glucagon, cortisol, growth hormone, or somatostatin. Metformin reduces glucose levels primarily by decreasing hepatic glucose production and by increasing insulin action in muscle and fat. The mechanism by which metformin reduces hepatic glucose production is controversial, but the preponderance of data indicates an effect on reducing gluconeogenesis (Stumvoll *et al.*, 1995). Metformin also may decrease plasma glucose by reducing the absorption of glucose from the intestine, but this action has not been shown to have clinical relevance.

Patients with renal impairment should not receive metformin. Hepatic disease, a past history of lactic acidosis (of any cause), cardiac failure requiring pharmacological therapy, or chronic hypoxic lung disease also are contraindications to the use of the drug. The drug also should be withheld for 48 hours after administration of intravenous contrast media. The drug should not be readministered until renal function is normal. These conditions all predispose to increased lactate production and hence to the fatal complications of lactic acidosis. The reported incidence of lactic acidosis during metformin treatment is lower than 0.1 case per 1000 patient years, and the mortality risk is even lower.

Acute side effects of metformin, which occur in up to 20% of patients, include diarrhea, abdominal discomfort, nausea, metallic taste, and anorexia. These usually are minimized by increasing the dosage of the drug slowly and taking it with meals. Intestinal absorption of vitamin B_{12} and folate often is decreased during chronic metformin therapy. Calcium supplements reverse the effect of metformin on vitamin B_{12} absorption (Bauman *et al.*, 2000).

Consideration should be given to stopping treatment with metformin if the plasma lactate level exceeds 3 mM. Similarly, decreased renal or hepatic function also may be a strong indication for withholding treatment. It also would be prudent to stop metformin if a patient is undergoing a prolonged fast or is treated with a very-low-calorie diet. Myocardial infarction or septicemia mandate stopping the drug immediately. Metformin usually is

administered in divided doses either two or three times daily. The maximum effective dose is 2.5 g daily. Metformin lowers hemoglobin A_{1c} values to a similar extent as do sulfonylureas (about 2.0%). Metformin does not promote weight gain and can reduce plasma triglycerides by 15% to 20%. There is a strong consensus that reduction in hemoglobin A_{1c} by any therapy (insulin or oral agents) can lead to diminished microvascular complications. Metformin, however, is the only therapeutic agent that has been demonstrated to reduce macrovascular events in type 2 DM (UK Prospective Diabetes Study Group, 1998b). Metformin can be administered in combination with sulfonylureas, thiazolidinediones, and/or insulin. A fixed-combination tablet containing glyburide (glibenclamide) and metformin (GLUCOVANCE) is available.

Thiazolidinediones

Three thiazolidinediones have been used in clinical practice (troglitazone, rosiglitazone, and pioglitazone). However, the first of these agents to be introduced (troglitazone) has been withdrawn from use because it was associated with severe hepatic toxicity. The structures of rosiglitazone and pioglitazone are shown below.

ROSIGLITAZONE

PIOGLITAZONE
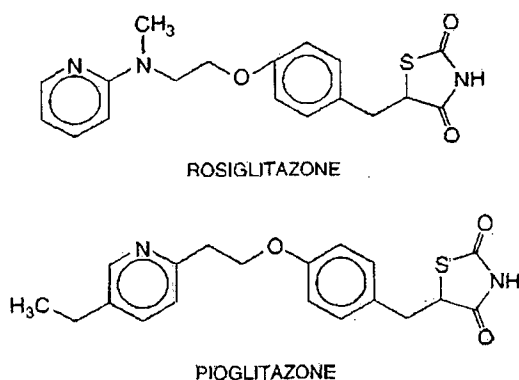
Thiazolidinediones are selective agonists for nuclear peroxisome proliferator–activated receptor-gamma ($PPAR_\gamma$). These drugs bind to $PPAR_\gamma$, which, in turn, activates insulin-responsive genes that regulate carbohydrate and lipid metabolism. Thiazolidinediones require insulin to be present for their action. Thiazolidinediones exert their principal effects by lowering insulin resistance in peripheral tissue, but an effect to lower glucose production by the liver also has been reported. Thiazolidinediones increase glucose transport into muscle and adipose tissue by enhancing the synthesis and translocation of specific forms of the glucose transporter proteins. The thiazolidinediones also can activate genes that regulate free fatty-acid

metabolism in peripheral tissue. Studies are in progress to determine if these agents reduce insulin resistance primarily by their actions on free fatty-acid metabolism.

Rosiglitazone (AVANDIA) and pioglitazone (ACTOS) are taken once a day. Both agents are absorbed within about 2 hours, but the maximum clinical effect is not observed for 6 to 12 weeks. The thiazolidinediones are metabolized by the liver and may be administered to patients with renal insufficiency, but these agents should not be used if there is active hepatic disease or if there are significant elevations of serum liver transaminases.

Regular monitoring of liver funtion should be instituted in patients receiving thiazolidinediones. Thiazolidinediones also have been reported to cause anemia, weight gain, edema, and plasma volume expansion. These drugs generally are not indicated for patients with New York Heart Association class 3 and 4 heart failure.

Rosiglitazone and pioglitazone can lower hemoglobin A_{1c} levels by 1.0% to 1.5% in patients with type 2 DM. These drugs can be combined with insulin or other classes of oral glucose-lowering agents. The thiazolidinediones tend to lower triglycerides (10% to 20%) but increase both HDL (up to 19%) and LDL (up to 12%) cholesterol. The increased LDL has been reported to reflect a change in particle size from a dense to a more buoyant, less atherogenic compound.

Both available thiazolidinediones are metabolized by cytochrome P450 enzymes in the liver. Rosiglitazone is metabolized by CYP2C8 and pioglitazone by CYP3A4 and CYP2C8. Metabolism by these hepatic enzymes provides the potential for interactions with other classes of drugs that are metabolized via these pathways. To date, no clinically significant interactions have been identified between the available thiazolidinediones and other drug classes, but further studies are in progress.

α-Glucosidase Inhibitors

α-Glucosidase inhibitors reduce intestinal absorption of starch, dextrin, and disaccharides by inhibiting the action of intestinal brush border α-glucosidase. Inhibition of this enzyme slows the absorption of carbohydrates; the postprandial rise in plasma glucose is blunted in both normal and diabetic subjects.

Acarbose (PRECOSE), an oligosaccharide of microbial origin, and miglitol (GLYSET), a desoxynojirimycin derivative, also competitively inhibit glucoamylase and sucrase but have weak effects on pancreatic α-amylase. They reduce postprandial plasma glucose levels in type 1 DM and type 2 DM subjects. α-Glucosidase inhibitors can have profound effects on hemoglobin A_{1c} levels in severely

McGraw-Hill

A Division of The McGraw-Hill Companies

EXHIBIT 4B

of April 5, 2010

Metformin modulates insulin post-receptor signaling transduction in chronically insulin-treated Hep G2 cells

YUAN Li[1], Reinhard ZIEGLER, Andreas HAMANN[2]

[2]*Department of Endocrinology and Metabolism in Hospital of University Heidelberg, Heidelberg 69115, Germany*

KEY WORDS metformin; insulin receptors; signal transduction

ABSTRACT

AIM: To study the effect of chronic insulin treatment on insulin post-receptor signaling transduction and whether the effects of metformin are transmitted throughout the cascade of insulin signaling intermediates in a human hepatoma cell line (Hep G2). **METHODS:** Hep G2 cells were incubated in serum free media containing either insulin 100 nmol/L or insulin 100 nmol/L plus different concentrations (0.01-10 mmol/L) of metformin for 16 h and then were stimulated with insulin 100 nmol/L for 1 min. **RESULTS:** Chronic treatment of insulin 100 nmol/L induced a significant reduction in the phosphorylation and protein expression of IRß, IRS1 and IRS2, which therefore resulted in a downregulation of association of PI3K with IRS. Therapeutic concentrations (0.01-0.1 mmol/L) of metformin prevented the changes induced by chronic insulin treatment in these post-receptor components of insulin signaling pathway. Tyrosine phosphorylation of IRβ, IRS1, and IRS2 was increased by 2.7 fold (*P*<0.01), 6.8 fold (*P*<0.01), and 2.3 fold (*P*<0.01) of chronically insulin-treated cells alone, respectively, after metformin 0.1 mmol/L was added. The association of p85 with IRS1 and IRS2 was also increased from 34 % to 86 % (*P*<0.01) and from 30 % to 92 % (*P*<0.01), respectively. In contrast, metformin in pharmacological concentration (1-10 mmol/L) further inhibited tyrosine phosphorylation of IRβ, IRS1, IRS2 and the interaction of PI3K with IRS. The association of IRS1 with p85 was further decreased by 58 % (*P*>0.05) and of IRS2 by 30 % (*P*<0.05). **CONCLUSION:** Chronic insulin exposure of Hep G2 cells induces the downregulation of insulin signal transduction via PI3K pathway. The effect of metformin on insulin signaling transduction represent a primary mechanism of metformin action in insulin resistant state.

INTRODUCTION

Metformin is an antihyperglycemic drug that treats insulin resistance and it has become a first-line choice of type 2 diabetes therapy. In recent years, research into the pharmacodynamic properties of metformin and their clinical implications has resulted in a renewal of interesting[1]. The liver is not only a key tissue for glucose metabolism, but also a major site of metformin action. Recently, the importance of hepatic insulin resistance in glucose homeostasis has been emphasized[2]. In hepatocytes, insulin resistance can result from impaired signaling downstream of the insulin receptor[3]. Antihyperglycemic effect of metformin is mainly a consequence of reduced hepatic glucose output.

[1] Correspondence to Dr YUAN Li, now in *Department of Endocrinology in Union Hospital of Tongji Medical College, Huazhong University of Science and Technology, Wuhan 430022, China.*
Phn 86-27-8572-6136. Fax 86-27-8577-6343.
E-mail yuanli18cn@yahoo.com.cn

However, the molecular basis of metformin effect on hepatocytes is largely unknown, involving the possible effects of metformin on insulin signaling tranduction, for instance, metformin could directly or indirectly influence protein-protein interactions within the signaling cascade.

Chronic hyperinsulinsm can induce insulin resistance[4]. Therefore, in the present study, we set up an insulin resistant cell model, with the Hep G2 cells chronic exposure to high concentration of insulin. The aim is: (1) to examine the changes in insulin signaling transduction after chronic insulin treatment. (2) to determine whether the antihyperglycemic action of metformin in hepatocytes is associated with effects on signaling protein expression and phosphorylation.

MATERIALS AND METHODS

Chemicals RPMI-1640 medium and fetal bovine serum (FBS) were obtained from Gibco BRL (Karlsruhe, Germany). Reagents for sodium dodecyl sulfate-polyacrylamide gel electrophoresis (SDS-PAGE) and immunoblotting were obtained from Bio-Rad (Hercules, CA). Rabbit polyclonal anti-insulin receptor β-subunit (IRβ), anti-insulin receptor substrate 1 (IRS1), anti-insulin receptor substrate 2 (IRS2), and anti-p85 subunit of phosphatidylinositol 3-kinase (PI3K) antibodies used for Western blotting were purchased from UBI (Lake Placid, NY). Anti-biotin and mouse monoclonal anti-phosphotyrosine (PY) antibody were from New England Biolabs (Frankfurt am Main, Germany). Protein A and protein G sepharose and BCA-assay reagents were purchased from Pierce (Hamburg, Germany). HRPO-conjugated anti-mouse and anti-rabbit antibodies, reagents for ECL were obtained from Amersham Pharmacia Biotech (Uppsala, Sweden). Human insulin (Actrapid) was obtained from Novo Nordisk (Deisenhofen, Germany). Metformin, aprotinin, pepstatin, leupeptin, and other reagents were from Sigma (Steinheim, Germany).

Cell culture Hep G2 human hepatoma cells were grown to confluence in 10-cm plastic culture dishes containing 10 mL RPMI-1640 medium supplemented with 10 % fetal bovine serum, HEPES 25 mmol/L (pH 7.4), 1 % penicillin /streptomycin and glutamine 25 mmol/L. The cells were incubated at 37 °C in a humidified atmosphere of 5 % CO_2 and 95 % air.

Confluent Hep G2 cells were incubated in serum free media including either insulin 100 nmol/L or insulin 100 nmol/L plus metformin 0.01-10 mmol/L for 16 h and then were stimulated with insulin 100 nmol/L for 1 min, as specified in the results section. Cells under basal conditions were used as controls.

Immunoprecipitation and Western blotting Phosphorylated proteins of IRβ, IRS1, IRS2 and interaction of PI3K with IRS were determined by immunoprecipitation assay. protein lysates 1000 μg were subjected to immunoprecipitstion using corresponding specific antibodies (anti-IRβ, anti-IRS1, anti-IRS2) and incubation at 4 °C for 2 h. Protein-antibody complexes were conjugated with protein A and Protein G for another 1 h. Precipitates were take up in 30 μL sample buffer containing Tris 62.5 mmol/L, dithiothreitol (DTT) 100 mmol/L, 10 % glycerol, 2 % SDS, 0.01 % bromphenolblue and denatured at 95 °C for 10 min. Protein samples were subjected to 7.5 % SDS-PAGE. After SDS-PAGE, electrotransfer of protein from the gel to nitrocellulose membranes was performed by Western blotting. Subsequently, nitrocellulose filters were incubates at 4 °C overnight with one of the following antibodies (1st antibody) at a concentration of 1 mg/L: anti-PY, anti-IRβ, anti-IRS1, anti-IRS2 or anti-p85, each of those suspended in 2.5 % non-fat dried milk. Blots were then incubated with 1:3000 HRPO conjugate (2nd antibody) at room temperature (28 °C) for 1 h. Immunoreactive bands were determined with the ECL detected reagents.

Immunoblotting Relative protein levels of IRβ, IRS-1, IRS-2, and p85 were determined by Western-immunoblotting in total cell lysates. Similar size aliquots of sample (150 μg) were processed for 7.5 % SDS-PAGE and proteins were separated by electrophoresis. Immunoblotting was performed as described above.

Statistical analysis Relative amounts of immunoreactive proteins were quantitated by Image Quant scanning densitometry. Experimental results were expressed as mean±SD. Statistical analysis was performed by Student's *t*-test. Statistical significance was assessed at $P < 0.05$.

RESULTS

Effect of metformin on protein levels and phosphorylation of signaling proteins following chronic insulin treatment In the basal state, no or little tyrosine phosphorylation of IRβ, IRS1, and IRS2 was detectable. Acute stimulation with insulin for 1 min resulted in an extensive phosphorylation on tyrosine

residues of signaling proteins. After cells were treated with insulin 100 nmol/L for 16 h, insulin-induced autophosphorylations of IRβ, IRS1, and IRS2 were significantly decreased. By comparison with control cells, tyrosine phosphorylation of IRβ was decreased to 22 % (*P*<0.01) of control level. For IRS1 an even more significant reduction in insulin-induced phosphorylation was observed, as anti-PY detectable protein was reduced to 15 % (*P*<0.01). Similar to the changes in IRS1, tyrosine phosphorylation of IRS2 was decreased to 22 % (*P*<0.01) of control levels (Fig 1).

Therapeutic concentrations of metformin 0.01 mmol/L and 0.1 mmol/L reversed the reduction of tyrosine phosphorylation of insulin signaling protein induced by chronic insulin treatment. Tyrosine phosphorylation of IRβ was increased by 2.3 fold (*P*<0.01) and 2.7 fold (*P*<0.01) of chronically insulin treated cells alone. Tyrosine phosphorylation of IRS1 was increased by 6.4 fold (*P*<0.01) and 6.8 fold (*P*<0.01), and phosphorylation of IRS2 was increased 2.8 fold (*P*<0.01) and 2.3 fold (*P*<0.05) after cells were preincubated with insulin 100 nmol/L for 16 h in the simultaneous presence of metformin 0.01 mmol/L and 0.1 mmol/L, respectively.

When the concentration of metformin was further increased to pharmacological doses (1-10 mmol/L), the effect of metformin on insulin signal transduction became inhibitory. Tyrosine phosphorylation of IRβ was further decreased to 3 % (*P*<0.01) of control levels. Quite similar observations were made for IRS1 and IRS2. When metformin 10 mmol/L was added, IRS1 tyrosine phosphorylation was further decreased to only 4 % (*P*<0.01) and IRS2 phosphorylation to 11 % (*P*<0.01) of control levels (Fig 1).

There were also significant changes in protein expression levels of IRβ, IRS1, and IRS2 following insulin 100 nmol/L chronic treatment. Protein level of IRβ was decreased to 42 % (*P*<0.01) of control levels, IRS1 was decreased to 63 % (*P*<0.01) and IRS2 was decreased to 47 % (*P*<0.05) compared to controls. However, this chronic hyperinsulinism induced reduction of protein levels was reversed after cells were preincubated with different concentrations of metformin. Level of IRβ was increased by 1.1 fold (*P*<0.01) in the presence of metformin 0.01 mmol/L and 1.6 fold (*P*<0.01) in the presence of metformin 10 mmol/L. Levels of IRS1 and IRS2 did not significantly changed following physiological concentration of metformin treatment and increased by 43 % (*P*<0.01) and 112 %
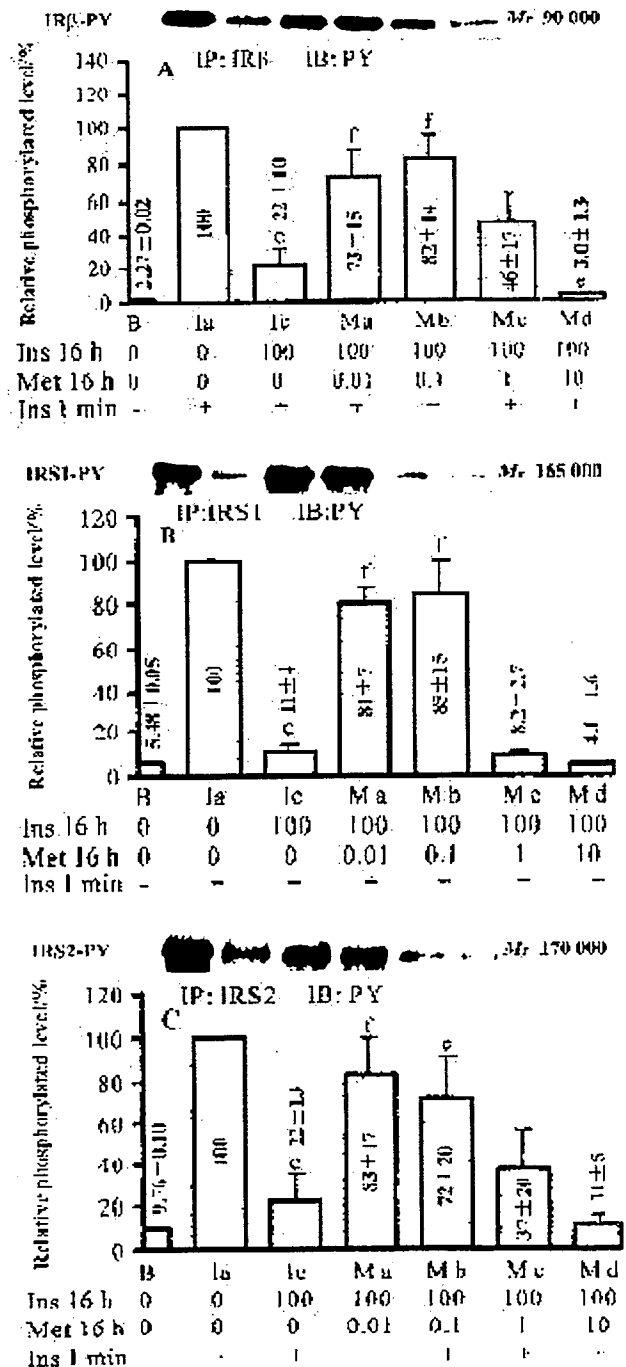

Fig 1. Effects of metformin on tyrosine phosphorylation of IRβ (A), IRS1 (B), and IRS2 (C) after chronic insulin treatment. Hep G2 cells were treated either without insulin (Ia), or with insulin 100 nmol/L (Ic) or with insulin 100 nmol/L and metformin 0.01, 0.1, 1, 10 mmol/L (Ma, Mb, Mc, Md) for 16 h and then were stimulated with insulin 100 nmol/L for 1 min, and cells cultured without these drugs were used to demonstrate the basal level (B). A typical blot for scanning densitometry by Image Quant (Molecular Dynamics) is shown above. *n*=4. Mean±SD. They are expressed as relative to Ia values, which were set at 100 %. [c]*P*<0.01 *vs* Ia. [e]*P*<0.05, [f]*P*<0.01 *vs* Ic. IP, immunoprecipitation; IB, immunoblot; Met, metformin; Ins, insulin.

($P<0.01$) by exposure to metformin 10 mmol/L (Tab 1).

Tab 1. Effects of metformin on protein levels of insulin signaling molecules after chronic insulin treatment. $n=4$. Mean±SD. $^c P<0.01$ vs control. $^e P<0.05$, $^f P<0.01$ vs Ic.

	IRβ	IRS1	IRS2	p85
Control	0.167±0.012	0.35±0.03	0.241±0.010	0.38±0.03
Ia	0.18±0.06	0.34±0.06	0.238±0.017	0.39±0.05
Ic	0.07±0.03^c	0.217±0.021^c	0.107±0.017^c	0.36±0.05
Ma	0.15±0.05^f	0.27±0.05^c	0.173±0.023	0.37±0.04
Mb	0.13±0.05^c	0.26±0.04^c	0.152±0.017	0.35±0.06
Mc	0.21±0.07^f	0.29±0.05^c	0.134±0.021	0.37±0.06
Md	0.19±0.04^f	0.31±0.03^f	0.24±0.05^f	0.38±0.05

HepG2 cells were treated either without addition of insulin (Ia), or with insulin 100 nmol/L (Ic) or with insulin 100 nmol/L plus metformin 0.01, 0.1, 1, 10 mmol/L (Ma, Mb, Mc, Md) for 16 h and then stimulated with insulin 100 nmol/L for 1 min, cells cultured without these drugs were used to demonstrate the basal control. The data are OD values of Scanning densitometry by Image Quant (Molecular Dynamics).

Effect of metformin on the interaction of IRS1 and IRS2 with PI3K following chronic insulin treatment To determine the effect of reduced IRS1 and IRS2 expression and phosphorylation after chronic insulin treatment on their interaction with the p85 subunit of PI3K, blots with immunopresipitates for IRS1 and IRS2 were immunoblotted with anti-p85 antibodies. As described above, cells pretreated in the absence of insulin responded to an acute maximal insulin stimulation with an increase in IRS-associated p85 of more than 10-fold. In contrast, after the cells were exposed to insulin 100 nmol/L for 16 h, immunodetectable p85 was significantly decreased, which was consistent with changes in phosphorylation of IRS1 and IRS2. However, in the presence of metformin 0.01 mmol/L, these effects of chronic insulin treatment on the association of IRS with p85 were reserved. Immunode-tectable p85 was increased from 34 % to 86% ($P<0.01$) of control levels in anti-IRS1 immunopre-cipitates and from 30 % to 92 % ($P<0.01$) in anti-IRS2 immunoprecipitates. When the dose of metformin was further increased to the pharmacological concentration 10 mmol/L, association of IRS1 with p85 was further decreased by 58 % ($P>0.05$) and of IRS2 by 30 % ($P<0.05$) of chronic treatment with insulin 100 nmol/L alone (Fig 2).
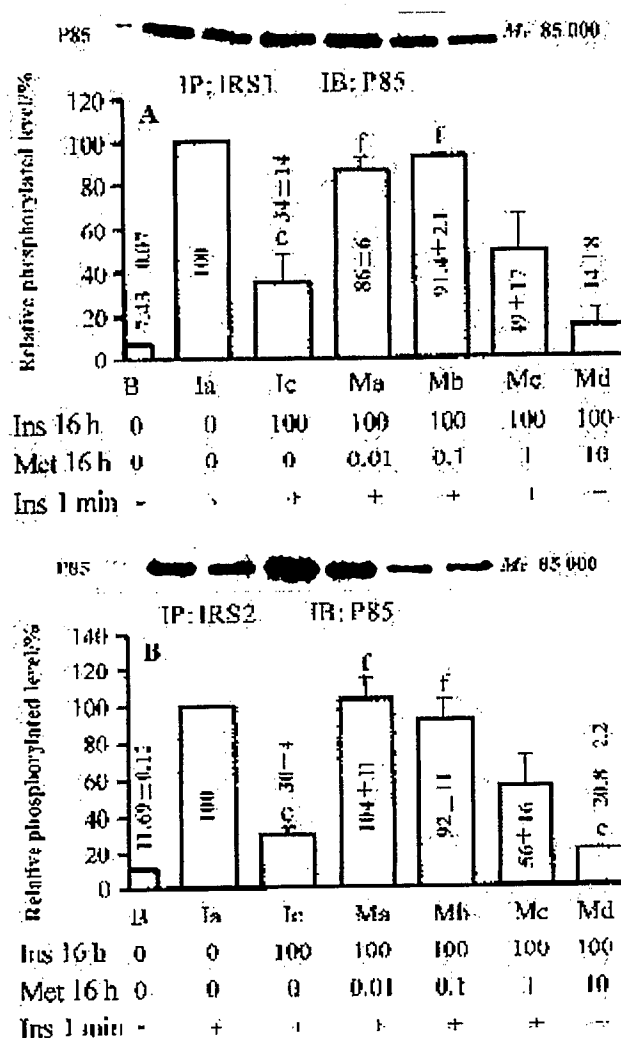

Fig 2. Effects of metformin on association of p85 subunit of PI3K with IRS1 (A) and IRS2 (B) after chronic insulin treatment. HepG2 cells were treated either without insulin (Ia), or with insulin 100 nmol/L (Ic) or with insulin 100 nmol/L and metformin 0.01, 0.1, 1, 10 mmol/L (Ma, Mb, Mc, Md) for 16 h and then were stimulated with insulin 100 nmol/L for 1 min, and cells cultured without these drugs were used to demonstrate the basal level (B). A typical blot for scanning densitometry by Image Quant (Molecular Dynamics) is shown above. $n=4$. Mean±SD. They are expressed as relative to Ia values, which were set at 100 %. $^c P<0.01$ vs Ia. $^e P<0.05$, $^f P<0.01$ vs Ic. IP, immunoprecipitation; IB, immunoblot; Met, metformin; Ins, insulin.

The protein expression of p85 was not significantly changed, either therapeutic or pharmacological concentrations of metformin added to the media (Tab 1).

DISCUSSION

Chronic hyperinsulinism can induce insulin resistance[4]. Cells cultured exposured to the high concentrations of insulin is an established model to induce

insulin resistance *in vitro*[4,5]. Thereby, in the present study, we first set up an insulin resistant model by using chronic treatment of Hep G2 cells with high doses of insulin. Such *in vitro* allows direct assessment of the effect of an additional treatment on the biological response to insulin stimulation. Since metformin exerts its beneficiary antihyperglycemic effect primarily in liver, this should also involve an alteration of the insulin resistant state in this organ. Therefore, it appeared interesting to focus on determining relevant molecules which transmit the effects of metformin within the insulin signaling cascade in a liver cell model system, in which insulin resistance had been induced. The data described here have suggested that impaired insulin signal transduction linked to IRβ, IRS1, IRS2, and PI3K is associated with insulin resistance, which was caused by chronic insulin treatment.

Metformin could interact with insulin at many potential steps, including the increased binding of insulin to its receptor[6], the intensified of insulin receptor tyrosine kinase activity[7-9], the elevated inositol-1,4,5-trisphosphate production, the augmented glycogen synthesis, and the inhibition of PEPCK as a key enzyme of gluconeogenesis[10]. In present experiment, the effect of chronic insulin treatment can be reversed by metformin. It suggests that metformin's action site is most likely located at an early post-receptor level and may directly or indirectly interact with the intracellular insulin signaling cascade.

Up to now, there were only a few reports regarding the effect of metformin on intracellular insulin signaling system and there has been a controversy in different experiments. Metformin was reported to increase insulin signaling transduction in cholesterol-treated Hep G2 cells[11] and to reverse chronic insulin effects on insulin signaling in rat adipocytes[5]. However, metformin treatment had no effect on insulin signaling cascade in human adipoctey[12] and skeletal muscle[13]. These different observations may be due to difference of tissues and cultured conditions. In the present study, therapeutic doses of metformin have reversed the reduction in phosphorylation of IRβ, IRS1, and IRS2 induced by chronic insulin treatment. Namely, through elevation of tyrosine phosphorylation of the insulin receptor metformin can increase further tyrosine phosphorylation of IRS1 and IRS2, as well as the association of IRS1 and IRS2 with PI3K. PI3K has been shown to play a critical role in many insulin-regulated metabolic processes, including stimulation of glucose transport, activation of glycogen synthase, and inhibition of PEPCK as the key enzyme of gluconeogenesis. Since the effect of metformin on insulin signaling processes was observed at concentrations reached in the serum of metformin-treated patients, these data are somewhat suggestive for the actual situation in humans. Thus, the primary mechanism of metformin's action to restore insulin sensitivity in hepatocytes might be related to the increased insulin post-receptor signal transduction linked to tyrosine phosphorylation of IRβ, IRS1 and IRS2 and the activation of PI3K.

In contrast to the effect of metformin at therapeutical concentrations, pharmacological concentrations of metformin inhibit further phosphorylation of signaling proteins and association of IRS with PI3K. These inhibitory effects may reflect the fact that higher metformin concentrations inhibit insulin action[9]. It should be noted that the changes in tyrosine phosphorylation associated with metformin treatment were not parallel to the alterations of protein expression level, which were increased in the presence of pharmacological concentrations of metformin. This suggests that effect of metformin on tyrosine phosphorylation of signaling protein could not be explained by the changes in the level of protein expression. Whether inhibitory effects of pharmacological concentrations of metformin are correlated with either the alteration in insulin receptor, IRS1 and IRS2 serine phosphorylation, or the direct action of metformin on insulin signal transduction or other regulatory event, remains to be investigated in future studies.

In conclusion, the present data suggest that chronic insulin exposure of Hep G2 cells results in down-regulation of insulin signal transduction via PI3K pathway. Therapeutic concentrations of metformin can reverse the effect of chronic hyperinsulinism on expression and activation of insulin signaling molecules, and pharmacological concentrations of metformin inhibit insulin signal transduction. The effect of metformin on insulin signal transduction represents a primary mechanism of metformin action in insulin resistant state.

REFERENCES

1   UK Prospective Diabetes Study (UKPDS) Group. Effect of intensive blood-glucose control with metformin on complications in overweight patients with type 2 diabetes (UKPDS 34). Lancet 1998; 352: 854-65.

2   Bergman RN. New concepts in extracellular signaling for insulin action: the single gateway hypothesis. Recent Prog

Horm Res 1997; 52: 359-85.

3　Nakajima K, Yamauchi K, Shigematsu S, Ikeo S, Komatsu M, Aizawa T, *et al.* Selective attenuation of metabolic branch of insulin receptor down-signaling by high glucose in a hepatoma cell line, HepG2 cells. J Biol Chem 2000; 275: 20880-6.

4　Bjornholm M, Kawano Y, Lehtihet M, Zierath JR. Insulin receptor substrate-1 phosphorylation and phosphatidy-linositol 3-kinase activity in skeletal muscle from NIDDM subjects after *in vivo* insulin stimulation. Diabetes 1997; 46: 524-7.

5　Pryor PR, Liu SC, Clark AE, Yang J, Holman GD, Tosh D. Chronic insulin effects on insulin signaling and GLUT4 endocytosis are reversed by metformin. Biochem J 2000; 348: 83-91.

6　Marena S, Tagliaferro V, Montegrosso G, Pagano A, Scaglione L, Pagano G. Metabolic effects of metformin addition to chronic glibenclamide treatment in type 2 diabetes. Diabete Metab 1994; 20: 15-9.

7　Santos RF, Nomizo R, Bopsco A, Wajchenberg BL, Reaven GM, Azhar S. Effect of metformin on insulin-stimulated tyrosine kinase activity of erythrocytes from obese women with normal glucose tolerance. Diabetes Metab 1997; 23: 143-8.

8　Stith BJ, Goalstone ML, Espinoza R, Mossel C, Roberts D, Wiernsperger N. The antidiabetic drug metformin elevates receptor tyrosine kinase activity and inositol 1,4,5 trisphosphate mass in Xenopus oocytes. Endocrinology 1996; 137: 2990-9.

9　Stith BJ, Woronoff K, Wiernsperger N. Stimulation of the intracellular portion of the human insulin receptor by the antidiabetic drug metformin. Biochem Pharmacol 1998; 55: 533-6.

10　Yuan L, Ziegler R, Hamann A. Inhibition of the phospho-enolpyruvate carboxykinase gene expression by metformin in cultured hepatocytes. Chin Med J 2003; 116: in press.

11　Meuillet EJ, Wiernsperger N, Mania-Farnell B, Hubert P, Cremel G. Metformin modulates insulin receptor signaling in normal and cholesterol-treated human hepatoma cells (Hep G2). Eur J Pharmacol 1999; 377: 241-52.

12　Ciaraldi TP, Kong AP, Chu NV, Kim DD, Baxi S, Loviscach M, *et al.* Regulation of glucose transport and insulin signaling by troglitazone or metformin in adipose tissue of type 2 diabetic subjects. Diabetes 2002; 51: 30-6.

13　Kim YB, Ciaraldi TP, Kong A, Kim D, Chu N, Mohideen P, *et al.* Troglitazone but not metformin restores insulin-stimulated phosphoinositide 3-kinase activity and increases p110 beta protein levels in skeletal muscle of type 2 diabetic subjects. Diabetes 2002; 51: 443-8.

EXHIBIT 4C

of April 5, 2010

SPECIAL REPORT

The endogenous lipid anandamide is a full agonist at the human vanilloid receptor (hVR1)

*,[1]D. Smart, [1]M.J. Gunthorpe, [1]J.C. Jerman, [1]S. Nasir, [1]J. Gray, [2]A.I. Muir, [2]J.K. Chambers, [1]A.D. Randall & [1]J.B. Davis

[1]Neuroscience Research, SmithKline Beecham Pharmaceuticals, New Frontiers Science Park, Third Avenue, Harlow, Essex CM19 5AW and [2]Vascular Biology, SmithKline Beecham Pharmaceuticals, New Frontiers Science Park, Third Avenue, Harlow, Essex CM19 5AW

The endogenous cannabinoid anandamide was identified as an agonist for the recombinant human VR1 (hVR1) by screening a large array of bioactive substances using a FLIPR-based calcium assay. Further electrophysiological studies showed that anandamide (10 or 100 μM) and capsaicin (1 μM) produced similar inward currents in hVR1 transfected, but not in parental, HEK293 cells. These currents were abolished by capsazepine (1 μM). In the FLIPR anandamide and capsaicin were full agonists at hVR1, with pEC$_{50}$ values of 5.94 ± 0.06 ($n=5$) and 7.13 ± 0.11 ($n=8$) respectively. The response to anandamide was inhibited by capsazepine (pK_B of 7.40 ± 0.02, $n=6$), but not by the cannabinoid receptor antagonists AM630 or AM281. Furthermore, pretreatment with capsaicin desensitized the anandamide-induced calcium response and vice versa. In conclusion, this study has demonstrated for the first time that anandamide acts as a full agonist at the human VR1.
British Journal of Pharmacology (2000) **129**, 227–230

Introduction The vanilloid receptor (VR1) has recently been cloned (Caterina *et al.*, 1997) and is a ligand-gated ion channel which plays an important role in nociception (Szallasi & Blumberg, 1999). Although the pungent plant extract capsaicin activates VR1 (Caterina *et al.*, 1997), the endogenous mammalian ligand remains to be identified (Szallasi & Blumberg, 1999).

We screened a collection of over 1000 bioactive substances for activity at the recombinant VR1, and identified the endogenous cannabinoid anandamide (Devane *et al.*, 1992) as an agonist at this receptor. This finding was of particular interest for several reasons. Firstly, the structure of anandamide (Pertwee, 1997) bears a striking similarity to several vanilloids (Szallasi & Blumberg, 1999), most notably olvanil (DiMarzo *et al.*, 1998). Secondly, anandamide has vasodilatory effects (Pertwee, 1997), which are not mediated by the cannabinoid receptors (White & Hiley, 1998). Thirdly, olvanil has been shown to inhibit the anandamide transporter (DiMarzo *et al.*, 1998; Beltramo & Piomelli, 1999). In addition anandamide has recently been reported to act as a partial agonist at the rat VR1 receptor (Zygmunt *et al.*, 1999).

Therefore, in the present study the effects of anandamide, and other cannabinoid ligands (Pertwee, 1997), on HEK293 cells stably expressing the hVR1 have been characterized using electrophysiology and a FLIPR-based calcium influx assay. This study has shown for the first time that anandamide acts as a full agonist at the human VR1.

Methods *Cloning and expression of VR1 receptors in HEK293 cells* Human VR1 cDNA was identified using the published rat VR1 sequence (GenBank accession AF029310) to search public nucleotide databases. Expressed sequence tag T48002 was identified and its sequence extended by rapid amplification of the cDNA ends using cDNA templates from a number of tissue sources. The full cDNA was amplified from brain cDNA, inserted into the expression vector pcDNA3.1, double strand sequenced, and stably expressed in HEK293 cells. Rat VR1 cDNA was amplified from rat DRG cDNA and similarly expressed in HEK293 cells.

Cell culture hVR1-HEK293 cells were grown as monolayers in minimum essential medium (MEM) supplemented with non-essential amino acids, 10% foetal calf serum, and 0.2 mM L-glutamine, and maintained under 95%/5% O$_2$/CO$_2$ at 37°C. Cells were passaged every 3–4 days and the highest passage number used was 20. Dissociated rat neonatal DRG cultures were prepared as described by Skaper *et al.* (1990).

Electrophysiological studies Cells were plated and cultured on glass coverslips at 26,000 cells cm^{-2} and whole-cell voltage-clamp recordings were performed at room temperature (20–24°C), using standard methods. The extracellular solution consisted of (mM): NaCl, 130; KCl, 5; CaCl$_2$, 2; MgCl$_2$, 1; Glucose, 30; HEPES-NaOH, 25, pH 7.3. For anandamide application this solution was supplemented with 0.2% lipid free bovine serum albumin. Patch pipettes of resistance 2–5 MΩ were fabricated on a Sutter Instruments P-87 electrode puller and were filled with the following solution (mM): CsCl, 140; MgCl$_2$, 4; EGTA, 10; HEPES-CsOH, 10, pH 7.3. All recordings were made from single, well isolated, phase bright

cells. Currents were recorded at a holding potential of -70 mV using a Axopatch 200B amplifier. Data acquisition and analysis were performed using the pClamp7 software suite. Drug applications were affected with an automated fast-switching solution exchange device (Warner Instruments SF-77B; time for solution exchange ~ 30 ms).

Measurements of $[Ca^{2+}]_i$ *using the FLIPR* hVR1-HEK293 cells were seeded into black walled clear-base 96-well plates (Costar U.K.) at a density of 25,000 cells per well in MEM, supplemented as above, and cultured overnight. The cells were then incubated with MEM containing the cytoplasmic calcium indicator, Fluo-3AM (4 μM; Teflabs, Austin, TX, U.S.A.) at 25°C for 120 min. The cells were washed four times with, and finally cultured in, Tyrode's medium containing 0.2% BSA, before being incubated for 30 min at 25°C with either buffer alone (control) or buffer containing various antagonists. The plates were then placed into a FLIPR (Molecular Devices, U.K.) to monitor cell fluorescence ($\lambda_{EX} = 488$ nM, $\lambda_{EM} = 540$ nM) (Sullivan *et al.*, 1999) before and after the addition of various agonists.

Data analysis Responses were measured as peak fluorescence intensity (FI) minus basal FI, and where appropriate, were expressed as a percentage of a maximum capsaicin-induced response. Data are expressed as mean$\pm$s.e.mean unless otherwise stated. Curve-fitting and parameter estimation were carried out using Graph Pad Prism 3.00 (GraphPad Software Inc., CA, U.S.A.). pK_B values were generated from IC_{50} curves for the antagonist vs a fixed EC_{80} concentration of agonist using the Cheng-Prusoff equation.

Materials All cannabinoids were purchased from Tocris (Bristol, U.K.) and all other ligands were obtained from RBI (Natick, MA, U.S.A.). All cell culture media were obtained from Life Technologies (Paisley, U.K.).

Results Application of either anandamide (10 μM) or capsaicin (1 μM) produced inward currents in HEK293 cells stably transfected with the hVR1 receptor. Neither agent produced responses in parental HEK293 cells. The currents produced by both agents developed slowly with mean time constants of 3.78 ± 0.93 s (1 μM capsaicin, $n = 7$) and 4.01 ± 0.65 s (10 μM anandamide, $n = 9$) reading peak amplitudes of 122 ± 27 and 44 ± 13 pA, respectively. The currents produced by either agonist exhibited substantial outward rectification and had similar interpolated reversal potentials (2.0 ± 1.4 mV, anandamide; -1.6 ± 1.2 mV, capsaicin; $n = 5$). The steady-state currents produced by both anandamide and capsaicin could be completely blocked by subsequent co-application of 1 μM capsazepine (Figure 1A); this antagonism developed with mean time-constants of 941 ± 205 ms ($n = 9$) and 3406 ± 930 ms ($n = 7$), respectively ($P < 0.05$, unpaired Student's t-test). In cultured rat DRG neurons anandamide (10 or 100 μM) produced capsazepine-sensitive inward currents in all capsaicin-responsive cells tested (Figure 1B,C). Even in response to 100 μM anandamide the amplitude of the currents recorded were smaller ($\sim 10 - 50\%$) than those generated by VR1 activation with a maximum concentration of capsaicin.

In the FLIPR, anandamide (100 pM $-$ 10 μM), like capsaicin (100 pM $-$ 10 μM), caused a concentration-dependent increase in $[Ca^{2+}]_i$ in hVR1-HEK293 cells (Figure 2), but was without effect in the non-transfected HEK293 cell-line (data not shown). Anandamide displayed a similar efficacy to capsaicin (Figure 2), but was markedly less potent (pEC_{50} values of 5.94 ± 0.06 and 7.13 ± 0.11, respectively, at pH 7.4). Moreover, the anandamide- and capsaicin-induced Ca^{2+} responses had indistinguishable kinetics in the FLIPR, with an initially rapid then slowing onset (peak ~ 30 s) followed by a gradually declining secondary phase.

The anandamide analogues methanandamide and palmitoylethanolamide also increased $[Ca^{2+}]_i$ in hVR1-HEK293 cells in a concentration-related manner, but were less potent
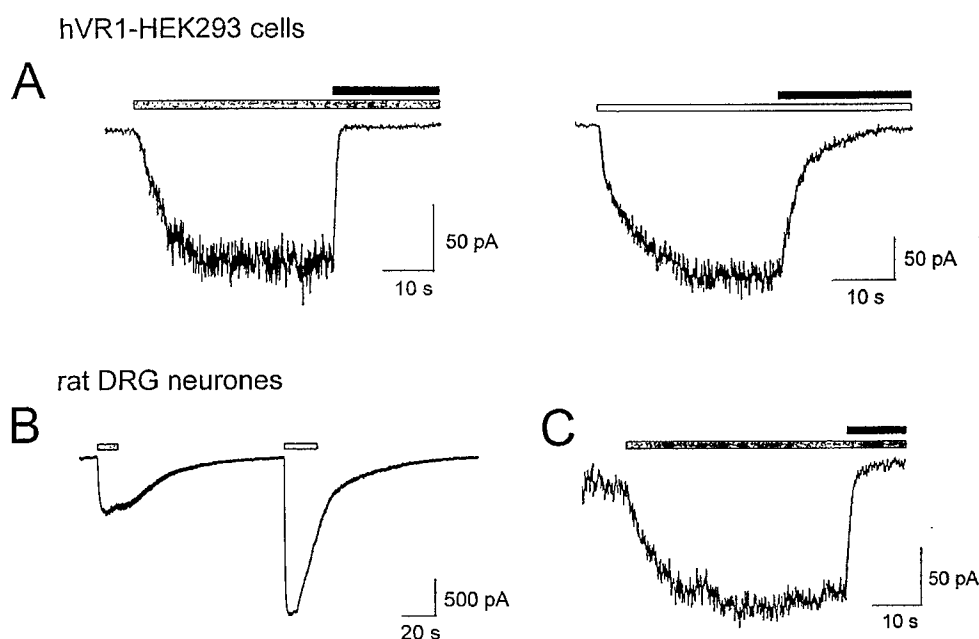
hVR1-HEK293 cells

rat DRG neurones

Figure 1 Anandamide-gated currents in hVR1-HEK293 cells and rat DRG neurons are capsazepine sensitive. (A) Application of anandamide (10 μM; grey bar) or capsaicin (1 μM; open bar) led to the appearance of inward currents in cells voltage clamped at -70 mV. These currents were blocked completely by co-application of capsazepine (1 μM; solid bar). Data are representative traces, typical of $n = 7-9$. (B) Application of anandamide (100 μM; shaded bar) led to the appearance of inward currents in DRG neurons voltage clamped at -70 mV. These cells were also shown to be sensitive to capsaicin (1 μM; open bar). (C) Anandamide-gated currents were blocked by capsazepine (1 μM; solid bar). Data are representative traces, typical of $n = 3$.

than anandamide, only evoking ~40% responses at 10 μM (Figure 2 and data not shown, n = 3). Like anandamide both these ligands were without effect in the non-transfected HEK293 cells. The synthetic cannabinoids CP-55,940 (((−)-cis-3-[2-hydroxy-4-(1,1-dimethylheptyl)phenyl] - trans - 4-(3-hydroxypropyl)cyclohexanol)) and WIN-55,212-2 (((R)-(+)-[2,3-dihydro-5-methyl - 3 - (4 -morpholinylmethyl)pyrrolo[1,2,3-de]-1,4-benzoxazin-6-yl]-1-naphthalenylmethanone)) were without effect in parental or hVR1-expressing HEK293 cells.

Interestingly, lowering the pH of the experimental buffer from 7.4 to 6.4 enhanced the potency of capsaicin (pEC_{50} of 7.13 ± 0.11 at pH 7.4 and 7.86 ± 0.18 at pH 6.4, n = 3), but had no effect on the potency of anandamide (pEC_{50} of 5.94 ± 0.06 at pH 7.4 and 5.76 ± 0.04 at pH 6.4, n = 3), or any of the other cannabinoid ligands tested (Figure 2 and data not shown).

The competitive VR1 antagonist (Szallasi & Blumberg, 1999) capsazepine (100 pM – 100 μM) inhibited both the anandamide (3 μM)- and capsaicin (100 nM)-induced Ca^{2+} responses, with pK_B values of 7.40 ± 0.02 and 7.31 ± 0.3 respectively (n = 6). However, the cannabinoid receptor antagonists AM630 ((6-iodo-2-methyl-1-[2-(4-morpholinyl)ethyl]-1H-indol-3-yl](4-methoxyphenyl)methanone)) and

AM281 ((1-(2,4-dichlorophenyl)-5-(4-iodophenyl)-4-methyl-N-4-morpholinyl-1H-pyrazole-3-carboxamide)) (100 pM – 10 μM) had no effect on either response (data not shown). Furthermore, pretreatment with 1 μM capsaicin for 30 min desensitized the response to 10 μM anandamide (16,271 ± 789 vs 332 ± 26 FI, n = 6) and 10 μM anandamide desensitized the response to 100 nM capsaicin (15,283 ± 1076 vs 1245 ± 83 FI, n = 6).

Discussion VR1 is a ligand-gated ion channel which plays an important role in nociceptive signalling (Szallasi & Blumberg, 1999). This receptor is activated by the plant extract capsaicin (Caterina et al., 1997), but the identity of the endogenous mammalian ligand remains unclear (Szallasi & Blumberg, 1999). Screening a wide range of bioactive substances revealed that anandamide, an endogenous cannabinoid (Devane et al., 1992), acted as an agonist at VR1. Anandamide displays a high structural similarity to the vanilloids, especially olvanil (DiMarzo et al., 1998; Beltramo & Piomelli, 1999), and has recently been reported to activate rat VR1 (Zygmunt et al., 1999). Therefore, the present study examined the pharmacology of anandamide at the recombinant human VR1 using electrophysiology and a FLIPR-based calcium assay, and has demonstrated for the first time that anandamide acts at human VR1 as a full agonist.

In the present study anandamide activated an inward current in hVR1-expressing, but not in parental, HEK293 cells. This current displayed similar kinetics to the capsaicin-induced current and was inhibited by capsazepine, a VR1 antagonist (Szallasi & Blumberg, 1999). Moreover, the anandamide- and capsaicin-induced currents had similar reversal potentials close to 0 mV, consistent with the gating of a non-selective ion channel and similar to findings for rat VR1 (Caterina et al., 1997). Anandamide also produced similar capsazepine-sensitive inward currents in capsaicin-sensitive cultured rat DRG neurons. In both the rat DRG neurones and hVR1-HEK293 cells the peak amplitude of the anandamide-induced current was significantly smaller (<50%) than that of the capsaicin-induced current. Similar results have recently been reported for anandamide at the recombinant rat VR1 (Zygmunt et al., 1999). Nevertheless, this apparent partial agonism probably reflects the technical difficulties in applying sufficiently high concentrations of such a lipophilic ligand in electrophysiological studies.

In the FLIPR anandamide and capsaicin both increased $[Ca^{2+}]_i$ in hVR1-expressing, but not non-transfected, HEK293 cells, and these responses displayed virtually identical kinetics. More importantly, the concentration-response relationship for anandamide was defined, and showed that anandamide was a full agonist compared to capsaicin. Capsaicin was more potent than anandamide, with an affinity consistent with that previously reported for rat VR1 (Caterina et al., 1997). Indeed, the potency of anandamide at hVR1 was ~20 fold lower than its binding affinity (55 nM) at the cannabinoid receptor (Devane et al., 1992), but was more consistent with the affinities (160 – 540 nM) reported from functional studies (Pertwee, 1997). Moreover, VR1 is structurally related to the transient receptor potential (TRP) channel family (Caterina et al., 1997), and certain TRP channels are activated by other lipid messengers with similar potencies (Chyb et al., 1999). Interestingly, the potency of capsaicin at hVR1 was enhanced by lowering the pH from 7.4 to 6.4, as reported for the rat VR1 (Caterina et al., 1997). In contrast the potency of anandamide was unaffected by pH, suggesting that anandamide and capsaicin may either bind to different
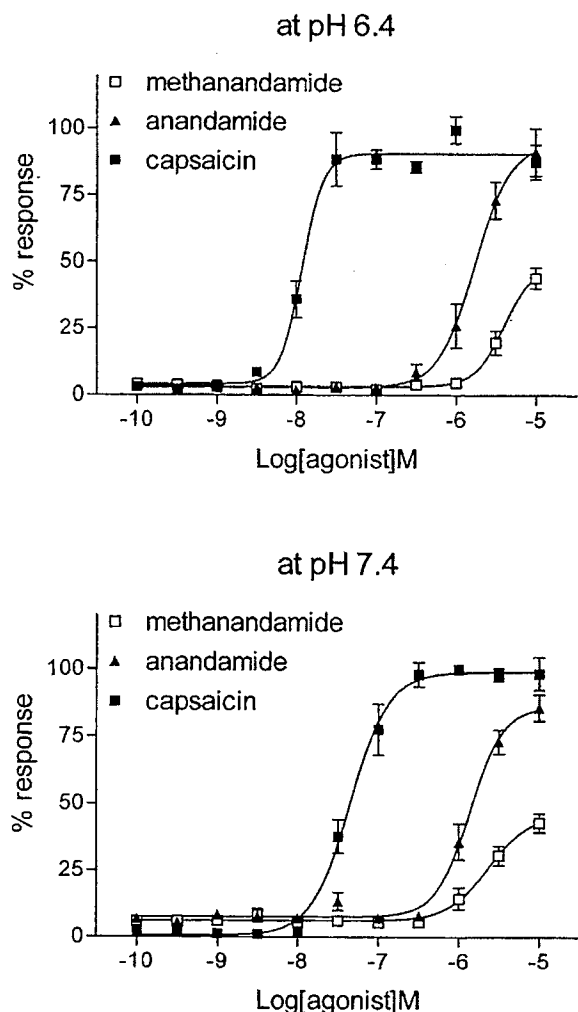
at pH 6.4

at pH 7.4

Figure 2 Anandamide-induced Ca^{2+} responses are concentration-dependent $[Ca^{2+}]_i$ was monitored using Fluo-3AM in hVR1-HEK293 cells before and after the addition of capsaicin (100 pM – 10 μM), anandamide (100 pM – 10 μM) or methanandamide (100 pM – 10 μM) at pH 6.4 or 7.4. Responses were measured as peak increase in fluorescence minus basal, expressed relative to the maximum capsaicin response and are given as mean ± s.e.mean, where n = 3 – 8.

sites on the human VR1 or gate the channel by different mechanisms.

Several lines of evidence demonstrate that the anandamide-induced Ca^{2+} response is mediated by hVR1. Firstly, anandamide has no effect in parental HEK293 cells. Secondly, the anandamide-induced Ca^{2+} response is inhibited by capsazepine, with a pK_B value consistent with the affinity of capsazepine at VR1 (Szallasi & Blumberg, 1999). Thirdly, the cannabinoid receptor antagonists, AM630 and AM281 (Pertwee, 1997) had no effect on the anandamide-induced response. Fourthly, capsaicin causes a homologous desensitization of the anandamide-induced response, and vice versa. Finally, the synthetic cannabinoid agonists, CP-55,950 and WIN-55,212-2 (Pertwee, 1997) were inactive at hVR1. These synthetic cannabinoids also failed to elicit a response in rVR1-

HEK293 cells (Zygmunt et al., 1999). However, in the present study the putative endogenous peripheral cannabinoid receptor ligand, palmitoylethanolamide (Pertwee, 1997) also activated hVR1, albeit more weakly than anandamide, despite having been reported to be inactive at the rat VR1 (Zygmunt et al., 1999). This demonstrates that other endogenous lipids can activate hVR1, suggesting possible roles for many different lipids in nociception. In conclusion, the present study has clearly demonstrated for the first time that the endogenous cannabinoid, anandamide acts as a full agonist at the human VR1.

References

BELTRAMO, M. & PIOMELLI, D. 1999). Anandamide transport inhibition by the vanilloid agonist olvanil. *Eur. J. Pharmacol.*, **364**, 75–78.

CATERINA, M.J., SCHUMACHER, M.A., TOMINAGA, M., ROSEN, T.A., LEVINE, J.D. & JULIUS, D. (1997). The capsaicin receptor: a heat-activated ion channel in the pain pathway. *Nature*, **389**, 816–824.

CHYB, S., RAGHU, P. & HARDIE, R.C. (1999). Polyunsaturated fatty acids activate the *Drosophila* light-sensitive channels TRP and TRPL. *Nature*, **397**, 255–259.

DEVANE, W.A., HANUS, L., BREUER, A., PERTWEE, R.G., STEVENSON, L.A., GRIFFIN, G., GIBSON, D., MANDELBAUM, A., ETINGER, A. & MECHOULAM, R. (1992). Isolation and structure of a brain constituent that binds to the cannabinoid receptor. *Science*, **258**, 1946–1949.

DIMARZO, V., BISOGNO, T., MELCK, D., ROSS, R., BROCKIE, H., STEVENSON, L., PERTWEE, R.C. & DEPETROCELLIS, L. (1998). Interactions between synthetic vanilloids and the endogenous cannabinoid systems. *FEBS Lett.*, **436**, 449–454.

PERTWEE, R.G. (1997). Pharmacology of cannabinoid CB1 and CB2 receptors. *Pharmacol. Therap.*, **74**, 129–180.

SKAPER, S.D., FACCI, L., MILANI, D., LEON, A. & TOFFANO, G. (1990). Culture and use of primary and clonal neural cells. In: Conn, P.M. (ed.). *Methods in Neurosciences.* vol.2. Academic Press, 17–33.

SULLIVAN, E., TUCKER, E.M. & DALE, I.L. (1999). Measurement of $[Ca^{2+}]_i$ using the fluorometric imaging plate reader (FLIPR). In: Lambert, D.G. (ed.). *Calcium Signaling Protocols.* Humana Press: New Jersey, pp. 125–136.

SZALLASI, A. & BLUMBERG, P.M. (1999). Vanilloid (capsaicin) receptors and mechanisms. *Pharmacol. Rev.*, **51**, 159–211.

WHITE, R. & HILEY, C.R. (1998). The actions of some cannabinoid receptor ligands in the rat isolated mesenteric artery. *Br. J. Pharmacol.*, **125**, 533–541.

ZYGMUNT, P.M., PETERSSON, J., ANDERSSON, D.A., CHUANG, H-H., SORGARD, M., DIMARZO, V., JULIUS, D. & HOGESTATT, E.D. (1999). Vanilloid receptors on sensory nerves mediate the vasodilator action of anandamide. *Nature*, **400**, 452–457.